The Dissertation Committee for Mark Allen Costello certifies that this is the approved version of the following dissertation:

Dexamethasone Intravitreal Implants: Characterization, Manufacture, and Elucidation of Drug Release Mechanisms

Committee:

Feng Zhang, Supervisor

Robert O. Williams III

Hugh D.C. Smyth

Nathaniel A. Lynd

Dexamethasone Intravitreal Implants: Characterization, Manufacture, and Elucidation of Drug Release Mechanisms

by

Mark Allen Costello

Dissertation

Presented to the Faculty of the Graduate School of

The University of Texas at Austin

in Partial Fulfillment

of the Requirements

for the Degree of

Doctor of Philosophy

The University of Texas at Austin

August 2023

Acknowledgements

I would like to thank several individuals that have supported my graduate work in a variety of ways over the last few years. First, I would like to thank my supervisor, Dr. Feng Zhang, for his valuable guidance and personal commitment to my success in graduate school. Dr. Zhang, thank you for pushing me to dig deeper, think bigger, and make the most of my time at UT. I would also like to thank the rest of my committee, Dr. Robert O. Williams III, Dr. Hugh D.C. Smyth, and Dr. Nathaniel A. Lynd, for their time and thoughtful recommendations regarding my research work. A special thanks to Dr. Lynd for being an excellent collaborator in our research and for educating me in polymer chemistry.

I would also like to acknowledge some of my former industrial colleagues that inspired me to pursue a graduate degree. Dr. Jonathan Miller was an excellent mentor at both AbbVie and Vertex Pharmaceuticals who provided me with a great example of what it means to be a scientist and encouraged me to invest in my professional growth. Dr. Eleni Dokou for giving me several opportunities to grow as a scientist at Vertex. Dr. Justin LaFountaine and Dr. Leena Prasad for leading me to the UT College of Pharmacy and for connecting me with Drs. Zhang and Williams early in the application process.

I would also like to thank our FDA collaborators in the Office of Generic Drugs and Office of Pharmaceutical Quality for guiding my research direction to maximize its impact and for thoroughly reviewing all my manuscripts: Yan Wang, Bin Qin, Xiaoming Xu, Qi Li, and William C. Smith.

A big thanks to my fellow graduate students in Dr. Zhang's lab for their helpful discussions, training, great listening skills, and excellent company throughout graduate school: Adwait Pradhan, Angela Ren, Ziyue Zhong, Coleman Johnson, and Dr. Tongzhou

Liu. I would also like to thank undergraduate research assistant Joseph Liu for his help executing numerous experiments in the lab and sticking with me for two years. Thanks to post-doc Dr. Beibei Chen for her time spent training me. I would also like to thank fellow graduate student Louise Kuehster from the Department of Chemical Engineering for being a great collaborator on our project, generating NMR data, and addressing all my polymer chemistry questions.

Several UT employees outside of the College of Pharmacy also deserve recognition. David Gray and Shallaco McDonald from the Department of Chemical Engineering for fixing all the broken parts I brought to their workshop. Kenny Schneider and Bryan McDonald from the Physics Machine Shop for their help manufacturing custom parts of all shapes and sizes. Jessie Maisano and Dave Edey from UT Geological Sciences for their help generating and analyzing microCT images.

I would like to thank my parents, Victor and Mary Costello, for their enduring support and for instilling in me the values that guide my life and career. Lastly, I want to thank my wife, Tracey Hwang, for her endless support throughout my time in graduate school. This would not have been possible without her understanding, patience, and encouragement.

Abstract

Dexamethasone Intravitreal Implants: Characterization, Manufacture, and Elucidation of Drug Release Mechanisms

Mark Allen Costello, Ph.D.

The University of Texas at Austin, 2023

Supervisor: Feng Zhang

Long-acting injectable products based on the biodegradable polymer poly(lactide-co-glycolide) (PLGA) have been available in the USA since 1989, with more than 20 PLGA–based formulations approved for use to date. Despite the clinical and commercial success of many of these drug products, no generic formulations have gained FDA approval at the time of this writing. The lack of PLGA–based generics can largely be attributed to the technical challenges associated with development of formulations with drug release profiles equivalent to the reference product. Despite extensive study of the drug release mechanisms of PLGA, the inherent complexity of the copolymer is largely to blame for the challenges associated with generic product development.

In this work, the FDA–approved product Ozurdex (dexamethasone intravitreal implant) was used as a model system to help address the challenges associated with generic product development of PLGA–based solid implants. Ozurdex is a small, rod-shaped implant (0.46 mm diameter, 6 mm long) formulated to deliver the corticosteroid dexamethasone to the posterior segment of the eye for 3–6 months. Ozurdex was thoroughly characterized and shown to be a porous implant consisting of a two-phase

system of dexamethasone crystals embedded within a PLGA matrix due to a limited drug-polymer interaction. Compositionally equivalent, reverse-engineered implants were produced using a continuous hot-melt extrusion process that required careful control to manufacture implants structurally equivalent to Ozurdex. The drug release mechanisms of the reverse-engineered implants were studied in detail using a variety of analytical techniques to examine the implant throughout the drug release period. This work also demonstrated how sourcing PLGAs with similar, but subtly different, physicochemical properties can affect the manufacture and drug release kinetics of dexamethasone intravitreal implants.

Table of Contents

List of Tables

List of Figures

List of Illustrations

Chapter 1. Introduction

1.1. MOTIVATION

Long-acting injectable drug products based on poly(lactide-*co*-glycolide) (PLGA) offer several advantages over standard dosage forms including reduced dosing frequency, maintenance of therapeutic levels of drug, and reduced incidence of side effects.[1] PLGA can be formulated to deliver a variety of therapeutic agents (e.g., small molecules, peptides, or proteins) for durations ranging from weeks to months.[2] The biodegradability of PLGA in combination with its documented biocompatibility and tunable degradation profile make it one of the most commonly investigated polymers to achieve long-acting release.[3] These drug products can take several forms including 1) a distribution of sub-millimeter particles (microspheres), 2) in-situ gels formed locally after diffusion of the PLGA solvent away from the injection site, and 3) solid, monolithic implants.[4]

PLGA has been used for more than 30 years to extend drug release with at least 25 PLGA–based formulations gaining FDA approval to date.[5] Despite many of these products existing beyond their marketing exclusivity period, no generic formulations of these drug products are available on the market, suggesting development of generic PLGA–based formulations is challenging. Indeed, several examples exist in the literature attempting to reverse engineer the innovator PLGA drug products.[6-9] Generic formulations save American consumers hundreds of billions of dollars per year, with cost savings growing to $338 billion in 2020 alone.[10, 11] This massive savings emphasizes the impact that lower-cost alternatives to brand-name drugs can have while remaining equally as safe and efficacious as the innovator product.

To achieve FDA–approval of a generic PLGA–based formulation via the abbreviated new drug application (ANDA) pathway, the generic formulation must be

qualitatively (Q1) and quantitatively (Q2) the same in terms of inactive ingredients as the reference-listed drug (RLD). Unfortunately, Q1/Q2 sameness does not guarantee equivalent drug release performance when compared to the RLD as the drug product manufacturing process can impart physicochemical changes to the dosage form that alter the release profile.[12] To further complicate matters, the inherent heterogeneity of PLGA (a statistical copolymer) can make achieving Q1/Q2 sameness difficult as properties beyond the polymer molecular weight and lactide/glycolide ratio can impact drug release kinetics, e.g., the monomer unit ordering (blockiness).[13]

1.2. PLGA CHEMISTRY

PLGA is a biodegradable polyester that degrades via hydrolysis in aqueous environments into the non-toxic monomer units lactic acid and glycolic acid. These two α-hydroxy acids are subsequently eliminated as carbon dioxide and water in vivo via the Krebs cycle.[14] Although the monomer units are readily soluble in water, the PLGA polymer is insoluble at industrially-meaningful molecular weights.

The tunable release characteristics attributed to PLGA derive from the chemical properties of the polymer. The five parameters that are primarily responsible for differences in the rate of PLGA degradation by hydrolysis include: 1) lactide/glycolide ratio, 2) stereochemistry of lactic acid, 3) molecular weight, 4) chain termination, and 5) repeat unit ordering (also known as blockiness). All these properties are controlled by the conditions of the polymerization reaction. Most of the PLGAs used in FDA–approved long-acting injectable formulations are synthesized using ring-opening polymerization (ROP).[15] ROP is performed with the cyclic diesters of lactic acid and glycolic acid, lactide and glycolide, respectively.[16] As lactic acid is a chiral molecule, lactide can exist as one of three diastereoisomers: D-, L-, or meso-lactide. A 50/50 racemic mixture of D-

and L-lactide (DL-lactide) is often used to prepare PLGAs. Figure 1.1 presents a typical reaction scheme for synthesis of acid-terminated 50:50 poly(DL-lactide-*co*-glycolide).

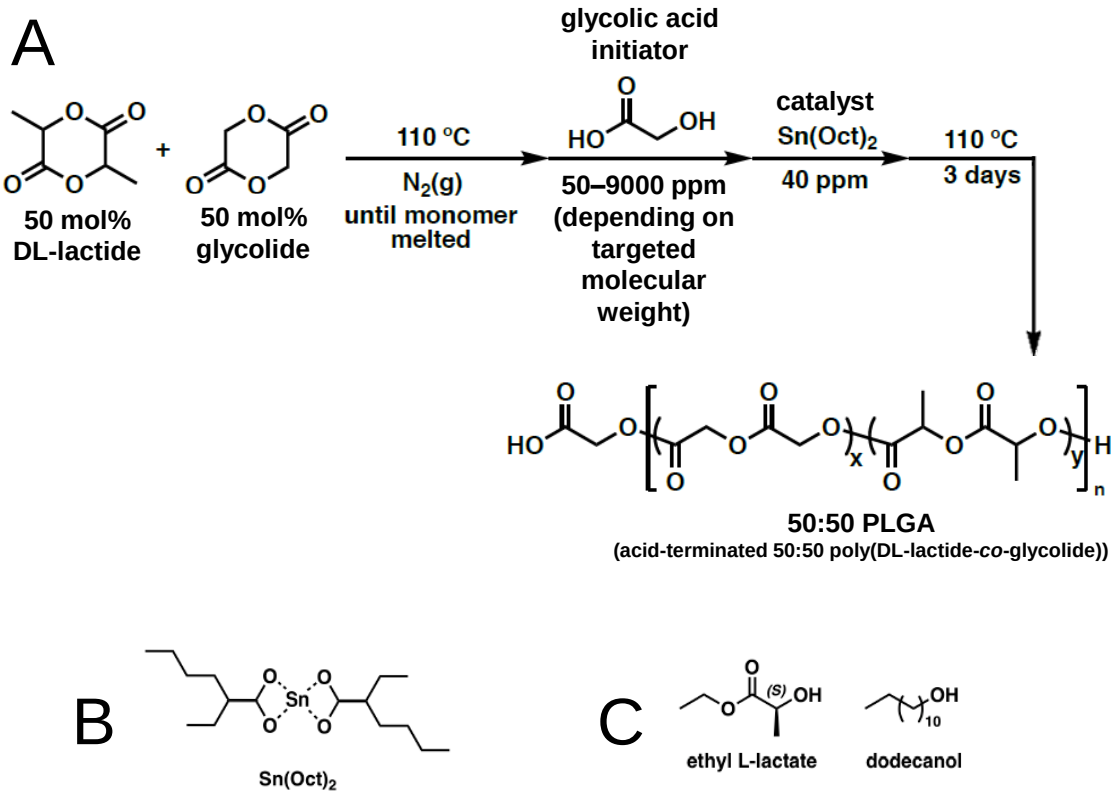

Figure 1.1. Reaction scheme for ring-opening polymerization of acid-terminated 50:50 PLGA (A). The structure of the tin(II) 2-ethylhexanoate catalyst (B) and the initiators used to produce ester-terminated PLGAs (C) are also shown.

The L/G ratio of PLGA is dictated by the molar ratio of the two monomers charged at the start of polymerization. The ratio can vary in any proportion of lactide and glycolide, though ratios between 50:50 L:G and 90:10 L:G are most common due to the poor solubility of glycolide-rich polymers in common organic solvents.[17] PLA (poly(DL-lactide)) is also applied in controlled drug release applications, but is out of scope for this discussion. Figure 1.2 shows the relationship between L/G ratio and the half-life of the

polymer during hydrolytic degradation in rat tissue. PLGAs with an equimolar ratio of lactide and glycolide tend to degrade the fastest of all other ratios. This effect of composition can be explained by the changes to copolymer hydrophilicity and crystallinity. Since PLGAs degrade by hydrolysis, access of water to the polymer backbone can be directly related to the polymer's degradation half-life. PLGAs with a high proportion of lactide or glycolide tend to be highly crystalline and correspondingly restrict access to water when compared to the completely amorphous 50:50 PLGA. Similarly, when D-lactide or L-lactide alone are used in the synthesis of PLGA, the polymers tend to be more crystalline and degrade more slowly than PLGAs prepared with the DL-lactide racemic mixture.

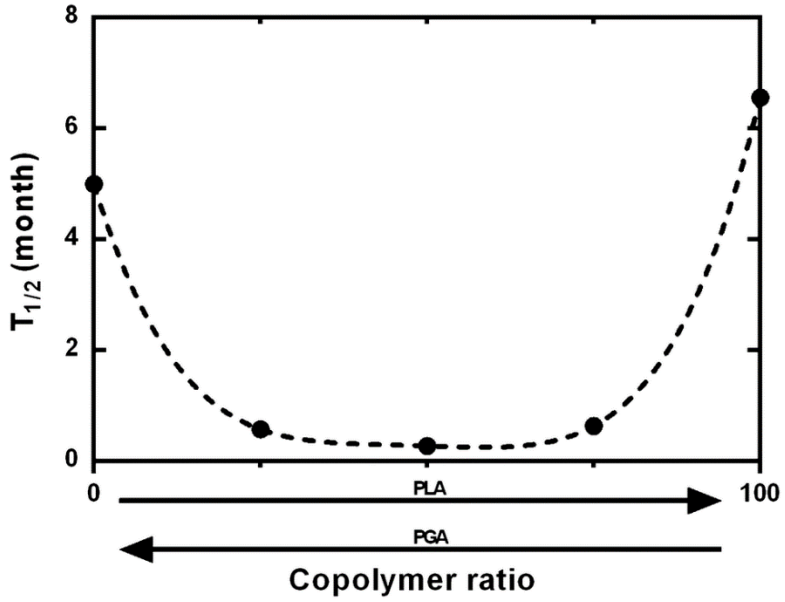

Figure 1.2. Half-life of various lactide/glycolide copolymers implanted in rat tissue.[18]

PLGA molecular weight is dictated by the amount of initiator charged at the beginning of polymerization. Lower concentrations of initiator result in PLGAs of higher molecular weight. PLGA degradation time increases with the average molecular weight

of the copolymer since the longer chains take longer to break down into water soluble monomers and oligomers. The nature of the initiator determines whether the PLGA is either acid-terminated or ester-terminated. If glycolic acid is used to initiate polymerization, the PLGA chain will be terminated with a carboxylic acid on one end and an alcohol on the other.[19] Alternatively, if polymerization is initiated with ethyl-lactate or dodecanol, the PLGA chain will be terminated with an ester on one end and an alcohol on the other. As previously discussed, the increased hydrophilic character of the acid-terminated PLGA would result in faster rates of hydrolysis compared to the ester-terminated PLGA.

In addition to the monomer ratio, the PLGA blockiness, or ordering of the lactic acid and glycolic acid monomers on the polymer backbone, can impact the rate of PLGA degradation. It is known that glycolic acid linkages are more hydrophilic (and therefore susceptible to hydrolysis) than lactic acid linkages as the methyl group on lactic acid reduces hydrophilicity and reactivity by steric hinderance.[20] As polymerization of PLGA progresses, transesterification, or mid-chain reactions, can occur resulting in scrambling of the expected G-G and L-L repeat units arising from the ROP of the cyclic dimers.[21] Glycolate-rich blocks degrade much more quickly than lactate-rich blocks, resulting in an overall faster rate of PLGA degradation from blocky polymers compared to PLGAs synthesized with alternating lactate-glycolate monomers.[22]

1.3. DISSERTATION OVERVIEW

The primary goal of this dissertation was to use the FDA–approved Ozurdex (dexamethasone intravitreal implant) as a model system for detailed investigation to help address the technical challenges associated with generic product development of PLGA–based dosage forms. Prior to experimentation, a review was conducted of the in vitro

release testing methods applied to evaluate the drug release kinetics of long-acting implants for drug delivery to the posterior segment of the eye (see Chapter 2). In Chapter 3, the Ozurdex implant was thoroughly characterized using a variety of analytical techniques and reverse engineered to produce structurally and compositionally equivalent implants for further study. This reverse-engineered implant was thoroughly characterized throughout the in vitro dissolution process in Chapter 4 to identify the critical physicochemical properties of the implant controlling drug release and how those properties change during the drug release process. Chapter 5 takes a deep dive into the continuous hot melt extrusion process used to manufacturing the dexamethasone intravitreal implants. The importance of accurate process control is discussed along with the impact of changes to the extrusion parameters on implant structure and drug release kinetics. Finally, this dissertation concludes in Chapter 6 with an evaluation of how dexamethasone intravitreal implants prepared with similar PLGAs sourced from different vendors (with subtly different properties) affected implant manufacture and drug release in vitro.

Chapter 2. In vitro release testing methodologies of long-acting implants for ocular drug delivery to the posterior segment: a review[*]

ABSTRACT

Drug delivery to the posterior segment of the eye offers a unique opportunity to treat several ocular conditions such as macular edema and uveitis. The extended-release nature of long-acting intravitreal implants helps to reduce frequency of intraocular injections, which can enable new treatments and improve clinical outcomes. Development of these long-acting implants requires a suitable in vitro dissolution method to tune and predict the rate of drug release in vivo. Multiple approaches have been developed for in vitro testing; however, these methods may not accurately predict in vivo drug release due to the complexity of ocular physiology. Drug elimination from the vitreous can occur through various transport pathways in the back of the eye or through the anterior segment (front of the eye), which is challenging to model in vitro. This review considers the different methods applied to predict drug release and the challenges associated with development of an in vitro-in vivo correlation for ocular implants.

[*] Mark A. Costello performed the literature review and wrote this chapter.

2.1. INTRODUCTION

Long-acting implant formulations for drug delivery to the posterior segment of the eye can serve as an effective alternative to frequent intravitreal injections and potentially enhance clinical outcomes. Long-acting implants can maintain drug concentrations at therapeutic levels for weeks to months while reducing the risk of complications stemming from frequent injections such as vitreous hemorrhage, retinal damage, and endophthalmitis.[23, 24]

The behavior of long-acting implants in ocular tissues is complex, requiring consideration of the blood-ocular barrier, vitreous viscosity, and drug transporter mechanisms in addition to the drug release mechanisms from the implant itself.[25] For this reason, no regulatory standard exists for in vitro dissolution methods for long-acting implants to the posterior segment of the eye. Currently, United States Pharmacopeia (USP) general chapter ⟨1771⟩ suggests using any existing apparatus described in Dissolution ⟨711⟩ or Drug Release ⟨724⟩. It also notes that non-compendial conditions and/or equipment may be applied for new ocular implant formulations with the goal of mimicking in vivo conditions.[26]

In vitro release testing to estimate the in vivo release rate is an important part of the development and commercialization of intraocular implants. Current methodologies range from basic, e.g., incubator-shaker setups, to complex, e.g., multi-compartment systems used to mimic the physiology of the eye, each having advantages and disadvantages. In this review, in vitro release testing methodologies for long-acting intraocular implants will be discussed.

2.2. INTRAOCULAR IMPLANTS FOR POSTERIOR SEGMENT DRUG DELIVERY

Today, only four implants for administration of a small molecule to the posterior segment of the eye have FDA approval for sale in the United States with others in development and under study in academic research labs.[27] Drug release from these implants can range from several months to several years depending on the unique structural and compositional design of the implant. Three of the four implants (Iluvien, Yutiq, and Retisert) deliver fluocinolone acetonide from a non-biodegradable implant and the fourth delivers dexamethasone from a biodegradable polymer matrix (Ozurdex).

Iluvien, Yutiq, and Retisert all make use of the Durasert® platform technology that consists of a combination of non-permeable polymer (polyimide and/or silicone) and semi-permeable polyvinyl alcohol (PVA) to control drug diffusion.[28] The implant core serves as a depot of fluocinolone acetonide, and diffusion is controlled by the drug's permeability through the PVA membrane (Figure 2.1). Release begins immediately after administration and occurs at a steady rate over a 2-3 year period.[29]

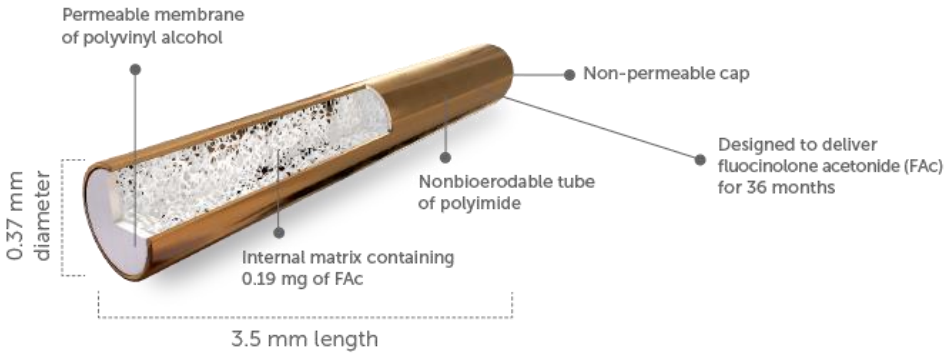

Figure 2.1. Structure of Iluvien non-biodegradable implant.[29]

The Ozurdex implant releases dexamethasone over the course of 6 months from a biodegradable poly(lactic-co-glycolic acid) (PLGA) polymer matrix (Figure 2.2). Due

to the autocatalytic nature of PLGA hydrolysis, a tri-phasic release profile of dexamethasone is observed. The first phase observed is a small burst (< 5%) of drug release immediately after administration, followed by a lag phase where limited drug release occurs while PLGA degradation is ongoing, and the final release phase where the remaining drug is released and the PLGA oligomers are solubilized and diffuse away with the dexamethasone.

Figure 2.2. Structure of Ozurdex biodegradable implant showing porous structure of PLGA. Magnified view (right) shows drug molecules (red spheres) interspersed in the pores and skeleton of the PLGA polymer.[24]

These two types of implants exhibit fundamentally different drug release mechanisms, which poses a challenge for predicting release in vitro using a standardized method. In vitro method parameters such as dissolution volume, pH, agitation rate, and buffer strength may all play a role in observed in vitro release rates. The following sections will discuss various methods applied for in vitro release testing of ocular implants.

2.3. STATIC DIFFUSION METHOD

The static diffusion method is perhaps the most straightforward in vitro method for evaluating drug release from ocular implants and has been applied extensively throughout implant research and development.[30-35] The implant is placed into a fixed volume of release media in a closed container and subjected to a fixed incubation

temperature with or without agitation (Figure 2.3). Drug released can be evaluated by either harvesting the media at regular intervals or by harvesting the entire implant. Common analytical methods, such as high-performance liquid chromatography (HPLC), can be applied to assay the quantity of drug in the media or in the solids after dissolving the remaining implant in an appropriate solvent. An incubation temperature of 37°C is most commonly used to mimic human basal body temperature. Phosphate buffered saline (PBS) pH 7.4 is the most commonly used media to simulate the osmolarity and ionic concentrations found in the body, however, other media can be applied in the static diffusion method such as unbuffered normal saline (0.9% w/v NaCl) or PBS with the addition of surfactants, e.g., Tween 80. Dissolution volume is selected to maintain sink conditions per USP guidelines (≤ ⅓ saturation solubility).[36]

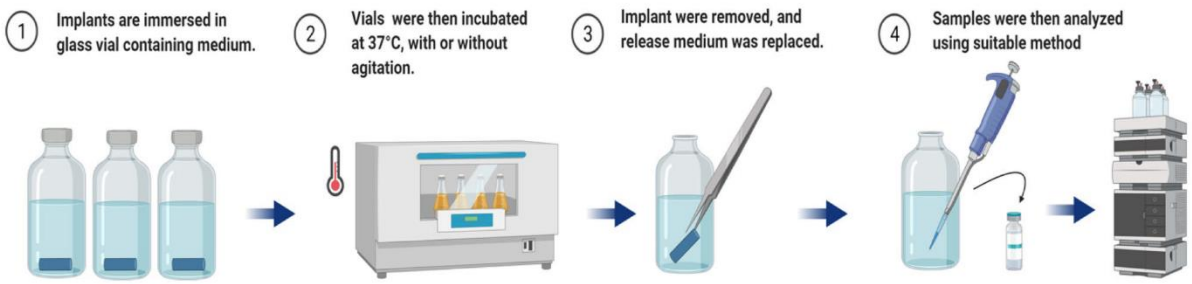

Figure 2.3. The static diffusion methodology.[25]

During the development of both the Durasert®-based fluocinalone acetonide formulations and Ozurdex dexamethasone formulation, the static diffusion method was applied. For fluocinolone acetonide, the developers (Control Delivery Systems, Watertown, MA) used 1 mL of PBS at 37°C without agitation in microcentrifuge tubes.[37] At each sampling timepoint, the tubes were vortexed and the entire 1 mL of dissolution media was sampled for assay followed by replacement with fresh PBS. This method was used for 168 days to illustrate the consistent release rate in vitro. For Ozurdex, the

developers (Allergan Inc., Irvine, CA) used 30 mL of Normal Saline at 37°C with gentle shaking.[38] At each sampling timepoint, 25mL of media was sampled for assay and replaced with 25mL of fresh saline. Normal saline was used in place of PBS due to its close match with in vivo rabbit data. This outcome is discussed further in Section 2.6.

2.4. USP DISSOLUTION METHODS

Despite no clear directive from USP regarding dissolution of intraocular implants, USP apparatus 3, 4, and 7 have been explored for in vitro release studies of long-acting formulations. Apparatus 3 and 7 use a vertical reciprocating mechanism that repeatedly moves the implant through the dissolution media held at constant temperature. The theoretical advantage of this methodology is that the constant shear due to the vertical movement captures the erosion component of implant dissolution which may not have been seen in the static diffusion setup. Stein et al. compared release from dexamethasone implants using the static diffusion method and USP apparatus 7.[39] The authors found the average release to be comparable after 28 days, however, the USP apparatus 7 showed significantly higher variability between replicates compared to the static diffusion method. This variability was attributed to fragmentation of the implants and adhesion to the apparatus 7 holder. Fragmentation was not seen in any of the static diffusion samples which may have contributed to less variability between replicates. Using apparatus 3 or 7 requires development of additional equipment-related parameters such as holder design, dip rate, and dip amplitude.

USP apparatus 4, the flow-through cell, uses a reservoir and a pump to continually circulate dissolution media across the sample from below. Control of the flow rate of dissolution media allows for control of the hydrodynamic conditions that the implant experiences. Rawat et al. demonstrated that a robust and reproducible method

could be developed for PLGA microspheres over the course of 40 days at both 37°C and 45°C.[40] The hydrodynamics during dissolution in apparatus 4 are a strong function of the flow rate and thus must be carefully considered during method development.[41]

2.5. OCULAR PHYSIOLOGY-BASED METHODS

A developing approach to in vitro dissolution of intraocular implants is to mimic the physiology of the eye as accurately as possible using a customized apparatus. Awwad et al. developed the PK-Eye with bioequivalent volumes of the posterior (4.2 mL) and anterior (0.2 mL) cavities, a semi-permeable dialysis membrane between the two cavities, and small ports to represent drug elimination through the front of the eye (Figure 2.4).[42]

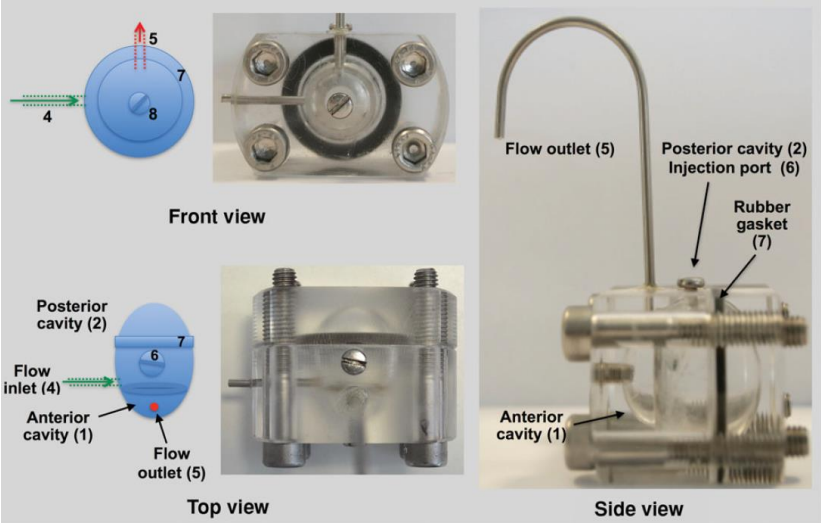

Figure 2.4 The PK-Eye model derived from human ocular physiology.[42]

The authors suggest that the PK-Eye is better suited to modeling release from protein-based therapeutics as these compounds are primarily cleared though the front of the eye due to their large size. For small, lipophilic molecules (e.g., dexamethasone) a combination of clearance through the retina into systemic circulation and through the

front of the eye can be expected, rendering this model less applicable. The authors also explored the impact of dissolution media viscosity in the posterior chamber: PBS vs. a vitreous humor substitute made of agar and hyaluronic acid.[43] Vitreous viscosity had a significant impact on clearance through the front of the eye for the two biologics evaluated but showed no impact for the small molecule suspension evaluated (Kenalog, triamcinolone acetonide). This result is consistent with rabbit in vivo data using Ozurdex in vitrectomized eyes replaced with balanced salt solution and unaltered eyes.[44]

Stein et al. also developed and evaluated the Eye Movement System (EyeMoS) in which a vitreous model of appropriate shape, volume, and temperature was linked to a drive belt that simulates the eye's natural movements.[45] The authors suggest that movement of the dissolution media alone, i.e., using an incubator/shaker, may not be biorelevant and that the nature of the movements in in vitro testing should be further considered.

2.6. IN VITRO-IN VIVO CORRELATION (IVIVC)

Based on the current state of the art, it is not possible to develop an in vitro-in vivo correlation in humans for intraocular implants. Even if the challenges associated with mimicking the complex drug transport mechanisms in the eye could be achieved in vitro, developing such a correlation would require frequent removal of human vitreous to determine actual drug release rate in vivo. Such sampling would pose too great a risk to the patient to perform in a clinical setting. In the European Medicines Agency (EMA) review of Ozurdex, one reviewer acknowledged that an a priori in vitro-in vivo correlation in humans is "impossible" to achieve, and that in vitro testing is more applicable for quality control applications.[46]

Nevertheless, developers of intravitreal implants attempt to simulate human eye behavior using an animal model such as rabbit or monkey. Neither model is perfect, but each may provide insight into possible human in vivo behavior. In the case of Ozurdex, the developers used normal saline as their dissolution media instead of PBS because of the close approximation in release rate in vitro and in vivo rabbit eyes (Figure 2.5).[47] Rabbit is the preferred model for studying intravitreal pharmacokinetics.[48] However, it is worth noting that release of dexamethasone in rabbit eye is significantly faster than monkey and human based on measured concentrations and observed clinical outcomes, respectively.[49] This further suggests that in vitro testing of ocular implants should be viewed more as a quality control and development tool rather than an accurate representation of release in the human eye.

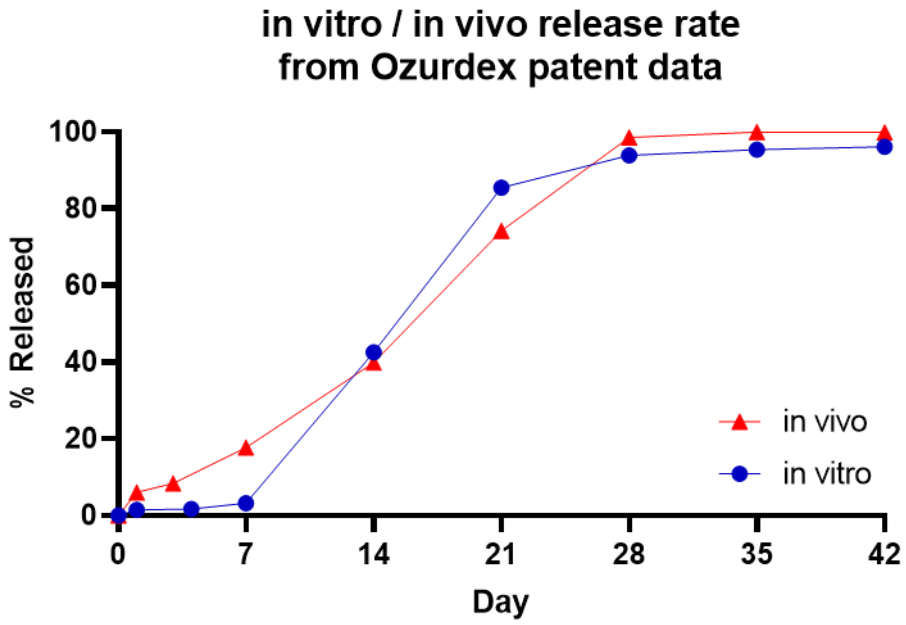

Figure 2.5. Overlay of in vitro and in vivo dexamethasone release. In vitro occurred in 37°C normal saline using the static diffusion method. In vivo reported from rabbit eye. Data replotted from [47].

2.7. RECOMMENDATIONS FOR IN VITRO RELEASE TESTING OF NEW OCULAR IMPLANTS

As discussed above, in vitro dissolution methods ranging from simple to complex have been developed for evaluating intravitreal implants. Alas, further development is needed to generate a physiologically relevant in vitro model that can be applied to a wide variety of new APIs. For this reason, the static diffusion method is recommended for in vitro release testing of new ocular implants. While the most simplistic method, its benefits arise from the ease of sample preparation, testing and method development. During the early phases of formulation development, rapid prototyping is required. Due to the long-acting nature of these implants, dissolution runtimes should not exceed more than 2-3 months for practical purposes.

Depending on the nature of the rate-limiting mechanism, media and temperature can be chosen to accelerate release to fit within this time frame. For example, PLGA is known to degrade via backbone hydrolysis of the polymer chain.[15] This hydrolysis is self-catalyzed by the acidic end groups produced during the degradation process.[50] The use of unbuffered media, such as normal saline, instead of PBS will accelerate the overall degradation rate of PLGA and ultimately increase the release rate of drug from the matrix. This can be useful for distinguishing fundamental changes in formulations in the early stages of development. During later stages of development, the media can easily be switched to PBS to provide a more biorelevant release rate due to a reduction in the autocatalysis of PLGA (Figure 2.6). Ultimately, animal models will still be required to validate this in vitro work; however, the PK-Eye methodology created by Awwad et al. shows promise in early studies as a biorelevant ocular model and should be considered as a final in vitro test prior to animal studies.

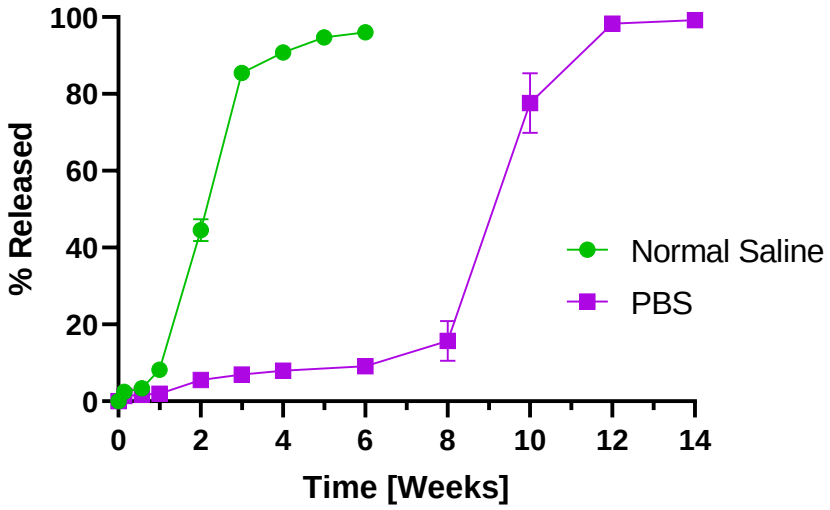

Figure 2.6. Dissolution of Ozurdex-like implants illustrating the impact of dissolution media on drug release.[51]

2.8. CONCLUSION

Development of a biorelevant in vitro dissolution model for a priori prediction of drug release from intravitreal implants in humans remains elusive. Numerous methods remain in development to close this gap; however, additional work is required to better correlate in vivo release rates with in vitro methods. A major hurdle facing this development is the inability to collect robust data sets of human in vivo release data due to ethical considerations. Nevertheless, as more intraocular implants are developed, animal data and human clinical data should be leveraged to better understand the relationships between in vitro dissolution parameters and in vivo release rates.

Chapter 3. Reverse engineering the Ozurdex dexamethasone intravitreal implant*

ABSTRACT

Ozurdex is a biodegradable implant formulated for sustained-release delivery of the corticosteroid dexamethasone to the posterior segment of the eye. The small, rod-shaped implant is administered directly to the vitreous using a dedicated applicator, and releases drug for up to 6 months after administration. Sustained release is achieved by embedding dexamethasone in a matrix of 50:50 poly(lactic-*co*-glycolic acid) (PLGA). In this work, the Ozurdex implant was thoroughly characterized to enable the reverse engineering of a compositionally and structurally equivalent implant. Advanced imaging techniques such as scanning electron microscopy (SEM) and microcomputed tomography (microCT) revealed that the Ozurdex implant exhibits an irregular surface and an internal porosity of 6% due to a large number of discrete voids approximately 3 μm in diameter. Thermal and spectroscopic analyses showed limited interaction between the drug and the polymer, resulting in a two-phase system of dexamethasone crystals embedded within a PLGA matrix. Reverse-engineered implants with properties similar to Ozurdex were prepared using a two-step hot-melt extrusion process. The reverse-engineered implants exhibited a triphasic drug release profile similar to Ozurdex. This work seeks to provide insight into the manufacturing process and characterization of PLGA–based solid implants to support future generic product development.

---

* Published in: Costello MA, Liu J, Wang Y, Qin B, Xu X, Li Q, et al. Reverse engineering the Ozurdex dexamethasone intravitreal implant. Int J Pharm. 2023;634:122625. Mark A. Costello wrote the manuscript and designed, executed, and interpreted the experiments.

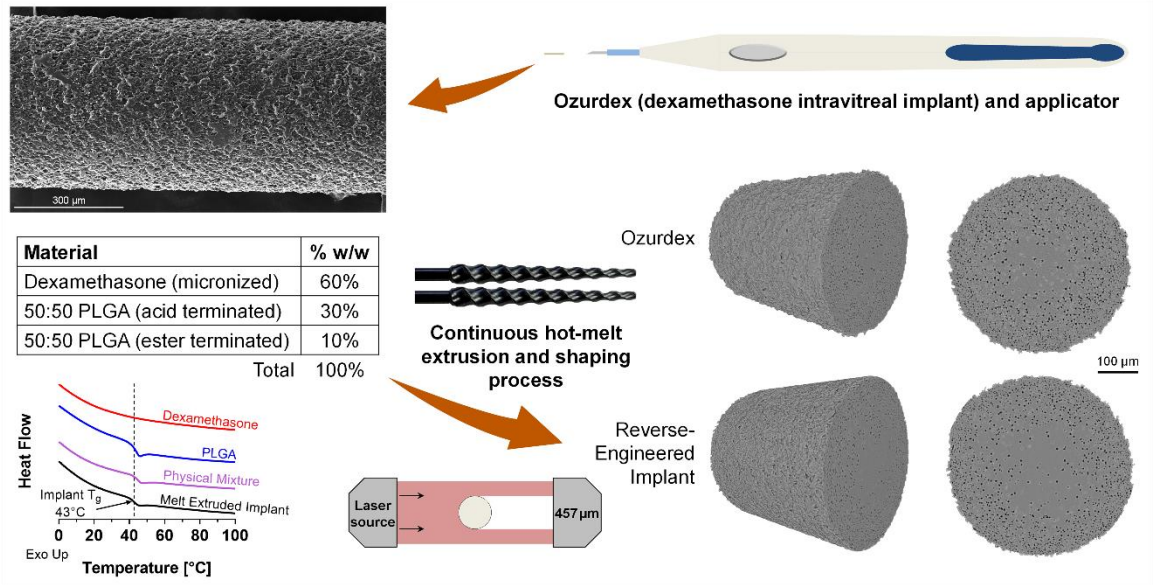

Illustration 3.1. Graphical abstract for Chapter 3.

3.1. INTRODUCTION

Several pathologies that affect the posterior segment of the eye carry a risk of permanent visual impairment or blindness without proper treatment. Some of these disorders (e.g., diabetic macular edema, which affects 7% of all persons with diabetes[52]) can be treated with anti-inflammatory agents, such as corticosteroids or anti-vascular endothelial growth factor (anti–VEGF) agents.[53, 54] The delivery of corticosteroids to the posterior segment of the eye poses challenges because both topical and systemic dosing often result in subtherapeutic concentrations in the retinal space as well as undesirable side effects.[55] The administration of drug directly to the vitreous is a solution to this problem. However, this solution is complicated by the short half-life of these compounds (3–6 h), which would require frequent injections and pose an increased safety risk to the

patient. To overcome this limitation, sustained-release dosage forms for intravitreal drug delivery have been developed.

Ozurdex is an FDA–approved, long-acting implant formulated to deliver the corticosteroid dexamethasone to the posterior segment of the eye for the treatment of non-infectious uveitis, macular edema following branch and central retinal vein occlusion, and diabetic macular edema.[56] Through a variety of anti-inflammatory mechanisms, dexamethasone serves to stabilize the blood-retinal barrier and reduce the retinal capillary leakage that causes loss of vision.[57] Dexamethasone, a synthetic derivative of hydrocortisone, is a non-ionizable small molecule with poor aqueous solubility (~90 µg/ mL).[58] Sustained release of dexamethasone is achieved by embedding the drug in a biodegradable poly(lactic-*co*-glycolic acid) (PLGA) matrix that gradually releases the drug directly into the vitreous over the course of 3–6 months.[24, 49]. The implant is produced using a continuous hot-melt extrusion process in which the drug and polymer are mixed between a pair of rotating screws at temperatures above the glass transition temperature (T_g) of the polymer. This process produces a melt that is extruded through a die to form rod-shaped filaments.[47] These filaments are then cut to the desired length to prepare unit doses of Ozurdex. The drug product is administered via a proprietary applicator in which the implant is housed in a 22-gauge needle to facilitate injection directly to the vitreous of the eye.[59]

Originally approved by the FDA in 2009, both the Ozurdex implant and its applicator are slated to lose patent exclusivity in 2023, thus opening the door for generic competition.[27] Generic medicines can help lower drug prices and improve access to care. New generic drug approvals from 2018 to 2020 saved Americans over $50 billion in the 12-month period following their approval.[11] Despite extensive study of the mechanisms of controlled drug release from PLGA–based formulations,[60] the development of generic

formulations of FDA–approved, PLGA–based products has been notoriously difficult.[4, 6, 61] At the time of this writing, there were no generic PLGA–based products available in the US, despite more than 20 branded drug approvals dating back to 1989.[1] This lack of generic drug products is attributed to a variety of factors, including (1) incomplete understanding of the impact of formulation and manufacturing process parameters on drug release, (2) lack of predictive in vitro release testing methods, and (3) difficulties in demonstrating bioequivalence in vivo.

The first steps taken to establish bioequivalence of a generic formulation of a parenteral injectable product typically involve demonstrating qualitative (Q1) and quantitative (Q2) formulation sameness, along with comparable drug release profiles from in vitro release testing.[12] Demonstrating Q1/Q2 sameness of PLGA–based formulations can be challenging due to the inherent variability of the random copolymer.[1] Advanced analytical techniques may be needed to appropriately characterize the polymer properties, such as molecular weight, polydispersity index, lactide:glycolide ratio, endcap, and blockiness.[13, 62] Changes in these properties may have an impact on drug release of the long-acting formulation. During in vitro release testing by the manufacturer, the Ozurdex implant exhibited a triphasic release profile with minimal burst release.[38]

In this work, we developed a compositionally and structurally equivalent implant of Ozurdex using a variety of analytical and processing techniques to better understand the unique characteristics of the dosage form. Compositional equivalence was inferred from both the literature and experimentation. Detailed analytical characterization of the PLGAs in Ozurdex was not included in the scope of this study. We first performed a thorough characterization of the Ozurdex implant along with characterization of the dexamethasone–PLGA interaction. This was followed by development of the hot-melt

extrusion manufacturing process used to produce the structurally equivalent implant. Our study concluded with in vitro release testing of the reverse-engineered implant formulation in normal saline and a comparison to the release profile of Ozurdex. The purpose of this study was to obtain a better understanding of the impact that formulation and process have on the quality and performance of PLGA–based implants to support future development of generic PLGA drug products, such as Ozurdex.

3.2. MATERIALS AND METHODS

3.2.1. Materials

Madison, NJ, USA) was purchased from a pharmacy supplier. Two grades of 50:50 poly(D,L-lactide-*co*-glycolide) (PLGA) were purchased from the Evonik Corporation (Darmstadt, Germany): Resomer RG 502 (ester terminated) and Resomer RG 502 H (acid terminated). Dexamethasone was purchased from Shenzhen Nexconn Pharmatechs Ltd. (Shenzhen, China). HPLC–grade acetonitrile, HPLC–grade acetone, and ACS–grade sodium chloride were purchased from Thermo Fisher Scientific (Waltham, MA, USA). Distilled, deionized water was obtained in the laboratory.

3.2.2. Methods

3.2.2.1 X-Ray powder diffraction (XRPD)

XRPD was performed using a Rigaku Miniflex 600 X-ray diffractometer (Rigaku Corporation; Tokyo, Japan). Samples were scanned with a step size of 0.01° and a dwell time of 0.5 s over a 2θ range of 5° to 45°.

3.2.2.2 Gel permeation chromatography (GPC)

The molecular weight and polydispersity index (PDI) of PLGA were determined using a Waters GPC system equipped with a 2414 refractive index (RI) detector and an integrated 2707 autosampler (Waters Corporation; Milford, MA, USA). The mobile phase (acetone) was pumped at a flow rate of 0.6 mL/min through two Tosoh TSKgel GMHHR-L columns connected in series (Tosoh Corporation; Tokyo, Japan). Nine polymethylmethacrylate (PMMA) standards (500–200,000 Da) (Agilent Technologies; Santa Clara, CA, USA) were used to generate a calibration curve. All samples and standards were prepared in acetone and injected with a volume of 50 μL.

3.2.2.3 Scanning electron microscopy

Scanning electron microscopy (SEM) was used to evaluate implant structure and morphology. Samples were prepared for imaging by attaching them to aluminum stubs using double-sided carbon tape. They were then sputter-coated with gold for 60 s at 40 mA (Electron Microscopy Sciences; Hatfield, PA, USA). Imaging was performed using a Quanta 650 FEG SEM (FEI Company; Hillsboro, OR, USA) with an accelerating voltage of 15 kV.

3.2.2.4 Polarized light microscopy

A hot-stage microscope fitted with a 50× objective and polarizing filters (BX53, Olympus Corporation; Tokyo, Japan) was used visualize the size of dexamethasone crystals in the implants. An implant fragment was heated to 150 °C, then gently smeared onto a glass slide. Linksys32 image capture software (Linkam Scientific Instruments Ltd.; Tadworth, UK) was used to record images. A 10 μm stage micrometer was used to calibrate a custom MATLAB program (MathWorks; Natick, MA, USA) that manually determined particle size.

3.2.2.5 Implant porosity

Total implant porosity can be estimated using geometric techniques by measuring the physical dimensions of the implant. The implant diameter was measured at several points (n = 5) along a 2–3 cm length of a melt-extruded implant using a laser micrometer (BETA LaserMike AccuScan 5012, NDC Technologies Inc.; Dayton, OH, USA). Digital calipers (Kobalt; Mooresville, NC, USA) were used to measure the length of the implant segment. Implant mass was measured using a microbalance with a precision of 0.001 mg (MSA3.6P0TRDM, Sartorius; Göttingen, Germany). Equation 3.1 was applied to determine the implant density:

Equation 3.1.

$$Implant\ Density = \frac{Implant\ Mass}{\pi \times \left(\frac{Avg.\ Diameter\ (n=5)}{2}\right)^2 \times Length}$$

To calculate implant porosity, the true density of the implant components was first determined using helium pycnometry performed on the powder blend (MVP-6DC, Quantachrome Instruments; Boynton Beach, FL, USA). Equation 3.2 was then used to determine the implant porosity:

Equation 3.2.

$$Implant\ Porosity = \left(1 - \frac{Implant\ Density}{True\ Density}\right) \times 100\%$$

Using the geometric approach to determine total implant porosity surface irregularities form voids between the imagined surrounding cylinder and the actual surface of the implant. Therefore, the *total porosity*, as applied in this work, includes both the external void volume generated by surface irregularities and the internal void volume generated from closed pores.[63] *Internal porosity*, calculated from microCT data, refers

specifically to the void volume generated from closed pores inaccessible from the surface. *External porosity* can be estimated by subtracting the internal porosity (calculated from microCT data) from the total porosity (calculated using the geometric method described above).

3.2.2.6 Thermal analysis

A Q20 DSC (TA Instruments; New Castle, DE, USA) was used to evaluate the T_g of the PLGA in various samples. Samples (1–5 mg) were sealed in an aluminum pan and subjected to a heat–cool–heat cycle from –10 °C to 110 °C. The T_g was determined by the midpoint of the transition during the second heating cycle.

3.2.2.7 Attenuated total Reflection–Fourier-Transform infrared spectroscopy (ATR-FTIR)

ATR-FTIR analysis was performed using a Nicolet iS50 FTIR Spectrometer equipped with a single-reflection Germanium ATR sampling accessory (Thermo Fisher Scientific; Waltham, MA, USA). Spectra were recorded in the range 675–4,000 cm^{-1} with 64 scans per sample.

3.2.2.8 Jet-Milling

An Alpine 50 AS Spiral Jet Mill (Hosokawa Micron; Summit, NJ, USA) was used to mill dexamethasone and both PLGAs using compressed nitrogen gas. For all materials, an injector pressure of 5–6 bar and a grinding pressure of 3–3.5 bar were used. The particle size of dexamethasone was evaluated using a Sympatec HELOS laser diffraction unit (Clausthal-Zellerfeld, Germany) equipped with an R3 lens (0.5–175 μm) and a RODOS dry dispersing unit set at 2 bar.

3.2.2.9 Melt extrusion and shaping

Dexamethasone intravitreal implants were manufactured using a double extrusion and shaping process. For the first extrusion, the pre-extrusion blend was fed into a Haake MiniLab twin-screw extruder (Thermo Electron (Karlsruhe) GmbH; Karlsruhe, Germany) using a single-screw force feeder rotating at 7 rpm. The blend was extruded at 105 °C using conical, co-rotating screws at 125 rpm, then shaped into rods using a 1 mm diameter heated die fitted at the extruder discharge port set to 97 °C. Before the second extrusion, these rods were manually broken into 1–2 cm segments and milled using a Wiley Mini Mill (Thomas Scientific; Swedesboro, NJ, USA) fitted with a 20-mesh screen to produce free-flowing granules.

For the second extrusion, a twin-screw volumetric feeder (MT-1, Brabender Technologie; Mississauga, ON, Canada) in tandem with a single-screw force feeder at 1 rpm was used to precisely control the feed rate of the milled extrudate (8–10 g/h) into a twin-screw Haake MiniLab extruder (set to 105 °C and 125 rpm) fitted with a heated die (0.48 mm diameter) at the discharge port set to 97 °C. A downstream puller (IMSTec USA, Inc.; Temecula, CA, USA) integrated with a dual-axis laser micrometer (BETA LaserMike AccuScan 5012, NDC Technologies Inc.; Dayton, OH, USA) was used to draw down the melt to the target diameter. Online process monitoring of the extruder parameters and the implant diameter was performed using custom MATLAB software (MathWorks; Natick, MA, USA) to trend real-time data from the extruder and laser micrometer. Implant rods 5–10 cm in length were collected and allowed to cool down to room temperature. After cooling, the rods from the second extrusion were manually cut to the desired length using a razor blade to produce individual implants.

3.2.2.10 HPLC assay

Dexamethasone assay of the dissolution media as well as the implant drug content was performed using a Waters HPLC equipped with a 2996 photodiode array (PDA) detector and integrated 717plus autosampler (Waters Corporation; Milford, MA, USA). The mobile phase consisted of a 60:40 acetonitrile:water (v/v) mixture. HPLC parameters consisted of a flow rate of 1 mL/min, a Luna 5 μm C18(2) 100 Å column (150 mm × 4.6 mm) (Phenomenex; Torrance, CA, USA), and a detection wavelength of 241 nm. Duplicate injections were used for all samples. Dexamethasone had a retention time of approximately 2.4 min.

Dissolution media samples were filtered through 0.45 μm PTFE centrifuge filters before a 50 μL injection. Implant solids that remained after the final dissolution timepoint were dissolved in 10 mL of mobile phase and filtered using a 0.45 μm PTFE syringe filter before a 50 μL injection. Duplicate 3-point calibration curves were generated from 0.1 to 10 μg/mL ($R^2 \geq 0.9999$) for both sample types.

For the assay of whole implants, the mass of the implant was recorded using a microbalance before completely dissolving the implant in 25 mL of mobile phase. A 20 μL injection volume was used. Duplicate 2-point calibration curves were generated for the range of 10–100 μg/ mL.

3.2.2.11 X-Ray microcomputed tomography (microCT) and analysis

X-ray microCT was used to characterize the internal pore structure of the implants. A ZEISS Xradia 620 Versa (ZEISS Microscopy; Jena, Germany), located at the University of Texas High-Resolution X-ray CT Facility, was used to generate image stacks corresponding to a 0.5 mm × 0.5 mm × 0.5 mm field of view, with a voxel size of 0.5 μm. Dragonfly (Object Research Systems (ORS); Montreal, QC, Canada) was used to

perform post-processing, including 3-D reconstruction and digital segmentation of the image stacks.

3.2.2.12 In vitro release testing

In vitro release testing was performed in 30 mL normal saline (0.9% NaCl (w/v)) at 37 °C and 100 rpm using a New Brunswick Innova 40 incubator/shaker (Eppendorf; Hamburg, Germany). Sampling occurred on Days 1, 4, 7, 14, 21, 28, 35, and 42. During sampling, 25 mL of the medium was removed for HPLC analysis and then replaced with 25 mL of fresh normal saline. Release data were normalized to the assay of the remaining implant fragment at the final timepoint on Day 42.

3.3. RESULTS AND DISCUSSION

3.3.1. Characterization of Ozurdex

3.3.1.1 Compositional analysis

The Ozurdex label claim is 700 μg dexamethasone and the drug loading was estimated to be 60% (w/w) based on a measured total implant mass of 1.186 mg (mean, *n* = 2). The dexamethasone drug substance has two reported polymorphs (Form A and Form B).[58] A comparison of Ozurdex XRPD data with the literature spectra reveals that the dexamethasone in Ozurdex is the Form B polymorph (see Figure S3.1).[64] The remaining 40% (w/w) of the implant is composed of a mixture of two grades of PLGA: 50:50 ester terminated and 50:50 acid terminated.[46] Ester terminated PLGAs are considered more hydrophobic, and they experience slower hydrolytic degradation rates than acid terminated PLGAs.[19] Patent literature suggests that the PLGAs used in Ozurdex are likely mixed in a 3:1 acid:ester ratio to achieve the desired drug release profile.[47]

Characterization of the PLGAs in Ozurdex to confirm this ratio was not included in this study.

Gel-permeation chromatography calibrated to PMMA standards shows that the weight average molecular weight (Mw) of the PLGA in Ozurdex is approximately 16,400 g/mol, with a polydispersity of 2.6 (n = 2). The 50:50 PLGAs with these properties and matching end groups are similar to the commercially available polymers from Evonik, Resomer RG 502 H (acid terminated) and Resomer RG 502 (ester terminated), which have an inherent viscosity (IV) of 0.2 dL/g.[65] These two polymers are referenced in both the patent literature and prescribing information, and were used throughout this study, blended in a 3:1 acid:ester ratio, to mimic the expected composition of Ozurdex (see Table 3.1).

Material	**Mass per implant (mg)**	**% w/w**
Dexamethasone (Form B, micronized)	0.700	60%
Resomer RG 502 H (50:50 PLGA, acid terminated)	0.350	30%
Resomer RG 502 (50:50 PLGA, ester terminated)	0.117	10%
Total	1.167	100%

Table 3.1. Estimated composition of Ozurdex.

3.3.1.2 Structural analysis

The majority of the FDA–approved PLGA–based drug products exist as *microparticles* (i.e., a distribution of submillimeter particles containing the active ingredient), while Ozurdex exists as a comparatively large rod. This unique form factor of Ozurdex demands unique criteria to consider when reverse engineering the drug product. The dimensional and structural characteristics of the implant were expected to

be critical for (a) enabling a proper fit within the injection device, (b) withstanding the forces experienced during administration, and (c) providing a consistent dose between implants.[46]

A qualitative analysis of the structural characteristics of Ozurdex was performed using SEM. Imaging confirms that Ozurdex is a cylindrical, rod-shaped implant 6 mm in length and 0.46 mm in diameter (see Figure 3.1). SEM images also reveal that Ozurdex consists of a uniform dispersion of dexamethasone particles embedded in a matrix of PLGA. The implant exhibits a rough, irregular surface, with few free crystals of dexamethasone visible under high magnification (1,000×).

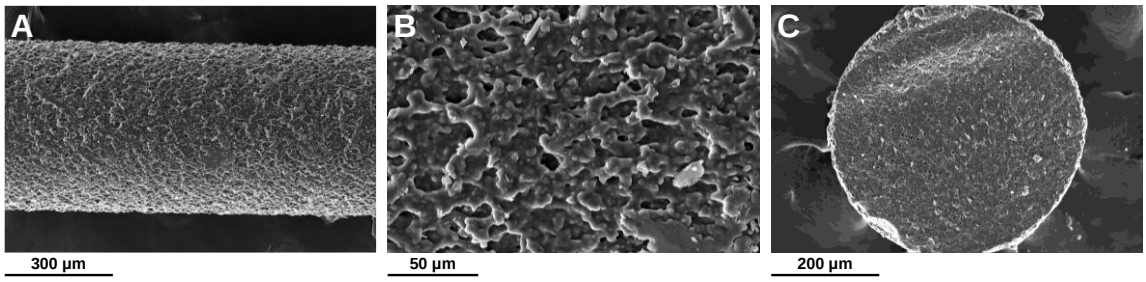

Figure 3.1. SEM images of Ozurdex. Side view at 200× (A), side view at 1000× (B), and cross-section at 300× (C).

The SEM cross-section reveals substantial internal porosity, with many pores less than 5 µm in diameter. The concentration of internal voids is enriched near the implant surface, with few pores present near the core. The total implant porosity (i.e., void fraction) can be calculated using the procedure described in Methods. It is important to note that the diameter used in the calculation of total porosity is derived from a scanning laser micrometer, which reports the diameter of the shadow cast by the implant when placed in the measurement field of the device. Therefore, when using this method, all

implant surface irregularities contribute to the total diameter, and the small indentations or valleys on the surface of the implant manifest as external porosity inside an imaginary cylinder that has a diameter equal to the diameter reported by the scanning laser micrometer.

Effectively, total implant porosity is a function of both surface roughness and internal porosity. To determine the total porosity of Ozurdex, helium pycnometry was used to measure the true density of the blended formulation components (1.365 g/cm3). Based on the theoretical mass and dimensions of Ozurdex, the estimated total porosity was 13.2%. Further discussion and quantification of internal porosity is included below.

Hot-stage polarized light microscopy was used to visualize the dexamethasone particles dispersed throughout the PLGA matrix and to estimate their size. The implant was heated to 150 °C and gently smeared across a glass slide to form a thin layer for visualization of individual drug particles. The dexamethasone particles exhibited birefringence while the PLGA matrix did not (see Figure 3.2). The observed birefringence suggested that Ozurdex is composed of crystalline dexamethasone embedded in an amorphous PLGA matrix. Few aggregates of dexamethasone crystals were visible, which suggested that the drug particles were uniformly dispersed throughout the PLGA matrix. The apparent diameter of the dexamethasone particles was determined by measuring the edge-to-edge distance of several particles (n = 150) after calibration using a slide micrometer. The crystals were small (<5 μm), which is consistent with the literature stating that Ozurdex contains micronized dexamethasone.[46]

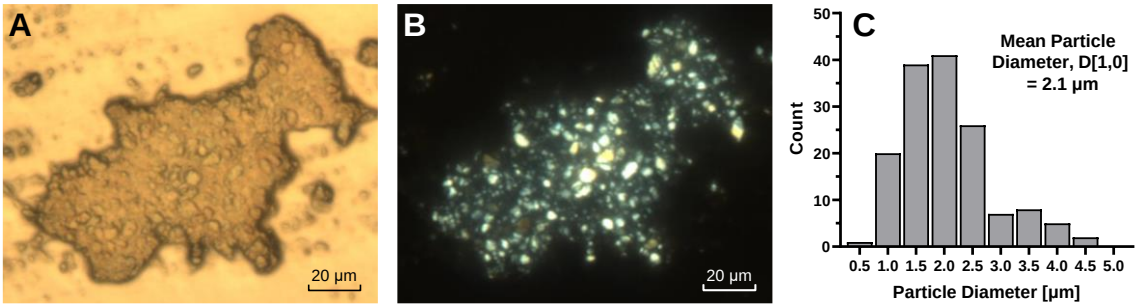

Figure 3.2. Hot-stage microscopy of Ozurdex: Bright field (A) and with cross-polarizers (B) showing crystals of dexamethasone exhibiting birefringence. Particle size distribution was estimated from 150 randomly selected birefringent particles from three different images (C).

3.3.2. Dexamethasone–PLGA interaction

During the hot-melt extrusion process, a portion of the crystalline dexamethasone may change physical state by dissolving in the PLGA to form a molecular dispersion of amorphous drug in the polymer. This amorphous form modification is often desired as a way to overcome the solubility limitations of poorly soluble drugs for oral delivery.[66] (Thompson et al., 2022) Such a modification of dexamethasone physical state would have implications for drug release, physicochemical stability, and manufacturing process control of the implant.[67, 68]

To investigate this phenomenon, the interaction between dexamethasone and PLGA was explored using thermal and spectroscopic techniques. Differential scanning calorimetry (DSC) was performed on Ozurdex, dexamethasone, PLGAs, and their mixtures before and after melt extrusion. Melting point depression of a drug in the presence of a polymer is a technique commonly applied to evaluate drug–polymer miscibility.[69] However, in this system, the melting point depression of dexamethasone could not be evaluated due to substantial thermal degradation of both dexamethasone and PLGA at temperatures below the apparent melting point of dexamethasone (~265 °C).

Alternatively, drug–polymer miscibility could be evaluated by observing a change in the T_g to a value that lies between the glass transition temperatures of the pure components. The estimated T_g of amorphous dexamethasone is between 115 °C and 120 °C.[64] The Gordon–Taylor equation can be applied to estimate changes in the T_g of amorphous dispersions of dexamethasone in PLGA.[70] Calculations showed that even a small fraction (e.g., 5%) of the dexamethasone dissolving in the PLGA would be expected to cause a detectable upward shift in the apparent T_g of the system (~4 °C). No such shift was apparent in the DSC thermograms of the drug, the polymer, or their mixtures both before and after extrusion (see Figure 3.3). The lack of shift in T_g suggests that the implant remains primarily a two-phase system of crystalline dexamethasone in amorphous PLGA after melt extrusion.

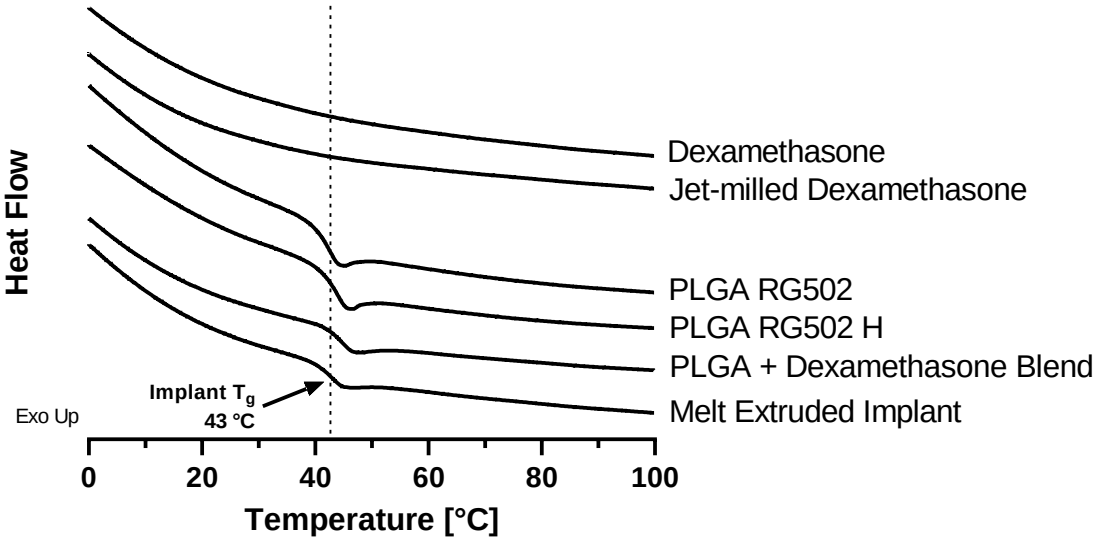

Figure 3.3. DSC thermograms of dexamethasone, PLGA, and their mixtures before and after melt extrusion. The estimated T_g of Ozurdex is 43 °C. The sample is not shown due to a very weak signal as a result of the small sample size (< 0.5 mg).

These findings corroborate the observations of Gasmi et al., who prepared dexamethasone-loaded PLGA microparticles using an oil-in-water (O/W) emulsion solvent extraction technique with drug loads ranging from 2 to 62%.[71] All formulations exhibited the same T_g as pure PLGA, including formulations that appeared to be X-ray amorphous.

To further probe the interaction between dexamethasone and PLGA, ATR-FTIR spectroscopy was performed on the pure components, their physical mixture, and the melt-extruded implant. Intermolecular interactions between dexamethasone and PLGA (e.g., hydrogen bonding) would be detectable through changes in the vibrational frequencies of key hydrogen bond donor/acceptor sites. These intermolecular interactions would manifest as a shift in the wavenumber in the FTIR spectra.[72] Changes to the ester carbonyl peak in PLGA (1,755 cm^{-1})[73], the aryl carbonyl peak in dexamethasone (1,664 cm^{-1}), and/or the broad hydroxyl peak in dexamethasone (3,410 cm^{-1})[74] could indicate hydrogen bonding interactions between the components. However, the formulation components exhibited no shifts or broadening in the characteristic peaks in the melt-extruded implant sample (see Figure 3.4). This further suggests limited interaction between the drug and the polymer in this system. Full IR spectra are available in the supplementary data (see Figure S3.2).

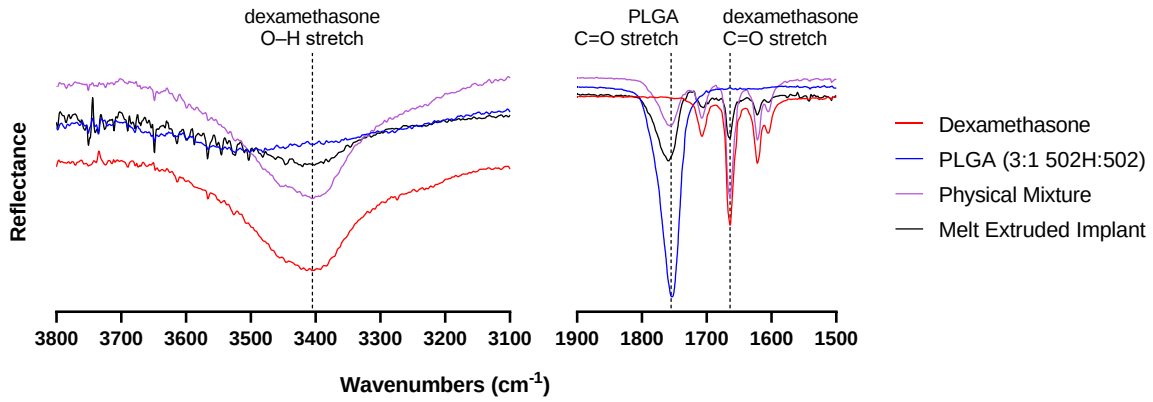

Figure 3.4. Select regions of ATR-FTIR spectra, illustrating the lack of hydrogen bonding interactions between dexamethasone and PLGA.

3.3.3. Implications for drug release

A truly biphasic system of dexamethasone embedded in a PLGA matrix may have significant implications for drug release. Drug diffusion through the polymer would be nearly eliminated, and drug release may be tied directly to the rate of PLGA degradation and erosion. Indeed, signs of this mechanism are evident in the in vitro release profile of Ozurdex published by the manufacturer.[38]

Ozurdex exhibits a triphasic release profile during in vitro release testing, a trait the implant shares with other previously described PLGA–based formulations.[75, 76] A limited burst release (≤3%) in the first 24 h may be caused by the reduced exposure of dexamethasone to the bulk dissolution medium as the drug is coated with PLGA in the matrix. This small amount of drug release may come from free drug (on or near the surface of the implant), which can dissolve immediately upon exposure to water. The second phase (i.e., the lag phase) shows very little drug release (≤10%) during the first week. In this phase, water ingress and PLGA hydrolysis can continue, but access of the bulk medium to the dexamethasone is still restricted due to the polymer coating. In the

final phase, release to completion occurs over 3–4 weeks in vitro in normal saline. In this phase, sufficient PLGA degradation can occur to enable the dissolution of oligomers and monomers from the implant matrix into the medium. As a result, the dexamethasone particles are exposed to substantial amounts of water, which leads to particle dissolution and drug release.

The internal pore structure may also have implications for the drug release rate and duration.[77] An interconnected pore system would increase the surface area–to-volume ratio and provide the dissolution medium with direct access to the center of the implant, thus reducing diffusion length and promoting drug release. The internal pore structure of Ozurdex was explored in detail using X-ray microCT, discussed below.

3.3.4. Importance of dimension control and implant structure during the melt extrusion process

We expected that accurate diameter control during the implant manufacturing process was important for ensuring the proper fit of the implant within the applicator and to maintain unit dose assay. Despite the irregular surface of Ozurdex observed under SEM, the diameter of the implant was observed to be very consistent across its entire 6 mm length. The 22-gauge, thin-wall needle used in the Ozurdex applicator has an inside diameter of 0.505 mm.[78] If the implant diameter exceeds this distance at any point along its length, it may not fit inside the device. Conversely, if the implant diameter is too small, it may not be held securely in the needle barrel, which may cause it to slip out prematurely before administration.

More importantly, both implant diameter and total porosity can be linked directly to unit dose assay through geometric constraints. For example, if two implants have the same total porosity and length, a smaller diameter decreases the volume of the PLGA–

dexamethasone matrix, which reduces the dose. Similarly, if two implants have the same diameter and length, a higher total porosity reduces the space available for the PLGA–dexamethasone matrix, which also reduces the dose.

Assuming a fixed length of 6 mm, a sensitivity analysis can be performed to evaluate the impact of small changes to implant diameter and total porosity on unit dose assay (see Figure 3.5). This analysis showed that a 4% increase in total porosity results in a 5% reduction in label claim, thus highlighting the importance of controlling total porosity as a critical quality attribute during manufacturing (i.e., both surface roughness and internal voids). Furthermore, a decrease of only 10 μm in the implant diameter can result in a 4% reduction in label claim. Clearly, maintaining accurate dimension control and consistent structural characteristics is critical for the manufacture of dexamethasone intravitreal implants.

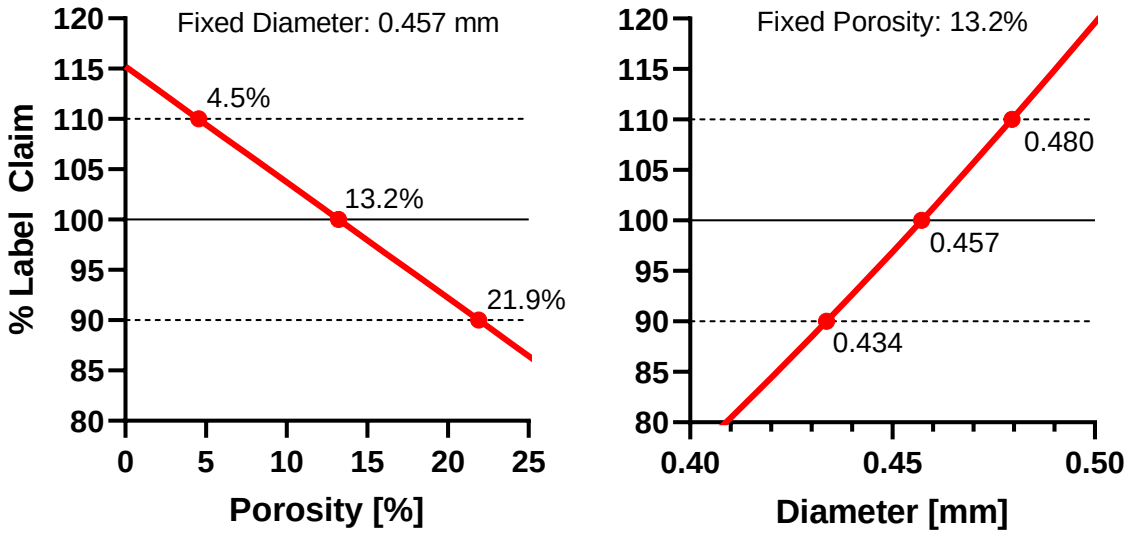

Figure 3.5. Sensitivity analysis of changes to porosity (A) and implant diameter (B) on % label claim for implants 6 mm in length. All values are calculated. Points show the values corresponding to 100% label claim and ± 10% label claim.

3.3.5. Production of a structurally equivalent implant

To produce dexamethasone intravitreal implants that are structurally equivalent to Ozurdex, all aspects of the implant need to be considered, including internal porosity, surface features, extent of mixing, and dimension control. A two-stage extrusion process was developed to prepare such implants.

First, all formulation components were jet-milled before blending. Dexamethasone was jet-milled to a $D_v(50)$ of 2.0 μm. Jet-milling of the PLGA served primarily to break apart large agglomerates (>0.5 mm) and granules to promote uniform powder mixing in the pre-extrusion blend. The dexamethasone and two PLGAs were mixed in the proportions listed in Table 3.1. Blending was performed by (1) manual shaking in a closed container for 2 min, (2) screening through a 16-mesh screen, and (3) an additional 3 min of manual shaking to produce the pre-extrusion blend. This blend was fed into a Haake MiniLab extruder fitted with a 1 mm diameter die to produce rods of extrudate for additional processing. The rods produced in this first extrusion were subsequently milled through a 20-mesh screen to produce free-flowing granules.

The primary goal of the first extrusion and milling process was to increase the density of the pre-extrusion blend into a free-flowing material that could be fed consistently during the second extrusion and shaping process. The low bulk density and cohesive nature of the pre-extrusion blend made it prohibitively difficult to maintain a steady feed rate into the extruder, which complicated implant dimension control during the shaping process. Additionally, the first extrusion allowed for further mixing of dexamethasone and PLGA, which improved dosage uniformity.

The second extrusion and shaping process is outlined in Figure 3.6. Briefly, steady feeding of the milled granules at 8–10 g/h was achieved using a twin-screw volumetric feeder in tandem with a single-screw stuffer feeder. The volumetric feeder

served to set the line rate, while the single-screw stuffer feeder served to buffer any flow variations and drove the material into the extruder barrel. A round reducing die (0.48 mm diameter) was fitted to the extruder discharge port to bring the melt diameter close to the target diameter of 0.457 mm (0.0180 in.).[47] The speed of a dual-wheel puller was adjusted to draw down (i.e., stretch) the molten extrudate to the target diameter. A faster puller speed resulted in a smaller diameter. An in-line laser micrometer measured the implant diameter in real time to enable appropriate adjustments of the puller speed. Finally, when the target diameter has been achieved and the extrudate rod has cooled sufficiently, the continuous rod was manually fractured into approximately 5–10 cm segments that could be later cut to 6 mm lengths with a razor blade to match the dimensions of Ozurdex.

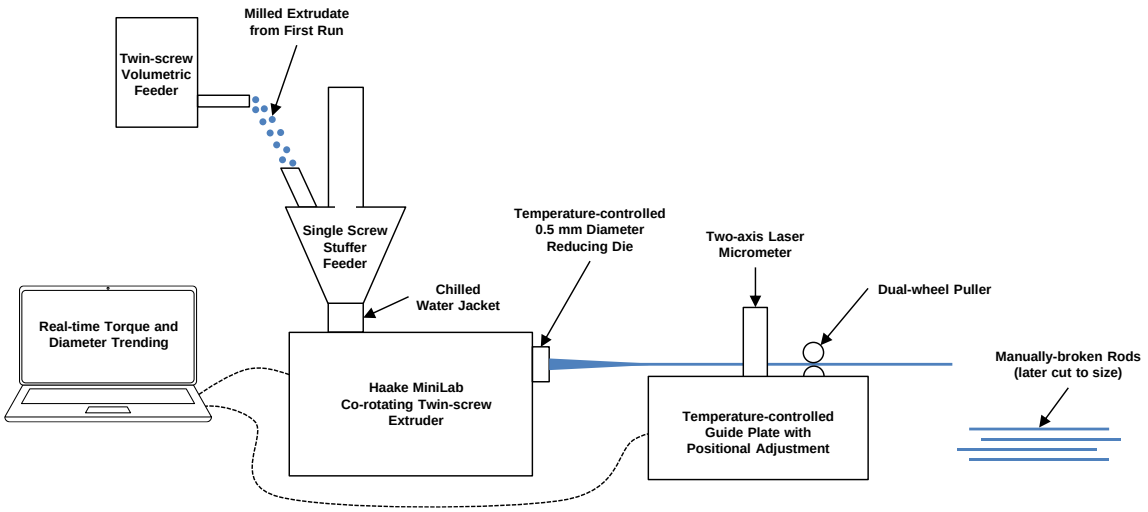

Figure 3.6. Illustration of the second extrusion and shaping process used to prepare dexamethasone intravitreal implants.

As previously discussed, precise diameter control was critical to produce implants with a consistent dose. The dual feeding setup provided a consistent flow of material into the extruder, which translated to a stable flow out of the extruder when operating at steady state. Under these conditions, minimal adjustments to the speed of the dual-wheel puller were required to maintain precise diameter control during the draw down process. The high solids content (i.e., dexamethasone crystals) in the molten extrudate imparted unique viscoelastic properties to the melt stream at the die exit, which severely limited the achievable draw down ratio (see Equation 3.3) to values less than approximately 1.5 under the processing conditions evaluated. This finding suggested that die design is also an important factor to consider in the manufacture of dexamethasone intravitreal implants.

Equation 3.3.

$$Draw\ Down\ Ratio\ (DDR) = \frac{Extruder\ Die\ Inside\ Diameter\ (mm)}{Implant\ Outside\ Diameter\ (mm)}$$

Internal porosity appeared to arise from the entrapment of air in the feeding zone and also from a combination of equipment and process parameters. Notably, the Haake MiniLab extruder did not have a vent port, which is common to many melt extruders. A vent port is used to release liberated gasses and trapped air during processing. The lack of venting, in combination with the melt seal formed in the feeding zone of the single-screw stuffer feeder, may have contributed to air entrapment and the formation of internal pores. The slow feed rate of 8–10 g/h resulted in a long residence time in the extruder barrel, promoting intimate mixing between dexamethasone and PLGA to create a uniformly dispersed two-phase system, as seen in Ozurdex. The surface roughness of the implant was not studied extensively in this work. However, it is thought that the slow feed rate, in combination with die design parameters (e.g., land length, surface

roughness), contributed to reduce melt fracture and produce implants with consistent surface characteristics.[79]

3.3.6. Characterization of the reverse-engineered implant

Figure 3.7 shows SEM images of the dexamethasone intravitreal implants prepared using the method described above. These implants exhibited structural characteristics remarkably similar to Ozurdex, including (a) an irregular surface with few free crystals of dexamethasone, (b) a consistent diameter, and (c) a cross-section that shows substantial internal porosity due to a large number of small pores. The distribution of internal voids also followed a pattern similar to Ozurdex, with a higher concentration of voids near the implant surface and few pores present near the core. Qualitatively, by eye, the reverse-engineered implant exhibited a somewhat smoother surface when compared to Ozurdex.

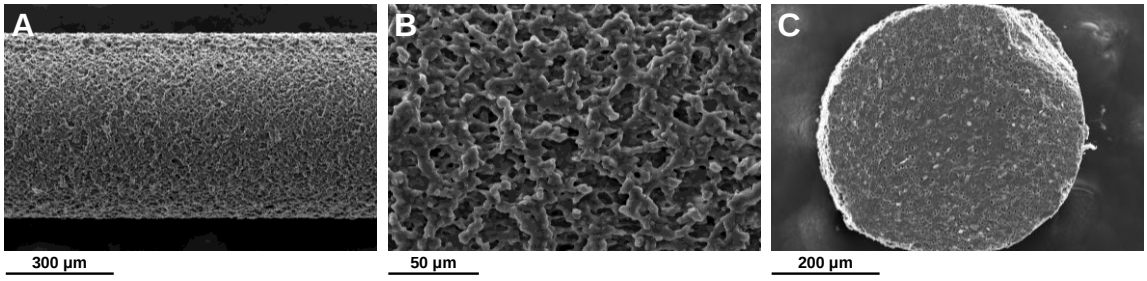

Figure 3.7. SEM images of a reverse-engineered dexamethasone intravitreal implant. Side view at 200× (A), side view at 1000× (B), and cross-section at 300× (C).

Table 3.2 shows the properties of the reverse-engineered implant compared to Ozurdex. No change in the dexamethasone solid form or assay by HPLC was observed

after melt extrusion, which suggested that the drug remained stable during thermal processing at 105 °C. In terms of polymer degradation during thermal processing, the molecular weight of PLGA in the reverse-engineered implant was similar to that of Ozurdex. However, after the two melt-extrusion runs, a 7% drop in PLGA number average molecular weight (Mn) was detected when compared to the pre-extrusion blend (see Figure S3.3).

Property	**Mean ± S.D. (where applicable)**	
	Reverse-Engineered Implant	**Ozurdex**
Dexamethasone Solid Form	Form B	Form B
Dexamethasone Assay	100.1 ± 0.2 % (*n* = 6)	N/A, not performed
PLGA Molecular Weight (M_w)	15,500 ± 300 g/mol (*n* = 3)	16,400 ± 1,300 g/mol (*n* = 2)
Diameter	0.464 ± 0.009 mm (*n* = 1,771)	0.462 ± 0.003 mm (*n* = 2)
Total Porosity	11.3 ± 1.1% (*n* = 5)	11.3 ± 2.7% (*n* = 2)

Table 3.2. Properties of the reverse-engineered dexamethasone intravitreal implant and Ozurdex.

Structurally, the average implant diameter and total porosity of the reverse-engineered implant were close to that of Ozurdex. The mean diameter for the reverse-engineered implant was calculated using real-time laser micrometer data collected each second during the 30 min steady-state collection period of the run. The total implant porosity, 11.3%, was slightly below the expected Ozurdex value of 13.2% but identical to the measured value for two Ozurdex implants.

3.3.7. X-Ray MicroCT analysis and comparison

X-ray microcomputed tomography (microCT) was performed on both Ozurdex and the reverse-engineered implant to obtain a detailed structural comparison and quantification of their internal porosities. MicroCT is a nondestructive, high-resolution method for visualizing internal morphology without sample modification.[80] Raw microCT data was received as a "stack" of several hundred 2- D images with known spacing between each "slice." These stacks were reconstructed into 3-D visualizations of the implants using advanced image processing software (Dragonfly, Object Research Systems (ORS)) (see Figure 3.8). After 3-D reconstruction, the images were digitally segmented to isolate the internal pores from the PLGA–dexamethasone matrix for quantitative analysis.

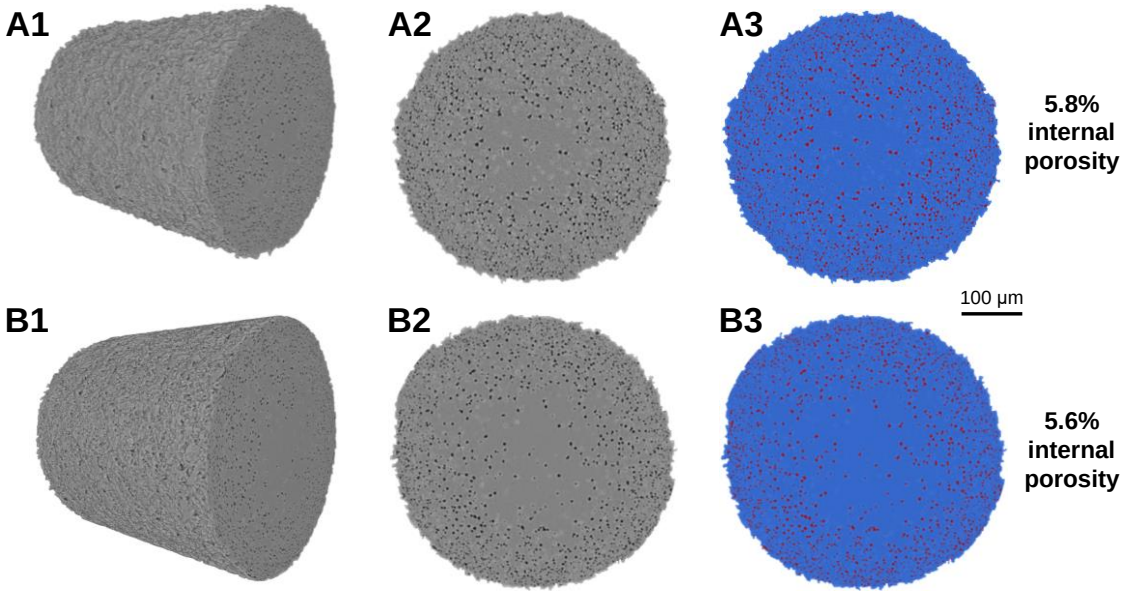

Figure 3.8. MicroCTs of Ozurdex (A1–A3) and the reverse-engineered implant (B1–B3). A1 and B1 show 3-D reconstructions. A2 and B2 show 2-D cross-sections. A3 and B3 show 2-D cross-sections with digital segmentation for the determination of internal porosity. Pores are shown in red, the dexamethasone–PLGA matrix is shown in blue.

After pore segmentation, the internal porosities of each implant were calculated on a volume-by-volume basis. The internal porosities of the two implants were similar: 5.8% (v/v) in Ozurdex and 5.6% (v/v) in the reverse-engineered implant. The internal porosities of the implants comprised about half the total porosity of each implant; the remaining porosity derived from surface pores generated by the uneven surface. A detailed analysis of the pore size distribution and radial volume distribution was also performed (see Figure 3.9). Both implants exhibited a mean pore diameter of approximately 3 μm, with a near-normal distribution. However, as shown in Figure 3.9B, the pores in the reverse-engineered implant tended to skew closer to the implant surface than the pores in Ozurdex.

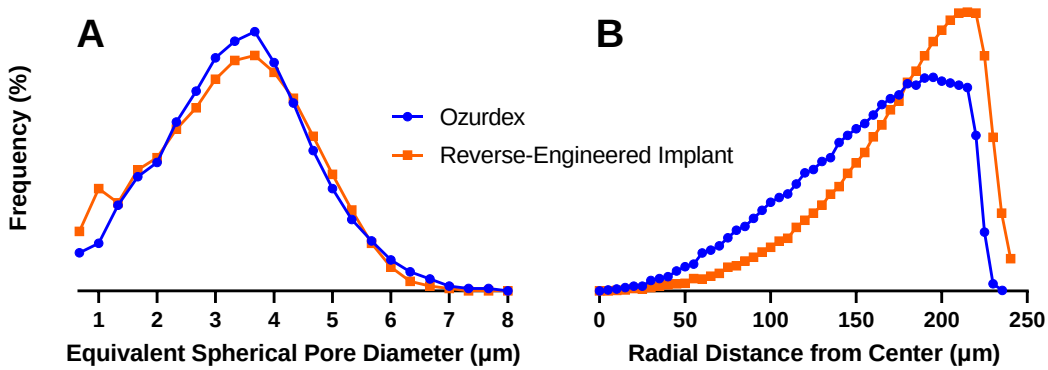

Figure 3.9. Internal pore size distribution (A) and radial pore volume distribution (B) calculated using microCT images after digital segmentation.

Most interestingly, the 3-D reconstructions reveal that the internal pores were isolated from one another and did not form a percolating network. The average distance from the edge of a given pore to the edge of its closest neighboring pore was calculated to be about 1.7 μm for both Ozurdex and the reverse-engineered implant (n = 180,219 and n

= 189,675, respectively). The discrete nature of these pores inhibits direct access of the bulk medium to the core of the implant at early timepoints during in vitro release testing, which may impact drug release.

3.3.8. In vitro release testing

The reverse-engineered implant and Ozurdex were remarkably similar based on the detailed compositional and structural analysis of the implants performed in this study. To confirm the successful reverse-engineering of the Ozurdex implant, in vitro release testing was performed using a method similar to the one published by the manufacturer that was applied to evaluate the impact of changes to the drug product.[38] The use of normal saline (0.9% (w/v) NaCl in water) as the dissolution medium instead of the commonly applied phosphate-buffered saline (PBS, pH 7.4) likely serves to accelerate the dissolution process to a more reasonable timeframe. PLGA hydrolysis is known to be autocatalytic.[15, 81] That is, the ends of the free carboxylic acid chains (liberated from a PLGA chain fracture due to hydrolysis) serve to reduce local pH, which can catalyze and further accelerate the hydrolysis reactions. When in vitro release testing is performed in unbuffered normal saline, the bulk medium likely experiences a significant decrease in pH as PLGA hydrolysis progresses. This pH shift contributes to an accelerated release rate compared to PBS, which is a buffered system (pH 7.4) in which free acids are likely neutralized and thus the bulk medium pH remains stable.[82].

The reverse-engineered implant exhibited a triphasic release profile nearly identical to the published data for Ozurdex (see Figure 3.10). The largest difference in drug release between the two datasets in the first 28 d of release was 3%, which occurred on Day 7. The discrepancy that appears on Day 35 in the reference data was notable, as a

negative slope is observed in the release profile between Day 28 and Day 35, which implied drug loss from the medium between the two timepoints.

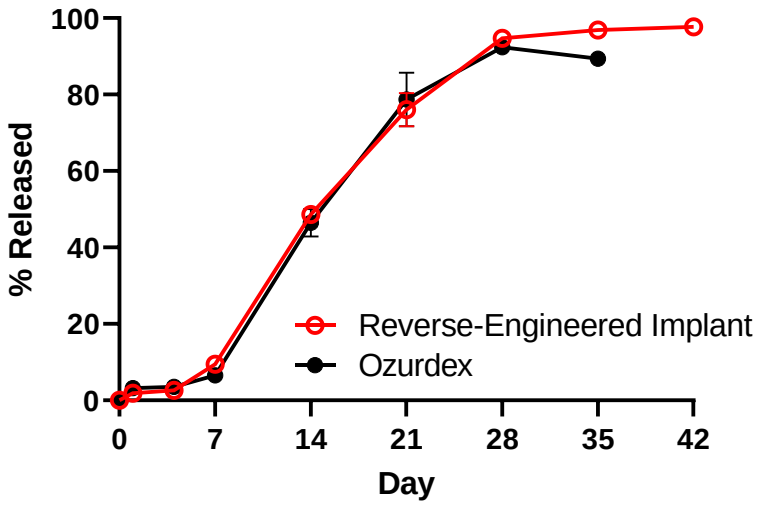

Figure 3.10. Overlay of the in vitro release profiles of the reverse-engineered implant and Ozurdex (republished from [38] with permission). Reverse-engineered implant in vitro release testing conditions: 30 mL normal saline, 37 °C, 100 rpm shaker, n = 6.

This discrepancy in the final two timepoints of the reference data may be attributed to degradation of the dexamethasone in solution, which is known to occur after release from dexamethasone–PLGA formulations.[83, 84] The in vitro release testing method published by the manufacturer does not comment on how (or whether) this degradation was considered in their analysis of Ozurdex. In the current experiment, the solid implant fragment remaining after the final timepoint (Day 42) was dissolved in HPLC mobile phase and assayed to determine the total remaining drug. The percentage of dexamethasone released on Day 42 was calculated by dividing the assay of the Day 42 implant fragment by the theoretical drug content based on the initial mass of the implant

on Day 0. The in vitro release profile was then normalized to this value to account for dexamethasone degradation in the medium.

3.4. CONCLUSIONS

The Ozurdex dexamethasone intravitreal implant was thoroughly characterized using a variety of analytical techniques to support the reverse engineering of the implant. Based on the literature and experimentation, the composition of Ozurdex was inferred to be 60% dexamethasone (micronized, Form B), 30% 50:50 acid terminated PLGA (Resomer RG 502 H), and 10% 50:50 ester terminated PLGA (Resomer RG 502).

Probing the interaction between dexamethasone and PLGA revealed that the implant consists of a two-phase system of dexamethasone crystals uniformly mixed into a PLGA matrix with limited interaction between the drug and the polymer. A compositionally and structurally equivalent implant was manufactured using a two-stage hot-melt extrusion and shaping process. The nature of the implant demanded accurate control of key structural characteristics to maintain dose uniformity. These characteristics included diameter, surface roughness, and internal porosity.

The compositional and structural similarities of the reverse-engineered implant and Ozurdex translated to an equivalent in vitro release profile using the accelerated normal saline method developed by the inventors of Ozurdex. In future work, this reverse-engineered implant will be used to explore the mechanisms of controlled drug release from dexamethasone intravitreal implants. The insights gathered in this study may be useful in supporting the development and approval of future generic formulations of PLGA–based drug products.

ACKNOWLEDGEMENTS

This work was supported by the Broad Agency Announcement (BAA) Contract # 75F40120C00198 from the U.S. Food and Drug Administration (FDA). The content reflects the views of the authors and should not be construed to represent the views or policies of the U.S. FDA. The authors would like to thank Jessie Maisano and Dave Edey of the University of Texas High-Resolution X-ray CT Facility (NSF EAR-1762458) for their assistance in acquiring, post-processing, and interpreting microCT images. The authors would also like to thank Andrew Clark and Shawn Zhang of DigiM Inc. for their helpful advice and valuable insight related to microCT image segmentation.

Chapter 4. Drug release mechanisms of high-drug-load, melt-extruded dexamethasone intravitreal implants[*]

ABSTRACT

Ozurdex is an FDA–approved sustained-release, biodegradable implant formulated to deliver the corticosteroid dexamethasone to the posterior segment of the eye for up to 6 months. Hot-melt extrusion is used to prepare the 0.46 mm × 6 mm, rod-shaped implant by embedding the drug in a matrix of poly(lactic-*co*-glycolic acid) (PLGA) in a 60:40 drug:polymer ratio by weight. In our previous work, the Ozurdex implant was carefully studied and reverse engineered to produce a compositionally and structurally equivalent implant for further analysis. In this work, the reverse-engineered implant was thoroughly characterized throughout the in vitro dissolution process to elucidate the mechanisms of controlled drug release. The implant exhibited a triphasic release profile in 37 °C normal saline with a small burst release (1–2 %), a one-week lag phase with limited release (less than 10 %), and a final phase where the remainder of the dose was released over 3–4 weeks. The limited intermolecular interaction between dexamethasone and PLGA rendered the breakdown of the polymer the dominating mechanism of controlled release. A close relationship between drug release and total implant mass loss was observed. Unique chemical and structural differences were seen between the core of the implant and the implant surface driven by diffusional limitations, autocatalytic hydrolysis, and osmotic effects.

[*] Published in: Costello MA, Liu J, Chen B, Wang Y, Qin B, Xu X, et al. Drug release mechanisms of high-drug-load, melt-extruded dexamethasone intravitreal implants. Eur J Pharm Biopharm. 2023. Mark A. Costello wrote the manuscript and designed, executed, and interpreted the experiments.

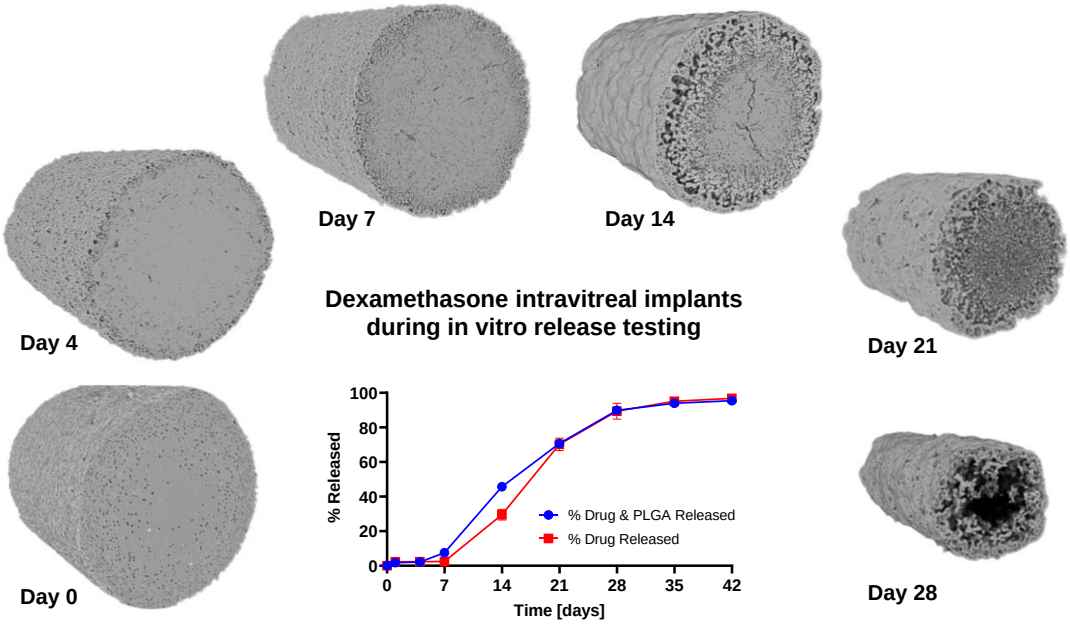

Illustration 4.1. Graphical abstract for Chapter 4.

4.1. INTRODUCTION

Ozurdex (dexamethasone intravitreal implant) is a long-acting, ophthalmic implant approved by the FDA for the treatment of non-infectious uveitis, macular edema following branch and central retinal vein occlusion, and diabetic macular edema.[4, 56] Dexamethasone is a synthetic corticosteroid that stabilizes the blood-retinal barrier and reduces the vascular leakage that leads to vision loss associated with the aforementioned conditions.[57, 85] To overcome the short half-life of dexamethasone (~5.5 h)[86], sustained-release is achieved in Ozurdex by embedding the dexamethasone in a biodegradable poly(lactic-co-glycolic acid) (PLGA) matrix using a continuous hot-melt extrusion process.[24, 47] The melt extrusion process produces rod-shaped filaments that are cut to the desired length to prepare unit doses of Ozurdex. The implant releases drug to the posterior segment of the eye over the course of 3–6 months after it is administered using a proprietary injector.[49, 59]

According to the FDA's Orange Book, the patent exclusivity associated with Ozurdex is slated to expire in 2023, rendering an opportunity for generic competition with the reference listed drug (RLD).[27] Generic medicines have been linked to lower drug prices, resulting in consumer savings and improved access to care. In 2019 alone, newly-approved generic drugs saved American consumers $25 billion in the 12 months following their approval.[11]

To date, the FDA has approved more than 20 PLGA–based branded drugs, with the first occurring more than 30 years ago.[1] However, at the time of this writing, no generic PLGA–based products are available for sale in the United States. This lack of generic products can be attributed to multiple factors, including challenges demonstrating bioequivalence, both in vivo and in vitro, and an incomplete understanding of how formulation and manufacturing parameters affect drug release.

The mechanisms of controlled drug release from PLGA–based dosage forms are known to be complex and have garnered significant study in recent years.[60] A number of physicochemical processes and characteristics have been identified as playing an important role in the drug process, including hydrolytic degradation of the polymer[87], water uptake[88], osmotic effects[89], pH gradients within the dosage form[90], drug-polymer interactions[91] (or lack thereof)[71], drug solubility[92], internal pore closure[77], system swelling[93], and erosion of the dosage form.[94] The relative importance of these phenomena to drug release may change throughout the duration of the sustained release period; ultimately, a unique combination of these factors dictates drug release from each unique PLGA–based formulation.

The primary goal of this work was to develop a mechanistic understanding of the factors driving drug release in Ozurdex by exploring the chemical and physical changes to the implant throughout the in vitro dissolution process. In our previous work, the

Ozurdex implant was studied in detail using a range of analytical techniques and reverse engineered to produce a compositionally and structurally equivalent implant.[8] This reverse-engineered implant was used as the model system for Ozurdex throughout this study.

Compositionally, the implants contained 60 % (w/w) micronized dexamethasone and a mixture of acid terminated and ester terminated 50:50 PLGA. Structurally, the reverse-engineered implant was shown to exhibit internal and external characteristics closely matching those of Ozurdex. Microscopy and microcomputed tomography (microCT) showed that both implants existed as a uniform dispersion of dexamethasone particles embedded in a PLGA matrix with 6 % internal porosity from many discrete voids approximately 3 μm in diameter. In vitro release testing of the reverse-engineered implant showed a nearly identical release profile to published data from the original inventors of Ozurdex (Allergan, Inc.; Irvine, CA, USA) when using a similar method.[38]

Ozurdex has several unique attributes that were expected to play an important role in its mechanisms of drug release. Firstly, Ozurdex is a relatively large (0.46 mm diameter × 6 mm long) solid implant.[38] The low surface-area-to-volume ratio and long diffusion length from the core of the implant to the bulk medium suggests a significant pH gradient could develop in the radial direction as trapped acidic byproducts of polymer hydrolysis are unable to diffuse out.[95] In this situation, autocatalytic degradation of the PLGA would dominate in the implant core and result in "bulk erosion" or "inside-out degradation" of the dosage form.[96]

Secondly, there is limited intermolecular interaction between the dexamethasone and PLGA, hindering the ability of drug to plasticize and diffuse through the polymer matrix.[8, 71] This lack of interaction results in a two-phase system of dexamethasone crystals uniformly embedded in a matrix of PLGA without any dissolution of drug into

the polymer after melt extrusion at elevated temperatures (105 °C). Significant drug–PLGA interactions that enable dissolution of drug into polymer have been observed with other compounds, which resulted in variable impacts to drug release.[67, 97, 98] The lack of interaction between dexamethasone and PLGA may diminish the impact of drug diffusion through the polymer matrix during dissolution and serve to simplify the mass transfer phenomena to erosion and bulk diffusion mechanisms.

Lastly, the exceptionally high drug loading of the formulation (60 % w/w) means that the implant is comprised of more crystalline drug particles than amorphous PLGA. The vast majority of PLGA solid implants studied in the literature have drug loadings less than 35 % (w/w).[30-32, 39, 99-101] The high drug content in the implant suggests water uptake and swelling behavior may be significantly different from previously described dexamethasone–PLGA solid implants prepared at lower drug loads.[35, 102]

4.2. MATERIALS AND METHODS

4.2.1. Materials

Ozurdex (dexamethasone intravitreal implant) (Allergan USA, Inc; Madison, NJ, USA) was purchased from a pharmacy supplier. Two grades of 50:50 poly(D,L-lactide-co-glycolide) (PLGA) were purchased from the Evonik Corporation (Darmstadt, Germany): Resomer RG 502 (ester terminated) and Resomer RG 502H (acid terminated). Dexamethasone was purchased from Shenzhen Nexconn Pharmatechs Ltd. (Shenzhen, China). HPLC–grade acetonitrile, HPLC–grade acetone, ACS–grade sodium chloride, and 10x phosphate buffered saline (PBS) solution were purchased from Thermo Fisher Scientific (Waltham, MA, USA). Distilled, deionized water was obtained in the laboratory.

4.2.2. Methods

4.2.2.1 Manufacture of dexamethasone intravitreal implants

The reverse-engineered dexamethasone intravitreal implants used in this study were prepared using the double melt extrusion and shaping process described in detail in our previous work.[8] The implant composition is presented in Table 4.1. The dual extrusion technique was necessary to accurately control the implant diameter during manufacture.

Material	**Mass per implant (mg)**	**% w/w**
Dexamethasone (Form B, micronized)	0.700	60%
Resomer RG 502 H (50:50 PLGA, acid terminated, inherent viscosity 0.2 dL/g)	0.350	30%
Resomer RG 502 (50:50 PLGA, ester terminated, inherent viscosity 0.2 dL/g)	0.117	10%
Total	1.167	100%

Table 4.1. Composition of the reverse-engineered dexamethasone intravitreal implants used in this study.

Briefly, both extrusions were performed using a Haake MiniLab twin-screw extruder (Thermo Electron (Karlsruhe) GmbH; Karlsruhe, Germany). For the first extrusion, a blend of dexamethasone and PLGA was extruded at 105 °C and shaped into rods approximately 1 mm in diameter. Before the second extrusion, these rods were milled to produce free-flowing granules that enabled consistent feeding during the second extrusion. For the second extrusion, a dual-feeder setup was used to precisely control the feed rate of the milled extrudate into the extruder (set to 105 °C) fitted with a 0.5 mm round die at the discharge port. A downstream puller (IMSTec USA, Inc.; Temecula, CA,

USA) was used to draw down the melt to the target diameter of 457 μm (0.0180 in).[47] Implant rods of variable length were collected and allowed to cool down to room temperature, after which they were manually cut to the desired length using a razor blade to produce individual implants. Table 4.2 compares the properties of the reverse-engineered implant and Ozurdex.

Property	**Mean ± S.D. (where applicable)**	
	Reverse-Engineered Implant	**Ozurdex**
Dexamethasone Solid Form	Form B	Form B
Dexamethasone Assay	100.1 ± 0.2 % (*n* = 6)	N/A, not performed
PLGA Molecular Weight (M_w)	15,500 ± 300 g/mol (*n* = 3)	16,400 ± 1,300 g/mol (*n* = 2)
Diameter	0.464 ± 0.009 mm (*n* = 1,771)	0.462 ± 0.003 mm (*n* = 2)
Total Porosity	11.3 ± 1.1% (*n* = 5)	11.3 ± 2.7% (*n* = 2)

Table 4.2. Properties of the reverse-engineered implant and Ozurdex (republished from [8] with permission).

4.2.2.2 In vitro dissolution

In vitro dissolution studies were conducted in 30 mL normal saline (0.9 % NaCl (w/v)) or phosphate-buffered saline (PBS, pH 7.4) at 37 °C and 100 rpm using a New Brunswick Innova 40 incubator/shaker (Eppendorf; Hamburg, Germany). Sink conditions greater than 3-fold were maintained throughout the study as dexamethasone is a non-ionizable molecule with a reported aqueous solubility of ~90 μg/mL at 37 °C.[35, 58] For in vitro dissolution in normal saline, sampling occurred on Days 1, 4, 7, 14, 21, 28, 35, and 42. For in vitro dissolution in PBS, sampling occurred on Days 1, 4, 7, 14, 21, 28, 42, 56, 70, 84, and 98. Two sampling methods were applied during in vitro release testing in this

study. In one method (media sampling), 25 mL of the medium was removed for assay at each timepoint and immediately replaced with 25 mL of fresh medium. Release data were normalized to the assay of the remaining implant fragment at the final timepoint: Day 42 for normal saline samples and Day 98 for PBS samples. In a second method (whole implant sampling), implants for all timepoints were staged on Day 0 and an implant was completely consumed at each timepoint for assay of the solids with no sampling or replacement of the medium. The two methods are discussed in detail in Section 4.3. Medium pH was measured prior to sampling using a calibrated pH meter (Denver Instrument Company; Arvada, CO, USA).

4.2.2.3 High-performance liquid chromatography (HPLC) assay

Dexamethasone assay of the dissolution media as well as the implant drug content was performed using a Waters HPLC equipped with a 2996 photodiode array (PDA) detector and integrated 717plus autosampler (Waters Corporation; Milford, MA, USA). The mobile phase consisted of a 60:40 acetonitrile:water (v/v) mixture. HPLC parameters consisted of a flow rate of 1 mL/min, a Luna 5 μm C18(2) 100 Å column (150 mm × 4.6 mm) (Phenomenex; Torrance, CA, USA), and a detection wavelength of 241 nm. Duplicate injections were used for all samples. Dexamethasone had a retention time of approximately 2.4 min.

Dissolution media samples were filtered through 0.45 μm PTFE filters before a 50 μL injection into the HPLC. Solid implant samples were dissolved in 10 mL of mobile phase using 2 min of sonication to aid dissolution and filtered using a 0.45 μm PTFE syringe filter before a 50 μL injection in to the HPLC. Duplicate 3-point calibration curves were generated from 0.1 to 10 μg/mL ($R^2 \geq 0.9999$) for both sample types.

4.2.2.4 Mass loss, water content and lyophilization

Implant mass loss and water content were evaluated throughout the in vitro dissolution process by measuring the implant mass before and after lyophilization using a microbalance with a precision of 0.001 mg (MSA3.6P0TRDM, Sartorius; Göttingen, Germany). Implants were completely consumed at each timepoint for this analysis. To determine an implant's wet mass, each implant was carefully recovered from the dissolution medium and gently patted dry with a Kimwipe (Kimberly-Clark Professional; Roswell, GA, USA) prior to measuring the mass with the microbalance. After recording the wet mass, all samples were transferred to a –20 °C freezer for holding until the final dissolution timepoint, at which all implants were lyophilized together. Lyophilization was performed using a VirTis AdVantage EL-85 Freeze Dryer (SP; Warminster, PA, USA) with the following three-step method: (1) 1200 min hold at –40 °C under 100 mTorr vacuum, (2) 1200 min ramp from –40 °C to 25 °C under 100 mTorr vacuum, and (3) 1200 min hold at 25 °C under 100 mTorr vacuum.

After lyophilization, the dry mass of each implant was measured using the microbalance. The total mass loss and moisture pickup were calculated using Equation 4.1 and Equation 4.2, respectively.

Equation 4.1.

$$\%\ Total\ Mass\ Loss\ (t) = \frac{Initial\ Mass\ -\ Dry\ Mass\ (t)}{Initial\ Mass} \times 100\%$$

Equation 4.2.

$$\%\ Moisture\ Pickup\ (t) = \frac{Wet\ Mass\ (t)\ -\ Dry\ Mass(t)}{Dry\ Mass(t)} \times 100\%$$

4.2.2.5 Gel permeation chromatography (GPC)

GPC was used to determine the molecular weight of the PLGA in the implants throughout the in vitro dissolution process. The molecular weight and polydispersity index (PDI) were determined using a Waters GPC system equipped with a 2414 refractive index (RI) detector and an integrated 2707 autosampler (Waters Corporation; Milford, MA, USA). The mobile phase (100 % acetone) was pumped at a flow rate of 0.6 mL/ min through two TSKgel GMHHR-L columns (Tosoh Corporation; Tokyo, Japan) connected in series. Nine poly(methyl methacrylate) (PMMA) standards (500–200,000 Da) (Agilent Technologies; Santa Clara, CA, USA) were used to generate a calibration curve. All samples and standards were prepared in acetone and injected with a volume of 50 μL. Dissolution samples from Days 0–28 were evaluated in triplicate. For Day 35 and Day 42 samples, n = 3 replicates were combined into a single sample to provide sufficient mass for GPC analysis.

4.2.2.6 Thermal analysis

A Q20 DSC (TA Instruments; New Castle, DE, USA) was used to evaluate both the wet and dry glass transition temperatures (T_g) of the PLGA in the implants throughout the in vitro dissolution process. Wet implant samples (n = 4) were patted dry of excess moisture, combined, and immediately sealed in a Tzero hermetic pan. To evaluate the wet T_g, the wet implant samples were first equilibrated to –30 °C and then subjected to modulated heating conditions: ±1 °C every 45 s with a ramp rate of 4 °C/min to 75 °C. After completion of the first heating cycle, the lid of the hermetic pan was manually punctured, and the sample was heated to 110 °C and held isothermally for 5 min to remove bound moisture. To evaluate the dry T_g, the sample was then re-equilibrated to –30 °C before undergoing a second heating cycle using the same modulated conditions

listed above. The reversible heat flow signal was used to determine T_g for all samples tested.

4.2.2.7 Scanning Electron Microscopy

Scanning electron microscopy (SEM) was used to evaluate implant structure and morphology throughout the in vitro dissolution process. Lyophilization of the dissolution samples was performed prior to SEM imaging using the parameters detailed in Section 4.2.2.4. Samples were prepared for imaging by attaching them to aluminum stubs using double-sided carbon tape. They were then sputter-coated with gold for 60 s at 40 mA (Electron Microscopy Sciences; Hatfield, PA, USA). Imaging was performed using a Quanta 650 FEG SEM (FEI Company; Hillsboro, OR, USA) with an accelerating voltage of 15 kV.

4.2.2.8 X-ray microcomputed tomography (microCT) and analysis

X-ray microCT was used to characterize the structure and morphology of the implants throughout the in vitro dissolution process. For each dissolution timepoint up to Day 28, X-ray microCT scanning was performed in situ by transferring the implant into a narrow tube filled with the dissolution medium. A ZEISS Xradia 620 Versa (ZEISS Microscopy; Jena, Germany), located at the University of Texas High- Resolution X-ray CT Facility, was used to generate image stacks corresponding to a 0.6 mm × 0.6 mm × 0.6 mm field of view, with a voxel size of 0.6 μm. Dragonfly (Object Research Systems (ORS); Montreal, QC, Canada) was used to perform post-processing, including 3-D reconstruction and digital segmentation of the image stacks.

4.3. RESULTS AND DISCUSSION

4.3.1. In vitro release testing in normal saline

Unbuffered normal saline (0.9 % NaCl (w/v)) was selected over phosphate-buffered saline (PBS, pH 7.4) as the primary in vitro release medium used in this work for several reasons. Notably, the literature shows that Allergan Inc. developed an in vitro release method using normal saline to identify changes in the drug release profile of Ozurdex. An in vitro comparison of fragmented and whole implants showed no difference in release profile in saline, which translated to rabbit eye in vivo.[59] Patent literature for Ozurdex also used saline to demonstrate the impact of changes to the drug release profile when altering the acid:ester ratio of the 50:50 PLGAs used in the formulation.[47]

The patent literature also noted that the drug release profiles in vivo in the vitreous of New Zealand White rabbits and in vitro in 37 °C normal saline were very similar. In both cases, most of the dexamethasone was released in 28 days and a sigmoidal curve shape with an inflection point around Day 17 was observed. The inventors did not claim an in vitro/in vivo correlation (IVIVC) with this method; however, the similarity between the two release profiles is noteworthy from a product development perspective.

Normal saline also accelerated drug release to a more reasonable timeframe compared to PBS (approximately 1 month vs. 3 months) by enabling the autocatalytic nature of PLGA hydrolysis to proceed unrestricted. It is suspected that during the hydrolytic degradation of the ester bonds along the polymer backbone, the ends of the free carboxylic acid chains (formed from a mid-chain breakage) reduced local pH, which catalyzed and further accelerated the hydrolysis reactions.[15] When in vitro release testing

was performed in unbuffered normal saline, both the bulk medium pH and local pH within the implant were expected to decrease as PLGA hydrolysis progressed. On the other hand, in PBS, the free acids were likely neutralized by the buffer, thus maintaining the bulk medium pH at 7.4 and reducing the local pH drop within the implant. As a result, acid-catalyzed hydrolysis and the rate of PLGA degradation were reduced, leading to slower drug release in the buffered system compared to normal saline.[82]

A complicating factor during in vitro release testing of dexamethasone intravitreal implants is the degradation of dexamethasone in the release medium. Dexamethasone is known to degrade into several structurally similar compounds under the conditions used in this study.[83, 84] Quantification of dexamethasone and its degradants is possible using an LC–MS/MS method as described by Matter et al.; however, such an analysis was out of scope for this study. Notably, Matter et al. found a protective effect when dexamethasone was formulated in a PLGA implant, suggesting that dexamethasone remains stable in the solid state prior to release, and that most of the degradation occurs in solution after release into the bulk medium.

Leveraging this assumption, the degradation of dexamethasone can be accounted for by normalizing the release profile to the assay of the remaining implant fragment at the final timepoint. This approach to in vitro release testing, referred to as the “media sampling” method, is advantageous in that the release profile from a single implant can be followed throughout the testing period by sampling the medium at regular intervals. The primary drawback of this method is the application of the correction factor from the final timepoint to the entire release profile, which may not be appropriate for the early timepoints when little drug has been released.

Alternatively, another in vitro dissolution method can be applied to correct for dexamethasone degradation whereby drug content is only measured in the implant solids,

referred to as the "whole implant sampling" method. In this method, one implant is staged for each timepoint on Day 0, and the entire implant is consumed for assay at each timepoint. The advantage of this method is that the degradation of dexamethasone in the release medium is of no concern, and no correction factor is required. However, this method requires multiple implants to generate a single release profile and relies on the critical assumption of low intra-batch variability in the implants.

In this study, both in vitro dissolution methods described above were applied for analysis of the reverse-engineered implants. Importantly, the two methods yielded similar release profiles for the implants tested. The media sampling method was favored because a similar method was applied by the inventors of Ozurdex, and it enabled analysis where samples were limited (i.e., when testing the Ozurdex commercial product; see Figure 4.1). The whole implant sampling method was applied when quantification of drug release at early-to-mid timepoints was crucial for the analysis (see Figure 4.5).

The reverse-engineered implant was not terminally sterilized by gamma irradiation, as in the case of Ozurdex.[103] It is known that PLGA experiences radiolytic degradation during exposure to gamma radiation that results in a reduction in molecular weight as a function of increasing irradiation dose.[104] Such a change in molecular weight could impact the kinetics of drug release in vitro, in which the non-irradiated sample would release drug more slowly.[105] Notably, in the Committee for Medicinal Products for Human Use (CHMP) Assessment Report for Ozurdex, it is stated that the radiation dose selected for terminal sterilization of Ozurdex did not impact drug release rates during product development.[46] Importantly, the molecular weights of the PLGA in the reverse-engineered implant and Ozurdex were very similar, as shown in Table 4.2.

The in vitro drug release profiles of the reverse-engineered implant and the Ozurdex commercial product in normal saline using the media sampling method are

presented in Figure 4.1. The release profile of the reverse-engineered implant closely matched that of Ozurdex. Both implants exhibited a triphasic release profile, consistent with other previously studied PLGA–based formulations.[75, 76] A small burst release (less than 2 %) in the first 24 h constituted the first phase of release. The second phase (i.e., the lag phase) exhibited limited drug release (≤ 10 %) during the first seven days of exposure to the medium. In the final phase, substantial drug release set on and release to completion occurred over 3–4 weeks. By visual observation, the two formulations were indistinguishable at all timepoints during in vitro release testing. In the following sections, observations of the reverse-engineered implant's chemical and physical changes throughout the dissolution process are discussed. The final sections of this work attempt to synthesize the various phenomena observed from the characterization data to accurately describe the release mechanisms of dexamethasone intravitreal implants.

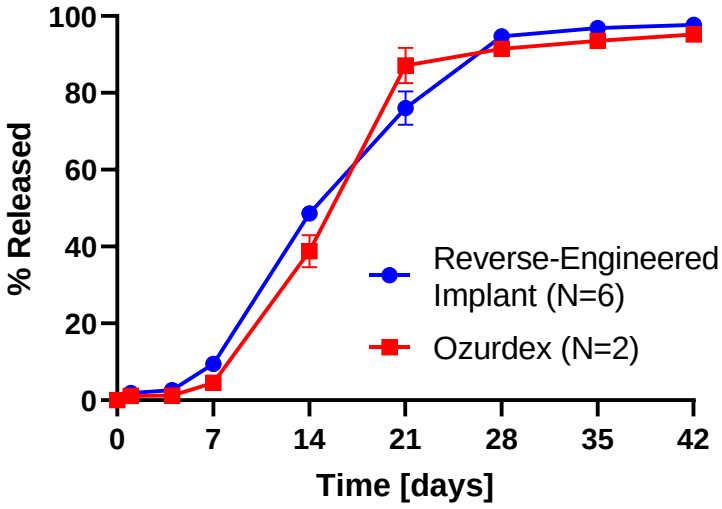

Figure 4.1. In vitro release profile of dexamethasone using the media sampling method from the reverse-engineered implant and the Ozurdex commercial product in 37 °C normal saline (mean ± S.D.).

4.3.2. Chemical changes during in vitro dissolution

Moisture uptake by the dexamethasone intravitreal implants was evaluated throughout the in vitro dissolution process in normal saline (see Figure 4.2). The data showed that the implant began to take up water immediately upon exposure to the release medium and continued to do so in exponential fashion for the first 21 days. After Day 21, the implant water content appeared relatively stable for the remainder of the study. As described in Section 4.2.2.4, when determining the mass of the wet implants, surface moisture was blotted away with a Kimwipe leaving behind moisture trapped in internal pores and dispersed in the polymer matrix. This moisture pickup calculation captured the sum of water in the two phases and did not have the ability to differentiate their distribution. Nonetheless, it is clear that the total implant water content remained dynamic throughout much of the drug release process.

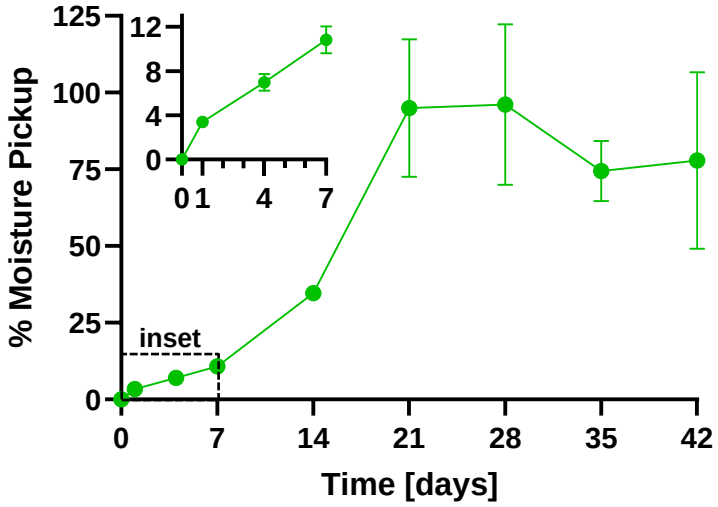

Figure 4.2. Moisture pickup by the reverse-engineered implant during in vitro dissolution in 37 °C normal saline (n = 6, mean ± S.D.).

Mechanistically, once water is taken up by the polymer matrix, hydrolytic degradation of the PLGA can begin. The uptake of significant amounts of water in the first few days of exposure to the medium suggested a drop in PLGA molecular weight would be expected as the hydrolysis began. Indeed, this phenomenon was observed when using gel permeation chromatography to quantify the molecular weight of the PLGA (see Figure 4.3). Despite less than 10 % drug release in the first week, the number average molecular weight (Mn) of PLGA dropped 57 % over the same period. Interestingly, the significant onset of drug release after Day 7 coincided with the system approaching the critical molecular weight, or the point at which the PLGA oligomers become soluble in the release medium.[106] Oligomers with molecular weights below this threshold can dissolve and diffuse out from the implant, initiating mass loss.

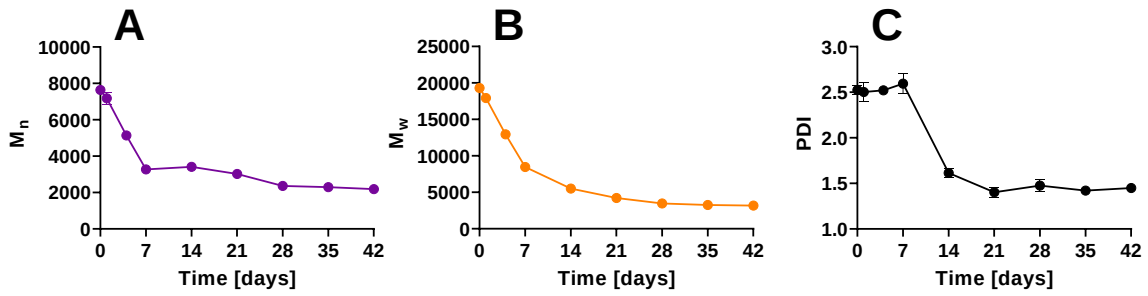

Figure 4.3. GPC number average molecular weight (Mn) (A), weight average molecular weight (Mw) (B), and polydispersity index (PDI) (C) during dissolution in 37 °C normal saline (n = 3, mean ± S.D.). Molecular weights are relative to poly(methyl methacrylate) standards.

The average molecular weight of the PLGA in the implant appeared to remain constant after Day 28. It is important to note that GPC analysis was performed on the implant solids remaining in the dissolution vial and does not consider hydrolytic byproducts like short chain oligomers or monomers of lactate and glycolate below the critical molecular weight that may be solubilized in the dissolution medium. The plateau

in the number average molecular weight plot at the later timepoints suggested oligomers below about 2,300 g/mol had sufficient solubility and/or chain mobility in 37 °C normal saline to dissolve and/or diffuse away from the implant matrix. These findings are consistent with previously reported PLGA degradation studies.[3]

As the PLGA molecular weight continued to drop during the dissolution process, it was expected that the acidic byproducts of hydrolysis would reduce the pH of the dissolution medium. Indeed, the pH of the medium dropped from Day 1 up to Day 21 (see Figure 4.4). After Day 21, a gradual increase in medium pH was observed. This increase in pH was attributed to a slowing rate of PLGA degradation along with the addition of 25 mL of fresh medium used to make up the sampling volume at each timepoint.

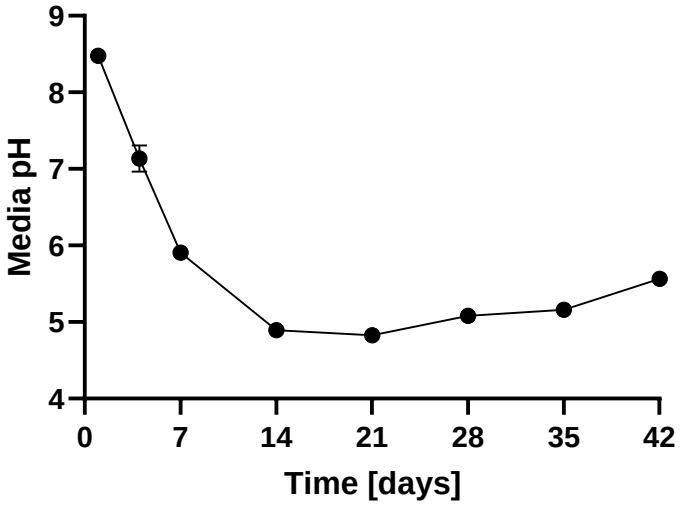

Figure 4.4. Medium pH during dissolution of the reverse-engineered implant in 37 °C normal saline (n = 6, mean ± S.D.).

4.3.3. Physical changes during in vitro dissolution

The total mass loss from the implant was evaluated throughout the in vitro dissolution process (see Figure 4.5). Interestingly, the total mass loss from the implant trended very closely with the total drug released (determined using the whole implant sampling method). Such a trend suggested an erosion-based mechanism driving drug release, where the polymer and drug leave the implant at similar rates.

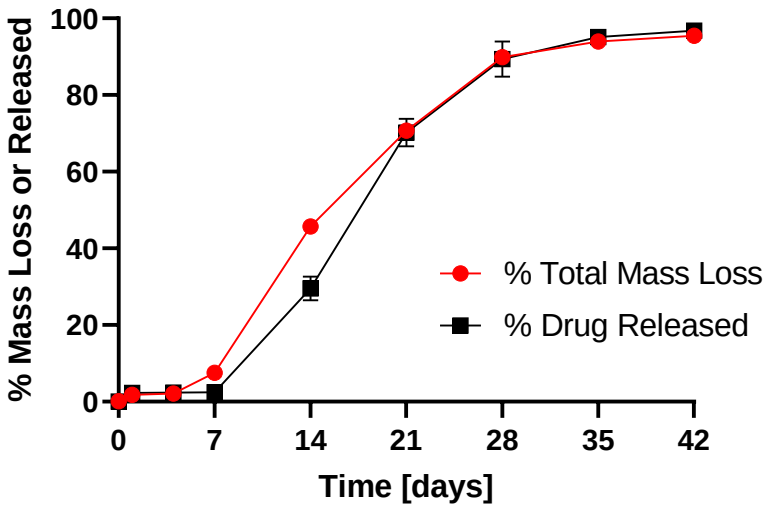

Figure 4.5. Overlay of total mass loss from the implant (n = 6) and drug release using the whole implant sampling method (n = 3) during dissolution of the reverse-engineered implant in 37 °C normal saline (mean ± S.D.).

As previously mentioned, dexamethasone has limited intermolecular interaction with the PLGA in the implant, limiting the ability of dexamethasone to diffuse through the polymeric matrix. Thus, it was hypothesized that PLGA sustains the release of dexamethasone in this formulation primarily by restricting access of substantial amounts of water to the dexamethasone crystals. Dexamethasone can only be released from the implant once the PLGA has sufficiently degraded to enable dissolution of oligomers and

monomers, resulting in exposure of each drug particle to sufficient amounts of water for dissolution.

The higher proportion of total mass lost compared to drug released on Day 7 and Day 14 indicated preferential release of polymer from the implant at these timepoints. Interestingly, this preferential polymer release occurred in tandem with the approach to the critical molecular weight of PLGA and just prior to the onset of significant drug release in the final phase of the triphasic release profile. Taken together, these results further supported the hypothesis that the PLGA must first degrade and leave the implant to expose the embedded dexamethasone to sufficient amounts of water for dissolution.

To better understand the physical changes happening during the dissolution process, SEM images were taken of implants at each timepoint after lyophilization (see Figure 4.6). The Day 0 images (prior to dissolution) showed that the implant exhibited an irregular, rough surface of dexamethasone crystals embedded in the PLGA matrix. By Day 1, no significant structural changes were observed; however, drug particles on the surface were largely absent. Dexamethasone on the immediate surface likely contributed to the initial burst release in the first 24 h. Close inspection of the Day 4 sample revealed numerous small pores formed on the surface of the implant, suggesting erosion of the PLGA matrix had started. By Day 7, the molecular weight of the PLGA had reduced significantly, and the polymer had been sufficiently plasticized by water to smooth over the rough surface features of the implant present from Day 0. After Day 7, when significant drug release had begun, the implant lost its rough surface characteristics entirely while becoming increasingly porous. From Day 14 onwards, the diameter of the implant continued to shrink as the PLGA matrix eroded away and the dexamethasone was released into the medium.

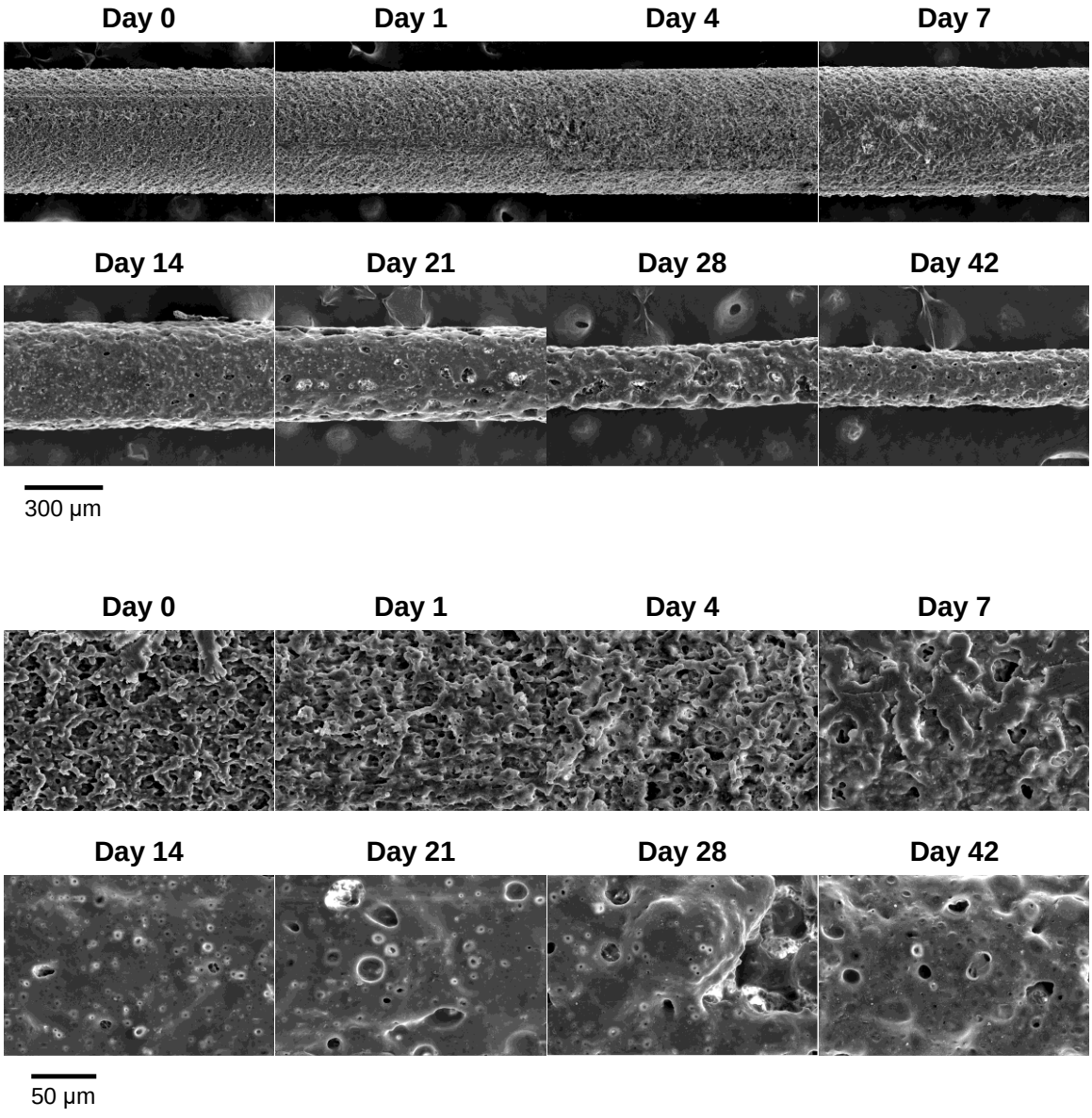

Figure 4.6. SEM images of the reverse-engineered implant during dissolution in 37 °C normal saline after lyophilization. Side view at 200× (top panel) and 1000× (bottom panel).

To characterize how the polymer molecular weight reduction and uptake of water affected the chain mobility of the PLGA in the implant, dissolution samples were removed beginning at 12 h, and each day thereafter, for 14 days and tested on the DSC

under modulated heating conditions to elucidate both the wet and dry T_g of each sample (see Figure 4.7A). In the Day 0 sample, prior to exposure to the dissolution medium, the T_g of PLGA was sensitive to moisture uptake from the ambient storage and handling conditions (approx. 20 °C, 30–70 % RH), which caused sufficient moisture uptake to depress the dry T_g of 43 °C to an apparent wet T_g of 34 °C. Subsequently, within hours of introduction to the dissolution medium, the wet T_g was depressed further to 22 °C while the dry T_g showed a modest decrease of 2 °C to 41 °C.

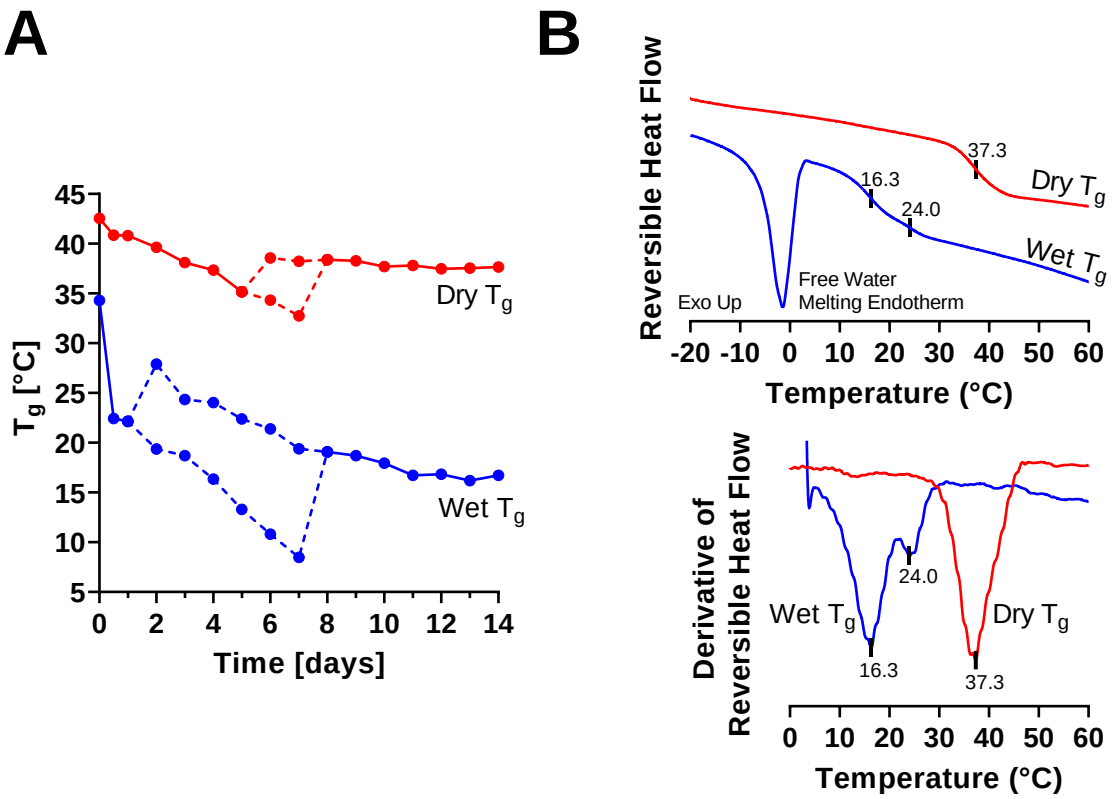

Figure 4.7. Wet and dry T_g of PLGA during the first fourteen days of in vitro dissolution (A). Regions with dashed lines indicate where two distinct T_g were observed in the thermogram. The DSC wet and dry thermograms for the Day 4 sample (B, top) are shown with the derivative of the heat flow signal used to elucidate the dual wet T_g (B, bottom).

Interestingly, the samples from Day 2 through Day 7 exhibited two distinct wet T_g in the DSC thermogram. To illustrate the method for determining these values, Figure 4.7B shows the reversible heat flow signals used to determine the wet and dry T_g for the Day 4 sample. The two wet T_g were not immediately apparent in the plot of reversible heat flow; however, the first derivative of the signal was applied to elucidate two sequential, overlapping transitions. After drying off the moisture at 110 °C to determine the dry T_g, only one glass transition emerged for all samples apart from Day 6 and Day 7, where two distinct dry T_g were detected. It is possible that the dual wet T_g observed in Day 2 to Day 7 samples emerged due to differences in both plasticization with water and differences in PLGA molecular weight between two structurally distinct regions of the implant.[107] For example, the core of the implant may have experienced accelerated PLGA degradation and increased water uptake compared to the implant surface due to trapped hydrolysis byproducts accelerating the autocatalytic degradation locally along with increased osmotic effects.

To explore how physical changes to the implant caused two PLGA T_g to emerge at several timepoints in the first week, SEM was used to evaluate their cross-sections throughout the dissolution process (Figure 4.8, top panel). The lyophilized implants showed physical changes to the implant began to occur from Day 1. The internal pores, clearly visible in the Day 0 sample, began to close near the surface of the implant within the first day. By Day 4, most of the internal pores had closed due to polymer plasticization. By Day 7, all the individual pores present at Day 0 had closed, and new, larger cracks in the matrix began to form, likely due to swelling associated with significant water uptake. An outside, “skin layer” of PLGA was apparent in all samples after Day 7. The thickness of this skin layer may represent the diffusion limit for

hydrolytic byproducts of PLGA, implying that solubilized oligomers and monomers underneath this layer may be trapped near the core of the implant.

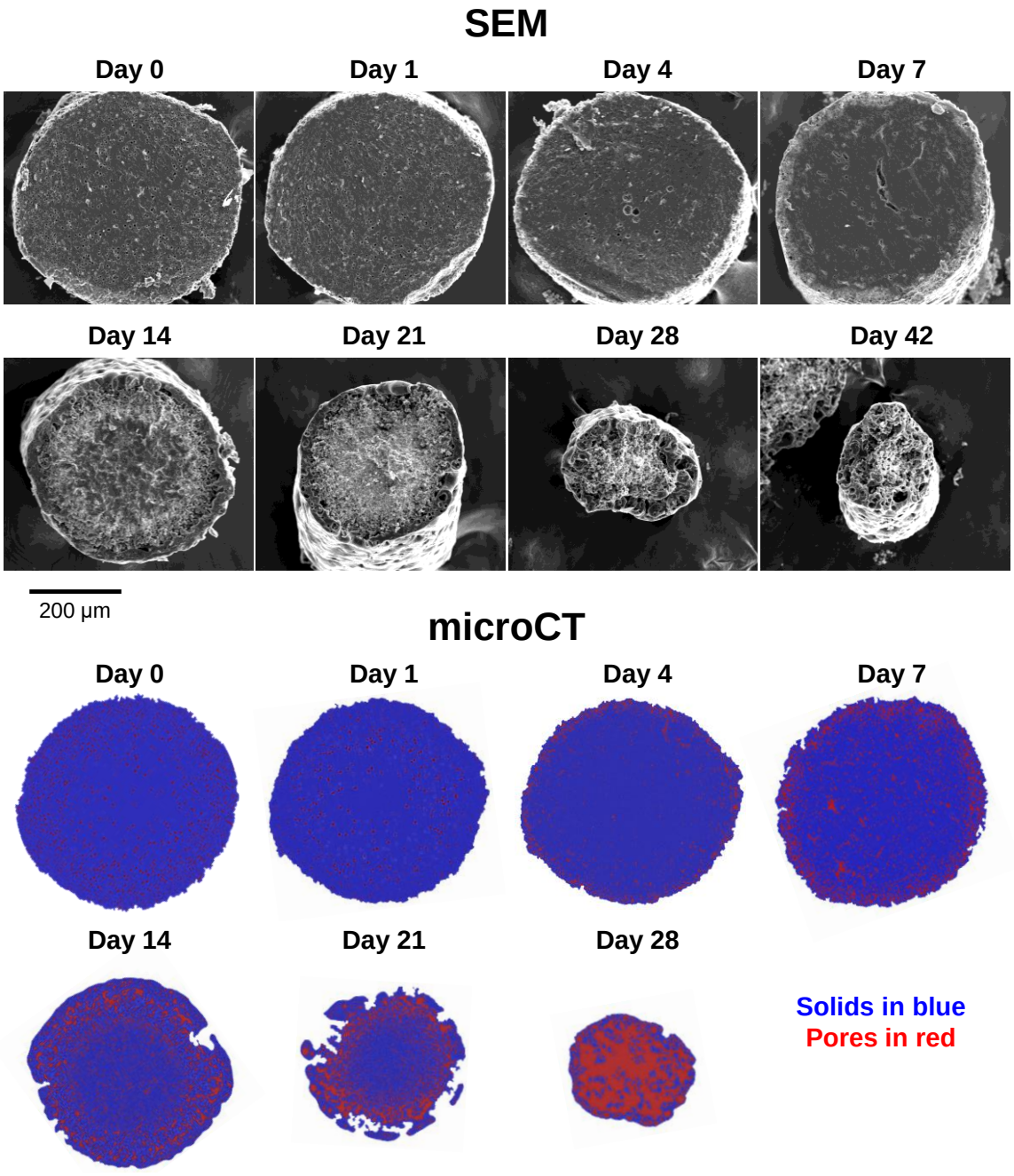

Figure 4.8. Cross-sections of the dexamethasone intravitreal implants throughout the in vitro dissolution process in normal saline, SEM after lyophilization (top panel) and in situ microCT (bottom panel). Digital segmentation was performed on the microCT images to differentiate implant solids from pores. Pores are shown in red, the dexamethasone–PLGA matrix is shown in blue.

Such a phenomenon could cause two distinct glass transitions to develop in the first week of dissolution. The higher T_g represented the outside skin layer where hydrolytic byproducts could more easily diffuse away into the bulk medium, reducing osmotic effects in this region and, thus, reducing the plasticization from additional water. On the other hand, the lower T_g represented the polymer chains in the core of the implant where hydrolytic byproducts of PLGA degradation were trapped. These trapped hydrolysis products reduced the apparent molecular weight and created an osmotic pressure that pulled additional water into the core and further plasticized the matrix. After Day 7, a single wet T_g was observed, suggesting that the matrix became sufficiently swollen and porous such that the trapped oligomers near the core could freely leave the matrix and the osmotic pressure was more evenly distributed throughout the implant. The absence of the lower wet T_g after Day 7 upholds this hypothesis as the new bulk wet T_g of the system then trended with the higher wet T_g, which always had exposure to the dissolution medium.

One drawback of using SEM to evaluate structural characteristics is the requirement to remove all water from the sample prior to imaging. Lyophilization was used in this case, which may have introduced structural artifacts such as shrinkage or collapse of implant features. To overcome this limitation, microCT was used to image the implants in situ in the dissolution medium without any sample modification (Figure 4.8, bottom panel).[80] Imaging the implants in situ enabled visualization of the swelling behavior as it occurred. A second advantage of microCT imaging is the ability to digitally segment the implant solids from internal pores in the implant, which was particularly useful for later timepoints where the implant was shown to carry larger amounts of water.

The in situ microCT images confirmed the findings of the SEM images: (a) closure of the internal pores began from the outside-in in the first 24 h, (b) internal pore

closure was nearly complete by Day 4, and (c) significant cracking and hydration of the PLGA matrix was apparent from Day 7 onwards. By Day 28, the internal structure of the implant was largely absent with only fragments of the skin layer formed in the first week of dissolution remaining, as seen in the SEM images, despite significant shrinkage from lyophilization occurring in the later timepoints.

4.3.4. Release mechanisms of dexamethasone intravitreal implants

To understand the release mechanisms of the dexamethasone intravitreal implants used in this study, the unique structural and physicochemical characteristics of the implant were considered. As previously mentioned, each dexamethasone crystalline particle was coated in PLGA because of the thorough mixing during the melt extrusion process; therefore, much of the drug was inherently restricted to bulk water from the dissolution medium in the initial stages of in vitro dissolution.

During the first day of dissolution testing, a small burst release of about 2 % was observed, driven by drug crystals on the surface of the implant that were lacking complete coverage from the polymer matrix. Although drug release was limited in this stage, water uptake throughout the entire matrix was rapid, reducing the T_g of the PLGA by 21 °C within 12 h. With the uptake of water, hydrolysis began, albeit at a modest rate, resulting in a 6 % drop in Mn in the first 24 h. Internal pores near the surface of the implant started to close as chain mobility increased due to the depressed T_g in combination with the 37 °C dissolution conditions.

Between Day 1 and Day 4, less than 1 % additional drug was released from the implant due to the polymeric coating acting as a barrier between the dexamethasone and the bulk dissolution medium. Further degradation of the polymer was required before it could erode and expose the drug to necessary quantities of water for dissolution. At this

stage, the Mn of the PLGA had reduced by 33 %, and two wet T_g emerged, suggesting the onset of PLGA's characteristic bulk erosion. The lower T_g represented the highly plasticized PLGA chains near the core of the implant. In this region, autocatalytic hydrolysis occurred at an accelerated rate due to diffusional limitations and osmotic effects from the degradation products pulling more water into the core. The higher T_g represented the PLGA near the surface of the implant, where the hydrolytic degradation byproducts readily diffused away, effectively enriching the proportion of larger polymer chains and limiting osmotic effects. By Day 4, the entire matrix was sufficiently plasticized to close all internal voids present at Day 0. Such a finding suggests that implant porosity may not be a critical quality attribute for drug release from dexamethasone intravitreal implants.

From Day 5 to Day 7, drug release had begun to pick up but was still limited to less than 10 %. On Day 7, the disparity between the two wet T_g was at its highest, manifesting in a detectable difference between two dry T_g as well. Since plasticization with water was not relevant in the dry T_g, the observed difference was attributed solely to differences in PLGA molecular weight. A small increase in polydispersity index was also observed on Day 7, highlighting the significant accumulation of low molecular weight PLGA trapped near the core of the implant. At this stage, moisture uptake continued to accelerate, and a 57 % drop in PLGA Mn was observed. The outside skin layer (the area where hydrolytic byproducts can readily diffuse away) had become apparent under both SEM and microCT.

Finally, on Day 8, sufficient water uptake and PLGA degradation had occurred to break down the internal structure of the implant core due to swelling and enabled the release of the trapped hydrolytic byproducts from the implant to begin the final phase of drug release. At this stage, preferential release of the polymer was observed in the total

mass loss data. GPC data showed a dramatic reduction in polydispersity index after Day 7 as trapped oligomers were released into the medium. Likewise, a single wet T_g and a single dry T_g were observed at all subsequent timepoints. SEM images of the implant surface showed newly formed pores in the skin layer, where the hydrolytic degradation byproducts and dissolved drug could diffuse out from the core. From this point on, erosion and diffusion of the implant core contents through the skin layer was the dominant mechanism driving drug release.

From Day 7 to Day 21, two-thirds of the 700 μg total dose was released. Correspondingly, 63 % of the total implant mass was lost, highlighting the erosion-based release behavior of this system, in which the PLGA acted as a barrier between the dissolution medium and the individually trapped crystals of dexamethasone. As seen in the microCT cross-sectional images, the dissolution medium displaced the lost solids in the newly formed internal pores beneath the skin layer, causing an apparent increase in total implant moisture content.

During the final 20 days of in vitro release testing (Day 22 to Day 42), 22 % additional drug was released, leaving just 2 % of the total dose remaining in the implant on Day 42. The rate of drug release in this final stage slowed slightly as the heavily hydrated, porous implant limited any autocatalytic degradation behavior and the remaining PLGA (largely from the remaining skin layer) slowly broke down via hydrolysis. The fact that the skin layer, formed by Day 7, remained near the final timepoints highlighted the importance of autocatalysis and osmotic effects on PLGA hydrolytic degradation. With the inability to leverage these effects, the PLGA in the skin layer degraded slowest despite always having direct contact with the bulk dissolution medium.

4.3.5. In vitro release testing in phosphate buffered saline

In vitro dissolution testing was performed in phosphate buffered saline to validate the proposed release mechanisms of the dexamethasone intravitreal implant (see Figure 4.9). Due to the buffering action of PBS, the autocatalytic degradation of PLGA was expected to be slowed compared to normal saline. The 30 mL of dissolution medium used in this method provided sufficient buffering capacity such that the free acid degradation products of the PLGA could be readily neutralized. This effect was expected to be most apparent during the second (lag) phase of drug release where the majority of the PLGA degradation occurred.

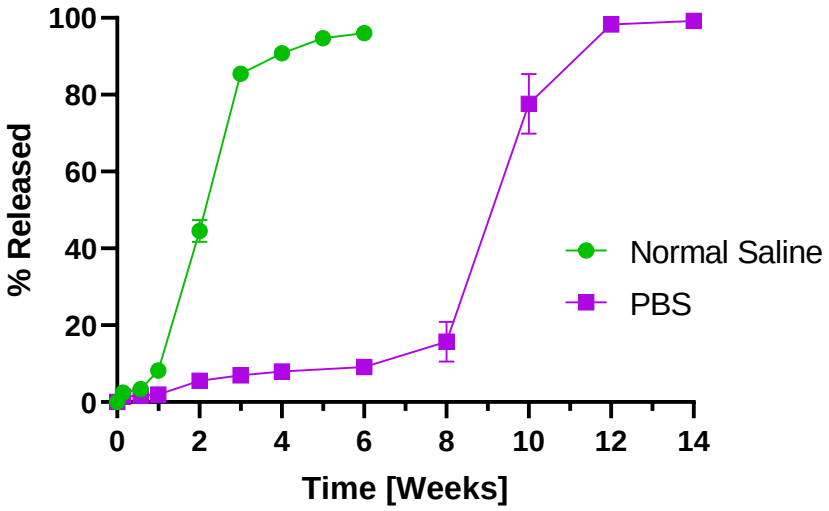

Figure 4.9. Overlay of the in vitro release profile of dexamethasone from the reverse-engineered implant in 37 °C normal saline and PBS using the media sampling method (n = 3, mean ± S.D.).

In the first phase of drug release, a 1–2 % burst release was seen in both PBS and normal saline over 24 h. A similar burst release was expected as solubilization of the exposed dexamethasone crystals on the surface of the implant was not impacted by media pH (i.e., dexamethasone is not ionizable)[47]. In the second phase of release, both

conditions showed a lag phase where drug release was slow as PLGA degradation was actively occurring. As expected, the lag phase in the PBS samples was dramatically extended compared to the normal saline samples. In normal saline, the lag phase lasted about one week. In PBS, the lag phase was extended to about eight weeks. In both cases, total drug release was about 10 % prior to the onset of the third and final phase of release.

The final phase of release showed a remarkably similar profile over the same 5–6-week period with nearly all drug released five weeks after completion of the lag phase. The mass transfer phenomena of erosion and diffusion of the contents in the implant core should have been similar between the two conditions once sufficient polymer degradation and hydration in the core had occurred to kick off drug release. Together, these data highlighted the importance of autocatalysis and osmotic effects in the degradation of the PLGA controlling drug release in the dexamethasone intravitreal implant.

While PBS is commonly used in vitro to simulate the in vivo conditions of the posterior segment of the eye, it remains challenging to develop a predictive IVIVC in human eyes.[25] The complexity of ocular physiology (including multiple routes of elimination and variations in vitreous viscosity), along with the inability to collect human ocular pharmacokinetic data, complicates the development of an IVIVC. Nevertheless, conservation of the release mechanisms between normal saline and PBS may assist with the assessment of drug release kinetics between similar formulations or equivalent batches of dexamethasone intravitreal implants during generic product development.

4.4. CONCLUSION

Using a variety of analytical techniques, the drug release mechanisms of the reverse-engineered Ozurdex implant during in vitro dissolution were elucidated. In both 37 °C normal saline and PBS (pH 7.4), the release profile was triphasic in nature despite

a difference in release duration. A small burst release was observed in the first 24 h, followed by a lag phase where limited drug release occurred, and a final release phase where the majority of the drug was liberated.

The 1–2 % burst release in the first day could be attributed to drug particles on the surface of the implant that were not completely coated by the polymer matrix and, thus, solubilized rapidly upon exposure to the dissolution medium. During the lag phase, total drug release was limited to less than ~10 % despite significant physical and chemical changes occurring in the implant. In this phase, autocatalytic hydrolysis of the PLGA dominated near the core of the implant. PLGA degradation occurred more slowly in the buffered PBS system, which extended the duration of the lag phase compared to normal saline.

The final phase of release began when sufficient PLGA degradation and moisture uptake had occurred to disrupt the structure of the implant via swelling. At this point, the trapped oligomeric degradation products near the core could diffuse out into the bulk medium, exposing the dexamethasone particles to enough water for dissolution. During this final phase of release, erosion/diffusion of the PLGA continued, releasing a directly proportional amount of drug. This proportionality suggested that the release of dexamethasone from these implants was linked directly to the breakdown of the PLGA barrier between the drug particles and the bulk dissolution medium.

The methods developed in this work for characterization of the dexamethasone intravitreal implant may facilitate the development of generic implants referencing Ozurdex. Additionally, the release mechanisms of dexamethasone from the reverse-engineered Ozurdex implant uncovered in this work provide valuable information for exploring non-clinical bioequivalence approaches in future generic formulations.

ACKNOWLEDGEMENTS

This work was supported by the Broad Agency Announcement (BAA) Contract # 75F40120C00198 from the U.S. Food and Drug Administration (FDA). The content reflects the views of the authors and should not be construed to represent the views or policies of the U.S. FDA. The authors would like to thank Jessie Maisano and Dave Edey of the University of Texas High-Resolution X-ray CT Facility (NSF EAR-1762458) for their assistance in acquiring and processing microCT images.

Chapter 5. Manufacturing dexamethasone intravitreal implants: process control and critical quality attributes[*]

ABSTRACT

Over 20 long-acting injectable formulations based on poly(lactide-co-glycolide) (PLGA) have been approved by the FDA to date. PLGA is a biodegradable polymer that can extend drug release from these dosage forms for up to six months after administration. Despite the commercial success of several of these formulations, there are still a limited number of products that utilize PLGA, and there are currently no generic counterparts of these products on the market. Significant technical challenges are associated with preparation of chemically and structurally equivalent formulations that yield an equivalent drug release profile to the reference listed drug (RLD) both in vitro and in vivo.

In this work, Ozurdex (dexamethasone intravitreal implant) was used as a model system to explore how the manufacturing process of PLGA–based solid implants impacts the quality and performance of the dosage form. Control of implant structural characteristics, including diameter, internal porosity, and surface roughness, was required to maintain accurate unit dose potency. Implants were prepared by a continuous hot-melt extrusion process that was thoroughly characterized to show the importance of precise feeding control to meet dimensional specifications. Five extruder die designs were evaluated using the same hot-melt extrusion process to produce five structurally-distinct implants. The structural differences did not alter the in vitro drug release profile when tested in both normal saline and phosphate-buffered saline (pH 7.4); however, implant

[*] This manuscript will be submitted for publication in the International Journal of Pharmaceutics. Mark A. Costello wrote the manuscript and designed, executed, and interpreted the experiments.

porosity was shown to impact the mechanical strength of the implants. This work seeks to provide insight into the manufacturing process of PLGA–based solid implants to support development of future novel and generic drug products.

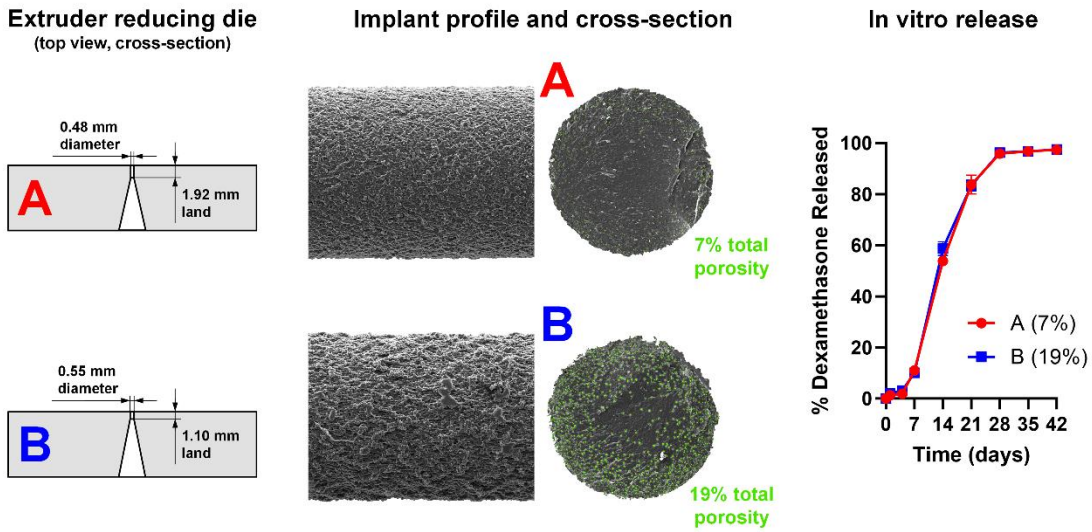

Illustration 5.1. Graphical abstract for Chapter 5.

5.1. INTRODUCTION

Poly(lactide-*co*-glycolide) (PLGA) is a biodegradable polymer used to sustain drug release in several FDA–approved long-acting dosage forms. These formulations can take several forms including solid implants, in situ gel implants, and (most commonly) microspheres. The sustained release conferred by these formulations helps to reduce dosing frequency, maintain stable concentrations of the active ingredient, and improve patient compliance.[1]

To date, the FDA has approved more than 20 PLGA-based drug products for use in the USA with the first approval dating back to January 1989.[4] Despite the clinical and commercial success of many of these products, no generic PLGA–based products have

achieved marketing approval. Even though several of these products are beyond their marketing exclusivity period and/or patent protection, technical challenges in formulation, characterization, and manufacture of equivalent drug products have hindered generic development.

Much of this complexity can be attributed to the multifaceted mechanisms of controlled drug release associated with PLGA–based dosage forms.[60] Several physicochemical processes and characteristics have been shown to play an important role in the drug release process from PLGA–based dosage forms, including water uptake[88], polymer degradation via hydrolysis[87], drug-polymer interactions[91] (or the absence of interactions[71]), drug solubility[92], system swelling[93], pH gradients within the dosage form[90], osmotic effects[89], and erosion of the dosage form[94]. The relative importance of these phenomena to drug release may change throughout the duration of the sustained release period, resulting in a unique combination of these factors driving drug release from each PLGA–based formulation.

To further complicate matters, the manufacturing process of PLGA–based products can have a major impact on the physiochemical properties of the final formulation, even in cases where the composition between two products is identical. For example, Park et al. described the large number of variables to consider during manufacture of PLGA microparticles using an emulsification-type process and discussed how their interplay is not fully understood to date.[108] Microparticles are most often prepared in a *batch process*, i.e., where the raw materials are charged together at the beginning of manufacture and the product is collected at the end of the process. Batch processes have inherent disadvantages over *continuous processes*, where raw materials are continually charged, processed, and collected throughout the procedure. Continuous processing offers easier scale-up, less batch-to-batch variability, and more

straightforward process monitoring.[109] Some PLGA–based dosage forms are produced via a continuous process; one such example is Ozurdex (dexamethasone intravitreal implant).[47]

Ozurdex is indicated for the treatment of non-infectious uveitis, macular edema following branch and central retinal vein occlusion, and diabetic macular edema.[56] The dosage form is a solid implant with a cylindrical profile approximately 0.46 mm in diameter and 6 mm long. The implant is produced via a continuous hot-melt extrusion process in which the drug and PLGA are thoroughly mixed at temperatures above the glass transition (T_g) of the polymer using a pair of rotating screws. This drug–polymer mixture is pushed through a die to form rod-shaped filaments that are subsequently cut to the appropriate length to produce unit doses of Ozurdex.[46] Release of dexamethasone from the dosage form is sustained for 3–6 months by embedding the drug in a matrix of PLGA. The long-acting implant is fitted inside the barrel of a 22-gauge needle and administered directly to the vitreous of the eye using a proprietary applicator.[59] Dexamethasone, a synthetic corticosteroid, exerts anti-inflammatory effects on the retinal tissues to stabilize the blood-retinal barrier and reduce the retinal capillary leakage that causes loss of vision in the aforementioned conditions.[57]

Ozurdex, first approved by the FDA in 2009, is slated to lose patent protection in 2023, providing a potential opportunity for generic competition.[27] Competition from generic drugs can help reduce prices and improve access to medicines for patients in need.[11] As of 2021, 90% of all dispensed prescriptions in the USA are generic drugs.[110] These generics offer billions of dollars in savings to Americans every year while providing the same clinical benefit as their branded counterparts.[111]

In this work, development, characterization, and optimization of the continuous manufacturing process used to prepare dexamethasone intravitreal implants like Ozurdex

is presented. The purpose of this study was to obtain a better understanding of how the manufacturing process used to prepare PLGA–based solid implants impacts the quality and performance of the dosage form to support future development of PLGA drug products.

5.2. MATERIALS AND METHODS

5.2.1. Materials

Ozurdex (dexamethasone intravitreal implant) (Allergan USA, Inc; Madison, NJ, USA) was purchased from a pharmacy supplier. Two grades of 50:50 poly(D,L-lactide-*co*-glycolide) (PLGA) were purchased from the Evonik Corporation (Darmstadt, Germany): Resomer RG 502 (ester terminated) and Resomer RG 502H (acid terminated). Dexamethasone was purchased from Shenzhen Nexconn Pharmatechs Ltd. (Shenzhen, China). Rhodamine B, HPLC–grade acetonitrile, ACS–grade sodium chloride, and 10x phosphate buffered saline (PBS) solution were purchased from Thermo Fisher Scientific (Waltham, MA, USA). Distilled, deionized water was obtained in the laboratory.

5.2.2. Methods

5.2.2.1 Manufacture of dexamethasone intravitreal implants

Dexamethasone intravitreal implants were manufactured using a double extrusion and shaping process. For the first extrusion, the pre-extrusion blend of micronized dexamethasone and PLGA was fed into a Haake MiniLab twin-screw extruder (Thermo Electron (Karlsruhe) GmbH; Karlsruhe, Germany) using a single-screw force feeder rotating at 7 rpm. The blend was extruded at 105 °C using conical, co-rotating screws at 125 rpm, then shaped into rods using a 1 mm diameter heated die fitted at the extruder discharge port set to 97 °C. Before the second extrusion, these rods were manually

broken into 1–2 cm segments and milled using a Wiley Mini Mill (Thomas Scientific; Swedesboro, NJ, USA) fitted with a 20-mesh screen to produce free-flowing granules. For the second extrusion, a twin-screw volumetric feeder (MT-1, Brabender Technologie; Mississauga, ON, Canada) in tandem with a single-screw force feeder set at 1 rpm were used to precisely control the feed rate of the milled extrudate (8–10 g/h) into a twin-screw Haake MiniLab extruder (set to 105 °C and 125 rpm) fitted with a heated reducing die (0.48 mm or 0.55 mm diameter) at the discharge port set to 97 °C. A downstream puller (IMSTec USA, Inc.; Temecula, CA, USA) integrated with a dual-axis laser micrometer (BETA LaserMike AccuScan 5012, NDC Technologies Inc.; Dayton, OH, USA) was used to draw down the melt to the target diameter. Online process monitoring of the extruder parameters and the implant diameter was performed using custom MATLAB software (MathWorks; Natick, MA, USA) to trend real-time data from the extruder and laser micrometer. Implant rods 5–10 cm in length were collected and allowed to cool down to room temperature. After cooling, the rods from the second extrusion were manually cut to the desired length using a razor blade to produce individual implants.

5.2.2.2 Residence time distribution (RTD)

RTD parameters of the extrusion process were determined by loading a small amount of tracer dye (Rhodamine B) to the feeding area of the extruder and monitoring the color change over time at the extruder die. A high-speed USB camera (Lt-C1950, Teledyne Lumenera, Ottawa, Canada) integrated into custom MATLAB software (The MathWorks, Inc., Natick, MA) was used to monitor the color change of the extrudate after introduction of the tracer dye. A linear relationship between the concentration of the tracer and the measured color intensity was assumed. Post-processing of the raw red-green-blue color channel data was completed in MATLAB to convert to the CIE 1976

L*a*b* color space and perform least squares fitting to an analytical solution of the Fokker-Planck equation for twin-screw extruders.[112] RTD parameters were calculated using the continuous best-fit function, E(t). Median residence time was estimated from the best fit function where 50% of the total area under the curve was reached, i.e., the time at which half the tracer dye had left the extruder. The mean residence time was determined by calculating the first moment of the distribution.[113]

5.2.2.3 Melt rheology[†]

Rheological properties of dexamethasone–PLGA mixtures were evaluated using a 25 mm parallel plate setup in a Physica MCR 301 rotational rheometer (Anton Paar, Graz, Austria). The rheometer was fitted with a Peltier temperature control hood (H-PTD200) to hold the sample at the desired temperature during testing. To prepare the dexamethasone–PLGA mixtures for testing, a powder blend of the components was first fed through the Haake MiniLab extruder to promote uniform mixing, then milled through a 20-mesh screen to produce granules of each sample. These granules were weighed to a target mass of 0.69 g and gently compressed in a hydraulic press (MTCM-I, GlobePharma, New Brunswick, NJ) fitted with a 10 mm round die to produce consistent slugs for testing. All tests were performed with a 1 mm gap height at 97 °C. Viscosity curves were generated using a rotational test with shear rates logarithmically ramped from 0.01 – 10 s^{-1}. Viscoelastic behavior was evaluated using an oscillatory amplitude sweep of shear strain ranging from 0.01-10% at a frequency of 10 rad/s.

[†] Joseph Liu collected all rheological data shown in this chapter.

5.2.2.4 Implant structural analysis

Scanning electron microscopy (SEM) was used to evaluate the internal and external structure of the melt extruded implants. To view the internal morphology, the implants were carefully fractured to reveal a cross-section. All SEM samples were prepared for imaging by attaching them to aluminum stubs using double-sided carbon tape. They were then sputter-coated with gold for 60 s at 40 mA (Electron Microscopy Sciences; Hatfield, PA, USA). Imaging was performed using a Quanta 650 FEG SEM (FEI Company; Hillsboro, OR, USA) using an accelerating voltage of 15 kV.

5.2.2.5 Total implant porosity

Total implant porosity can be derived from the implant's mass and physical dimensions along with the true density of its components. First, implant diameter was measured at five equidistant points along a 2–3 cm segment of melt extrudate with a precision of 0.1 µm using a laser micrometer (BETA LaserMike AccuScan 5012, NDC Technologies Inc.; Dayton, OH, USA). Digital calipers (CD-6" ASX, Mitutoyo Corp., Kanagawa, Japan) were used to measure the length of the implant segment with a precision of 0.01 mm. Implant mass was determined using a microbalance (MSA3.6P0TRDM, Sartorius; Göttingen, Germany) with a precision of 0.001 mg. The true density of the dexamethasone–PLGA powder blend was determined to be 1.365 ± 0.004 g/cc (mean ± S.D., n = 5) using a helium pycnometer (MVP-6DC, Quantachrome Instruments; Boynton Beach, FL, USA). Equation 5.1 was used to calculate the total implant porosity:

Equation 5.1.

$$Total\ Implant\ Porosity = \left(1 - \frac{\left(\frac{Implant\ Mass}{\pi \times \left(\frac{Avg.Diameter}{2} \right)^2 \times Length} \right)}{True\ Density} \right) \times 100\%$$

5.2.2.6 Implant breaking force

A three-point bend test based on Procedure A of ASTM D7264 was used to evaluate the breaking force of the dexamethasone intravitreal implants.[114] Individual implants were placed on two supports placed 5 mm apart. A TA-XT Plus Texture Analyzer (Stable Micro Systems, Surrey, United Kingdom) was used to apply a loading force to the center of the implant. The loading nose and supports had a radius of 0.5 mm. The crosshead was set to move at 0.01 mm/sec until fracture of the implant was detected. The maximum force recorded prior to fracture was reported as the breaking force.

5.2.2.7 In vitro release testing

In vitro release testing was performed in 30 mL normal saline (0.9% NaCl (w/v)) or phosphate-buffered saline (PBS, pH 7.4) at 37 °C and 100 rpm using a New Brunswick Innova 40 incubator/shaker (Eppendorf; Hamburg, Germany). The 30 mL volume of both media was sufficient to maintain sink conditions (greater than three-fold the saturation volume) throughout in vitro release testing as dexamethasone is a nonionizable molecule with a reported aqueous solubility of ~90 μg/mL at 37 °C.[35, 58] For the normal saline samples, sampling occurred on Days 1, 4, 7, 14, 21, 28, 35, and 42. For the PBS samples, sampling occurred on Days 0, 1, 4, 7, 14, 21, 28, 42, 56, 70, 84, and 98. When sampling, 25 mL of the medium was removed for HPLC analysis and immediately

replaced with 25 mL of fresh medium. Release data were normalized to the assay of the remaining implant fragment at the final timepoint: Day 42 for the normal saline samples and Day 98 for the PBS samples.

5.2.2.8 Dexamethasone assay

Dexamethasone assay of the release media as well as the implant drug content was performed using a Waters HPLC equipped with a 2996 photodiode array (PDA) detector and integrated 717plus autosampler (Waters Corporation; Milford, MA, USA). The mobile phase consisted of a 60:40 acetonitrile:water (v/v) mixture. High-performance liquid chromatography (HPLC) parameters consisted of a flow rate of 1 mL/min, a Luna 5 μm C18(2) 100 Å column (150 mm × 4.6 mm) (Phenomenex; Torrance, CA, USA), and a detection wavelength of 241 nm. Duplicate injections were used for all samples. Dexamethasone had a retention time of approximately 2.4 min. Implant solids that remained after the final dissolution timepoint were dissolved in 10 mL of mobile phase using 1–2 min of sonication to aid dissolution and filtered using a 0.45 μm PTFE syringe filter. The injection volume for all samples was 50 μL. Duplicate 3-point calibration curves were generated from 0.1 to 10 μg/mL ($R^2 \geq 0.9999$) for both sample types.

5.3. RESULTS AND DISCUSSION

5.3.1. Dimensional and structural specifications of dexamethasone intravitreal implants

The composition of the dexamethasone intravitreal implants similar to Ozurdex prepared in this study is presented in Table 5.1. The implant composition was inferred from both the literature and experimentation, as discussed in our reverse engineering study of the Ozurdex implant.[8]

Material	**Mass per implant (mg)**	**% w/w**
Dexamethasone (Form B, micronized)	0.700	60%
Resomer RG 502 H (50:50 PLGA, acid terminated, inherent viscosity 0.2 dL/g)	0.350	30%
Resomer RG 502 (50:50 PLGA, ester terminated, inherent viscosity 0.2 dL/g)	0.117	10%
Total	1.167	100%

Table 5.1. Composition of the dexamethasone intravitreal implants prepared in this study.

Based on observations from the reverse engineering study, the dexamethasone and PLGA in Ozurdex were assumed to be intimately mixed during the hot-melt extrusion manufacturing process, resulting in a uniformly-dispersed, two-phase system of drug and polymer in the implant. This uniformity within the continuously produced implants leads to consistent drug loading between unit doses. Applying the assumption of 60% w/w drug loading in the implant, the theoretical % label claim of the implant can be derived from its dimensional and structural characteristics (i.e., diameter, length, and total porosity), as described in Equation 5.2. See Figure S5.1 for a derivation of this equation.

Equation 5.2.

$$\%\ Label\ Claim = \frac{\pi \times \left(\frac{Diameter\ (mm)}{2}\right)^2 \times Length\ (mm) \times True\ Density\ \left(\frac{mg}{mm^3}\right) \times Drug\ Loading\ (\%) \times \left(1 - Porosity(\%)\right)}{Label\ Claim\ (mg)} \times 100\%$$

Where:

$$True\ Density = 1.365 \frac{mg}{mm^3} \left(or \frac{g}{cm^3}\right)$$

$$Drug\ Loading = 60\%$$

$$Label\ Claim = 0.700\ mg$$

The relationship between implant structure and unit dose potency is important to consider during implant manufacture and allows for creation of in-process controls (IPCs) to maintain acceptable unit dose potency (95–105%). Furthermore, accurate diameter control is essential to achieve proper fitting of the implant inside the needle barrel of the applicator. From patent literature, the IPC specification for Ozurdex implant diameter is ≥ 80% yield within 0.0175–0.0185 inch (0.445–0.470 mm).[47] The 22-gauge, thin-wall needle used in the applicator has an inside diameter of 0.505 mm, which serves as an effective maximum diameter for the implant, above which the implant will not fit into the device.[78] Conversely, implants with a diameter that is significantly smaller than the lower IPC limit may not be properly secured inside the needle barrel and may slip out of the applicator prior to administration.

Total implant porosity, a consequence of process parameters and equipment parameters during manufacture, also plays an important role in unit dose potency. An implant with a high total porosity has a larger total void volume, which leaves less space for the dexamethasone–PLGA matrix and results in a reduced total dose. The geometric approach used to quantify total implant porosity in this work (as discussed in Methods)

assumes that the implant is a perfect cylinder. In reality, surface imperfections form voids between the imagined surrounding cylinder and the actual surface of the implant. The diameter reported by the laser micrometer represents the shadow cast by the implant when placed in the path of its collimated laser beam. Under these conditions, surface imperfections on either side of the implant are included in the reported implant diameter. Consequently, the *total implant porosity*, as used in this work, comprises both the external void volume caused by surface imperfections and the internal void volume generated from closed pores.[63] Using this geometric approach to quantify total implant porosity enables near-real-time acquisition of porosity data that can be used to adjust process parameters during production. For a more detailed analysis of total implant porosity, including the ability to quantify the internal void volume fraction, orthogonal methods such as microcomputed tomography (microCT) can be applied.[8]

Patent literature for Ozurdex lists the IPC specification for implant density as 1.10–1.30 g/cm^3, corresponding to a total implant porosity range of 4.8–19.4%, calculated using the measured true density for the dexamethasone–PLGA mixture of 1.365 g/cm^3. Alternatively, Equation 5.2 can be used to determine the maximum possible range in total porosity for a label claim of 95–105%, a diameter range of 0.445–0.470 mm, and an implant length of 6 mm. In this window, the calculated range for possible variation of total implant porosity is 3.6–22.0%.

The target values and possible ranges for implant structural properties required to maintain unit dose potency between 95–105% are summarized in Table 5.2 and visualized in Figure 5.1 for implants 6 mm in length. During manufacture of the dexamethasone intravitreal implants, the total implant porosity remained consistent throughout a manufacturing run when operating at steady-state (see Section 5.3.3). The diameter was easily adjusted in-process by changing the speed of the dual wheel puller

used to drawdown the melt to the desired diameter. As shown in Figure 5.1, the contour corresponding to the target total implant porosity of 13.2% has the longest length inside the box corresponding to the target operating window compared to any other contour of total porosity. In other words, it is advantageous to adjust the process parameters and equipment parameters to achieve a total porosity near the 13.2% target to maximize the collection of material near 100% label claim and account for normal variation in implant diameter during processing. However, despite adding additional complexity, variations in total porosity from the target value that cause a shift in % label claim can be corrected after melt extrusion is complete by adjusting the length to which each implant is cut.

Implant Property	**Target**	**Possible Range**
Diameter (mm)	0.4572	0.4445 – 0.4699
Total Porosity (%)	13.2	3.6 – 22.0
Length (mm)	6.00	5.43 – 6.63

Table 5.2. Target dimensional and porosity specifications for the dexamethasone intravitreal implants and corresponding possible ranges to maintain 95–105% unit dose potency.

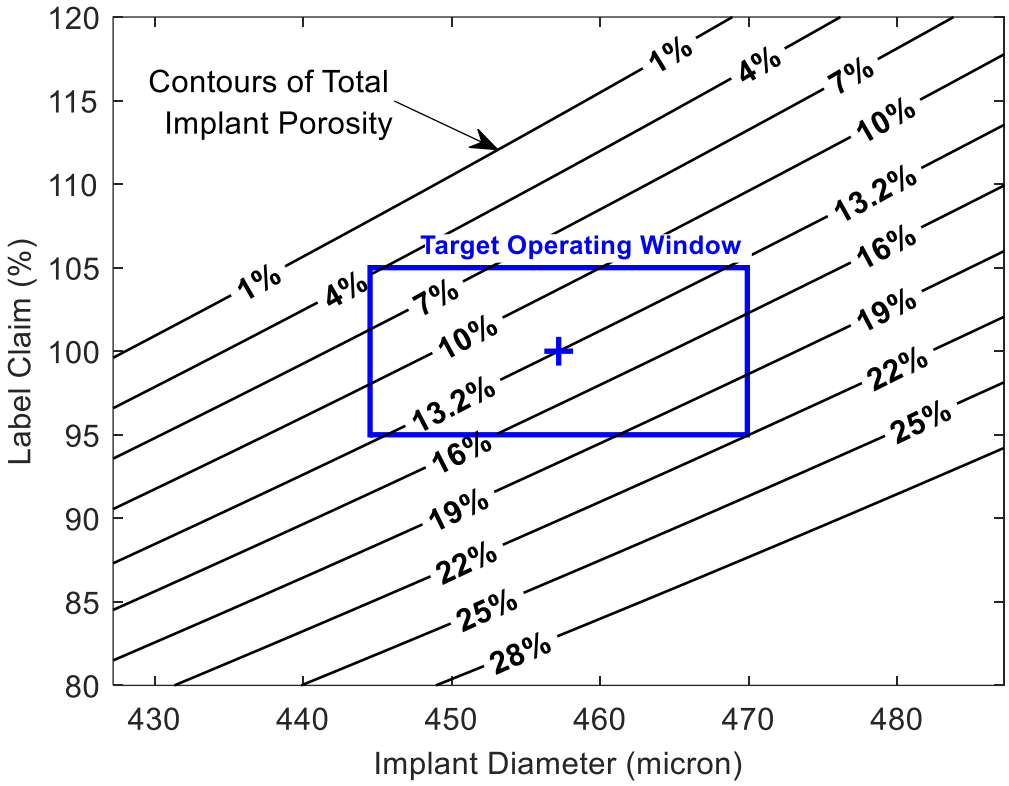

Figure 5.1. Contour plot illustrating how the label claim of dexamethasone intravitreal implants is influenced by total implant porosity and implant diameter. A fixed implant length of 6.00 mm was assumed for these calculations. The target operating window is overlaid to show the operating region required to maintain 95–105% label claim and all specifications shown in Table 5.2.

Melt extruded rods of known diameter and total porosity can be cut to lengths other than 6 mm to refine the % label claim of the unit doses. Interestingly, there is evidence that this approach was applied in the commercial manufacture of Ozurdex. Table 5.3 shows the measured properties of two Ozurdex implants from different production lots. Sample #1 exhibits properties very close to the theoretical values for diameter, length, and total porosity, which leads to an estimated label claim close to 100% using Equation 5.2. Sample #2 has a higher average diameter and a lower total

porosity than the target values. Notably, this implant was measured to be shorter in length, with a length of 5.79 mm. Had the implant been cut to a fixed length of 6 mm, the estimated label claim according to Equation 5.2 would be 108.1%, outside of the 95–105% target window. Reducing the length to 5.8 mm resulted in an estimated unit dose potency of 104.3% that is within the target specification.

Implant Property	**Sample #1**	**Sample #2**
Average Diameter (*n*=4) (mm)	0.4599	0.4643
Length (mm)	6.02	5.79
Mass (mg)	1.189	1.217
Total Porosity (%)	12.9%	9.1%
Estimated % Label Claim	101.9%	104.3%

Table 5.3. Properties of two commercial Ozurdex implants from different production lots. Estimated % label claim was calculated using Equation 5.2.

5.3.2. In-process implant diameter control

To appropriately control the diameter of the dexamethasone intravitreal implants during manufacture, a two-stage melt extrusion process was implemented, as discussed in Methods. The low bulk density (0.18 g/cm^3, *n*=5) and cohesive properties of the pre-extrusion blend, composed of jet-milled dexamethasone and jet-milled PLGAs, resulted in inconsistent feeding to the melt extruder. This poor feeding was attributed to variable compaction and unpredictable slip-stick behavior in the funnel of the single-screw stuffer feeder. This poor feeding control manifested as large variability in extruder torque and

pulsations in material flow from the extruder die during the first stage of the extrusion process that rendered accurate diameter control practically impossible.

The extrudate produced in the first extrusion was milled to produce dense, free-flowing granules that enabled improved feeding during the second extrusion. After milling the extrudates produced in the first extrusion through a 20-mesh screen using a rotary mill, the bulk density of the milled granules was measured to be 0.62 g/cm^3 (n = 5). This significant densification and improved bulk flow, compared to the pre-extrusion blend, was expected to improve feeding performance in the stuffer feeder.

Initial attempts to achieve good diameter control during the second extrusion process using the milled granules were curbed by feeder limitations. Despite the use of a chilled water jacket to cool the base of the stuffer feeder funnel, premature softening of the milled granules in the transition between the funnel and the feed throat of the extruder was unavoidable. This premature softening caused the granules to reach temperatures slightly above the glass transition temperature (T_g) of the PLGA, resulting in a highly viscous melt that the single-screw stuffer feeder struggled to feed. With insufficient feeder power, the rotation rate of the stuffer screw was variable and contributed to pulsation in flow and, correspondingly, poor diameter control (see Figure 5.2A). Extruder torque variations ± 35% of the mean value were common with this setup. Periodic shifts in torque resulted in corresponding periodic changes to implant diameter on a time lag of about 75 seconds, as shown in Figure 5.2A. This observed correlation between process torque and implant diameter emphasized the importance of consistent feeding to the extruder to stabilize extruder torque, and ultimately, achieve good control of implant diameter during continuous processing.

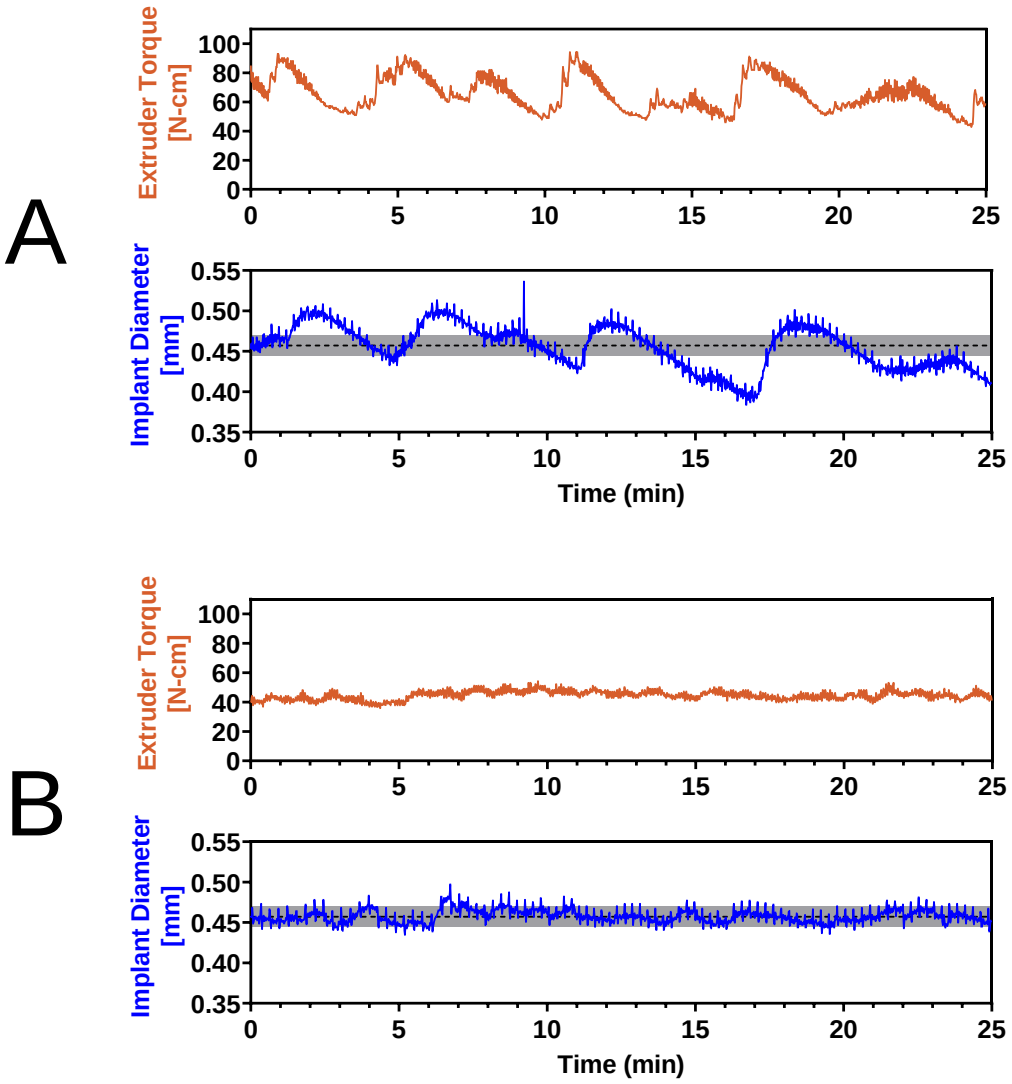

Figure 5.2. In-process extruder torque and implant diameter for a 25-minute segment of a second extrusion run with the single feeder setup (A) and the dual feeder setup (B). Implant diameter control was improved with the dual feeder setup. The shaded area represents the target operating range for implant diameter per the IPC specification listed in Table 5.2.

To overcome the limitations of the single-screw stuffer feeder, alternate feeding options were considered. It is feasible that a stuffer feeder with a more powerful motor

could provide sufficient torque during force feeding of the viscous melt to avoid stalling, but such custom equipment was not readily available in the laboratory. An alternative approach made use of a small, twin-screw volumetric feeder, the Brabender MT-1. For materials with excellent bulk flow properties and consistent bulk density, such as the milled granules, twin-screw volumetric feeders can be used to accurately deliver powder blends during continuous manufacturing.[115, 116] Feeding performance of the milled granules from the Brabender feeder at 10 g/h was evaluated using an analytical balance capable of recording the mass each second to a precision of 0.001 g. The mass vs. time data was recorded for approximately 15 minutes and post-processed to determine the real-time feed rate on a 10-second and 1-minute rolling basis, as shown in Figure 5.3. While the real-time feed rate varied considerably on a 10-second basis, the feed rate on a minute-by-minute basis was deemed satisfactory for feeding the hot-melt extrusion process due to the extended residence time of the process (discussed in Section 5.3.3).

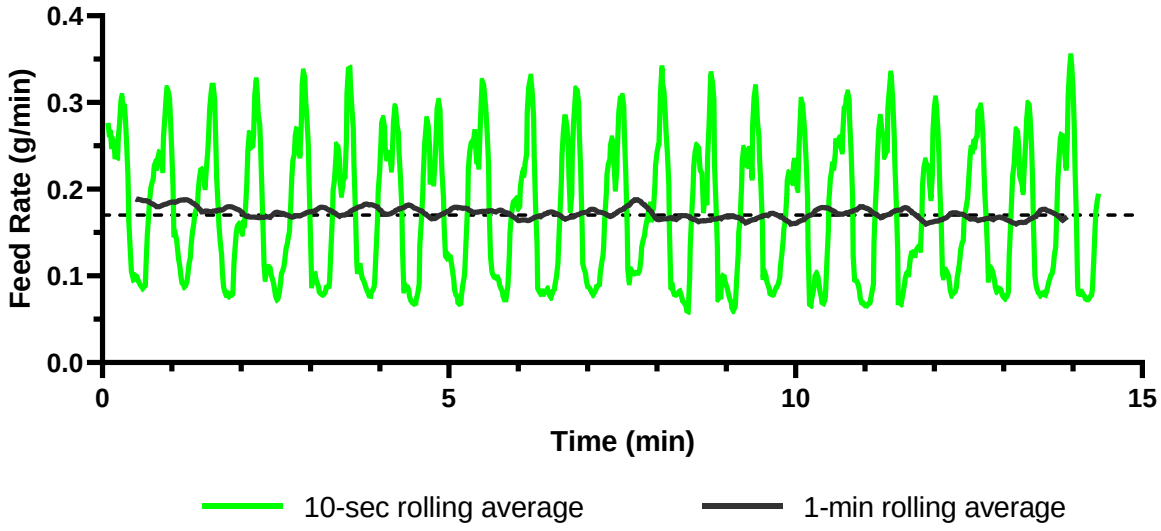

Figure 5.3. Evaluation of milled granule feeding performance from the Brabender MT-1 twin-screw volumetric feeder. The target feed rate of 10 g/h (0.17 g/min) is shown by the dashed line.

Initial attempts to feed the milled granules into the extruder using only the volumetric feeder failed due to the granules bridging over the screws in the feed zone of the extruder. The single-screw stuffer feeder was reintroduced between the volumetric feeder and the extruder to force the material into the extruder while enabling consistent feeding from the volumetric feeder (see Figure 3.6 for an illustration of the process). Beneficially, during process startup, a small amount of the granules dispensed from the volumetric feeder had accumulated in the stuffer feeder, which allowed it to act as a buffer to the short-term variations in flow of the volumetric feeder, further stabilizing the flow of material into the extruder. Using the dual feeder setup, variations in extruder torque were considerably reduced and diameter control was improved sufficiently to meet the IPC specifications for implant diameter, as shown in Figure 5.2B. In this setup, the line rate, or total throughput at steady-state, is dictated by the volumetric feeder.

5.3.3. Steady-state operation and residence time distribution

A feed rate of 8–10 g/h was targeted during production of the dexamethasone intravitreal implants. Feed rates considerably higher than this range resulted in a rougher surface of the implant, which contributed to higher total porosity. Additionally, due to the small total mass of the dosage form (1.167 mg), the production rate was a reasonable ~130 implants/min at this speed. Attempts to feed any slower with the volumetric feeder would likely introduce additional variability into the process, as seen in Figure 5.3, potentially complicating diameter control.

At feed rates of 8–10 g/h, the time required to reach the steady-state collection period was approximately 90 minutes (see Figure 5.4). No process torque was measured by the melt extruder during the first 20 minutes of feeding from the volumetric feeder, as the material was accumulating in the stuffer feeder and not reaching the extruder screws. After this accumulation in the feeding zone, material began to reach the twin screws of the melt extruder and a corresponding increase in process torque was observed for the next 25 minutes as the twin-screw extruder barrel filled with melt. Material was first visible exiting from the extruder die approximately 45 minutes after the start of feeding. For a further ~40 minutes, the process torque continued to increase and remained dynamic until leveling out and remaining steady after about 85 minutes. As previously mentioned, accurate diameter control could only be achieved when process torque variability was reduced; therefore, waiting the full 1.5 hours to reach steady-state operation was required before collecting dexamethasone intravitreal implants that met IPC criteria. Additionally, total implant porosity was found to be consistent (standard deviation < 1%) between implants when operating at steady-state. The total porosity of the implants during startup tended to be lower and variable, further emphasizing the importance of waiting for steady-state operation prior to material collection.

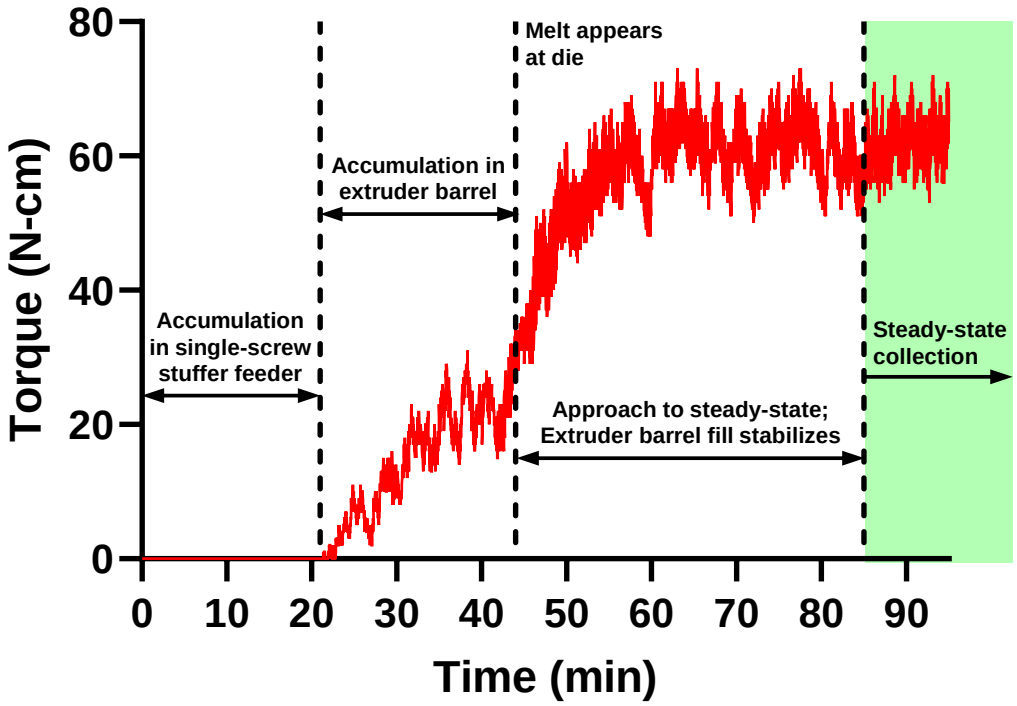

Figure 5.4. Plot of extruder torque during startup and approach to steady state for the manufacture of dexamethasone intravitreal implants. Select regions of the startup sequence are labelled.

With such a long approach to steady-state, it was expected that the mean residence time for a randomly selected particle in this system would also be long. To evaluate the residence time distribution (RTD) of this process, a pulse of red tracer dye was introduced directly into the space between the stuffer feeder and the extruder feed throat. The color change of the melt at the extruder die was recorded using a high-resolution scientific camera with a frame rate of approximately 12.7 frames/s for a two-hour period. A select region of each frame was post-processed in a custom MATLAB program to quantify color change and fit a continuous RTD function to the raw data for calculation of RTD parameters (see Figure 5.5 and Table 5.4).

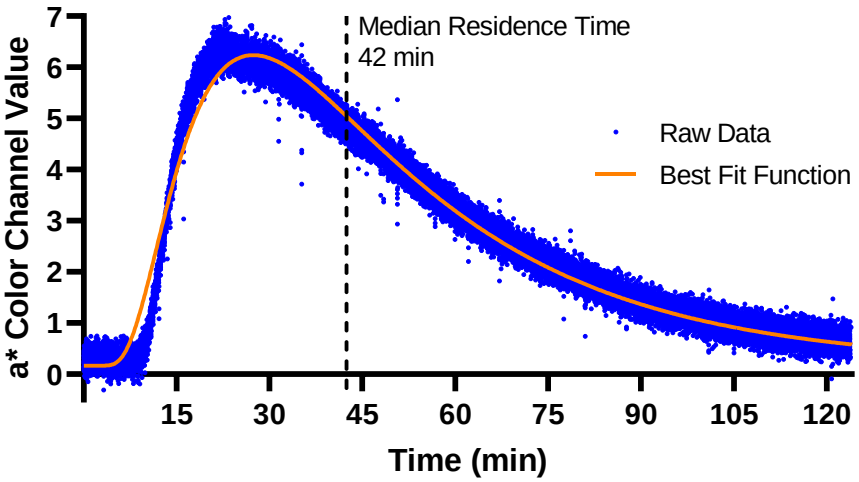

Figure 5.5. Measured color change during evaluation of residence time distribution using a tracer dye (*n*=94,440 frames). The corresponding best-fit function is overlaid with the raw color change data.

Parameter	**Time (min)**
T_{start}	5.2
T_{max}	27.4
Median Residence Time	42.4
Mean Residence Time	51.2
$T_{90\% \text{ Cumulative}}$	94.8

Table 5.4. Residence time parameters derived from the best-fit function for the second extrusion and shaping process of the dexamethasone intravitreal implants.

The median residence time for this system, or the time required to purge half of the total tracer added, was estimated to be 42 minutes. Color change from the dye was first detected by the camera at the extruder exit in less than 10 minutes, however a

long tail in the distribution was observed after recording the peak concentration at 27 minutes. This long tail in the distribution suggested substantial back mixing within the extruder barrel. Extensive back mixing, as opposed to plug-flow behavior, was expected with this setup due to the slow feed rate in combination with extensive mixing from the extruder screws turning at 125 rpm. This extensive back mixing likely contributed to high uniformity within the dosage form and well dispersed crystals of dexamethasone in the PLGA matrix, as seen under SEM.[8]

5.3.4. Rheological properties and drawdown to target diameter

A reducing die affixed to the end of the extruder was used to achieve the cylindrical profile of the implants to match Ozurdex. The Haake MiniLab extruder used to produce the dexamethasone intravitreal implants had a discharge port with a rectangular profile approximately 4.1 mm × 1.1 mm, significantly larger than the diameter of the implant (see Figure S5.2). A custom reducing die with a smooth internal surface was manufactured using electrical discharge machining (EDM) to gradually taper the extrudate melt from the rectangular profile to the cylindrical profile. The first protype die of this design was manufactured to a diameter of 1 mm.

Initial attempts to draw down the extrusion melt from the 1 mm diameter die to the target implant diameter of 0.457 mm failed due to strand breakage. The minimum diameter achievable after drawdown using the 1 mm die was approximately 0.65 mm, corresponding to a maximum draw down ratio of approximately 1.5 (see Equation 5.3). It was suspected that the high content of dexamethasone crystals (60% w/w) in the PLGA melt significantly altered the rheological properties compared to pure PLGA, making draw down more challenging than originally anticipated.

Equation 5.3.

$$Draw\ Down\ Ratio\ (DDR) = \frac{Extruder\ Die\ Inside\ Diameter\ (mm)}{Implant\ Outside\ Diameter\ (mm)}$$

The rheological properties of three dexamethasone/PLGA blends and pure PLGA were evaluated using a rotational rheometer. A parallel plate setup was employed with a heated chamber used to hold the sample at 97 °C to match the setpoint of the extruder die temperature. Drug loadings of 60%, 40%, 20%, and 0% were evaluated, with the balance of each composition being the 3:1 blend of acid terminated:ester terminated 50:50 PLGA, as described in Table 5.1.

First, a rotational test was performed to evaluate differences in the viscosity, or resistance to deformation, of the four blends in the low-shear range (see Figure 5.6A). It was observed that the viscosity of the melt increased dramatically with increasing dexamethasone loading. A small difference in viscosity was seen between the pure PLGA and 20% drug loaded sample; however, a 10-fold and 100-fold increase was seen relative to the pure PLGA for the 40% drug loaded and 60% drug loaded samples, respectively. The curve associated with the 60% drug loaded sample terminates early in the plot due to reaching the upper torque limitation of the rheometer. All samples exhibited some extent of shear-thinning behavior, as expected for polymeric melts. Interestingly, the shear thinning behavior was most apparent in the 60% drug loaded sample. The increase in shear thinning may be due to alignment of the dexamethasone crystals within the melt after experiencing an increasing number of rotations throughout the testing period. The higher viscosity of the 60% drug loaded sample used to produce the dexamethasone intravitreal implants implies that a higher stretching force from the dual-wheel puller would be required to draw down the melt to the target diameter.

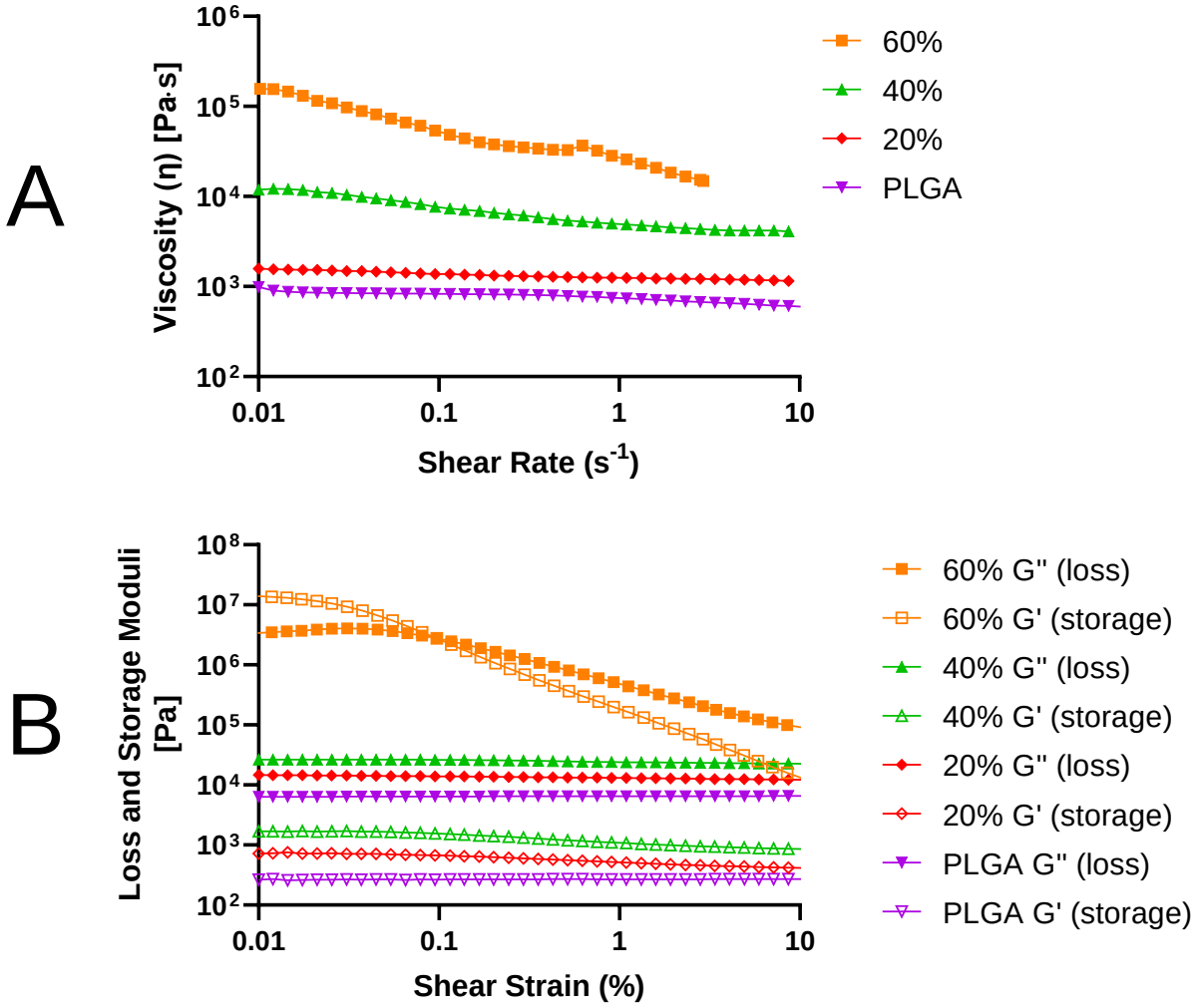

Figure 5.6. Melt rheology of dexamethasone/PLGA blends of various drug loadings at 97°C. Viscosity curves from a rotational test (A) and viscoelastic behavior from an oscillatory test (B) are shown.

To better understand the viscoelastic properties of the four blends, an oscillatory amplitude sweep was performed (see Figure 5.6B). Oscillatory rheological tests can elucidate the elastic portion (i.e., the solid-state behavior) and the viscous portion (i.e., liquid-state behavior) of the overall viscoelastic behavior. The *storage modulus* (G′) represents the solid-like behavior, or the stored deformation energy when shear is applied. The *loss modulus* (G″) represents the liquid-like behavior, or the

deformation energy lost when flowing via internal friction when shear is applied. For the 40%, 20%, and 0% drug loaded samples, the loss modulus is significantly higher than the storage modulus at all levels of strain tested. This implied that, at the 97 °C test conditions, these polymer melts behaved in a fluid-like manner and lacked dimensional stability. These samples would be expected to flow (albeit slowly) into the shape of their container at this temperature.

Interestingly, the 60% drug loaded sample exhibited drastically different viscoelastic behavior. At low strain, the storage modulus exceeded the loss modulus, implying a solid, gel-like consistency of the sample that would hold its shape over time. Most notably, a transition from solid-like to liquid-like behavior occurred at shear strains less than 0.1% where the G′ and G″ curves crossover. The overall reduction in both moduli and the increasingly dominant viscous behavior at higher strains may explain why achieving high drawdown ratios in the 60% drug loaded sample was difficult during melt extrusion. The draw down process involves pulling, or straining, the extrudate melt to reduce the diameter. Initially, a high pulling force would be required to deform the material and initiate the transition to liquid-dominant behavior. This high pulling force then rapidly deforms the increasingly fluid-like material resulting in strand breakage. Drawdown of the samples with lower drug loads would be easier as these materials are inherently prone to deformation at all strain rates.

5.3.5. Impact of die design on implant structure

To overcome the challenges associated with drawdown of the gel-like formulation to the target diameter observed using the 1 mm die, a series of dies with a smaller diameter were manufactured to reduce the draw down ratio. Two different diameters were evaluated: 0.55 mm and 0.48 mm, corresponding to draw down ratios of 1.20 and

1.05, respectively. These ratios were significantly smaller than the DDR of 2.19 required for the 1 mm die. In addition to diameter, a second parameter of the die was varied to improve draw down behavior. The *land length*, or length of the segment within the die that has the same diameter as the outlet, was varied for each of the two new diameters tested. Increasing land length in the die provides additional time for the melt to align with the desired profile before drawdown. In an ideal case, the land length would be on the order of 10× the outlet diameter to provide ample time for polymer chain alignment, which eases the draw down process.[117] However, when processing highly viscous materials, long land lengths compounded with small outlet diameters can be very restrictive to flow resulting in high back pressure within the extruder barrel. In the case of the dexamethasone intravitreal implants, changes to back pressure within the extruder could have implications for internal porosity of the implants, where high pressure could drive out any trapped air that forms the internal voids. Alternatively, an overly restrictive die may render processing impossible due to insufficient pressure buildup in the extruder barrel required to force material through the die. Such a scenario could be compensated for by increasing extrusion barrel temperature to reduce the viscosity of the melt; however, other factors, such as thermal degradation of the drug and polymer, become increasingly important considerations.

Figure 5.7 illustrates the basic design of the reducing dies used to prepare the dexamethasone intravitreal implants. Table 5.5 lists the five unique die designs evaluated in this study, two with a diameter of 0.48 mm and three with a diameter of 0.55 mm. Melt extrusion was performed with the five dies under identical extruder processing conditions, as described in Methods.

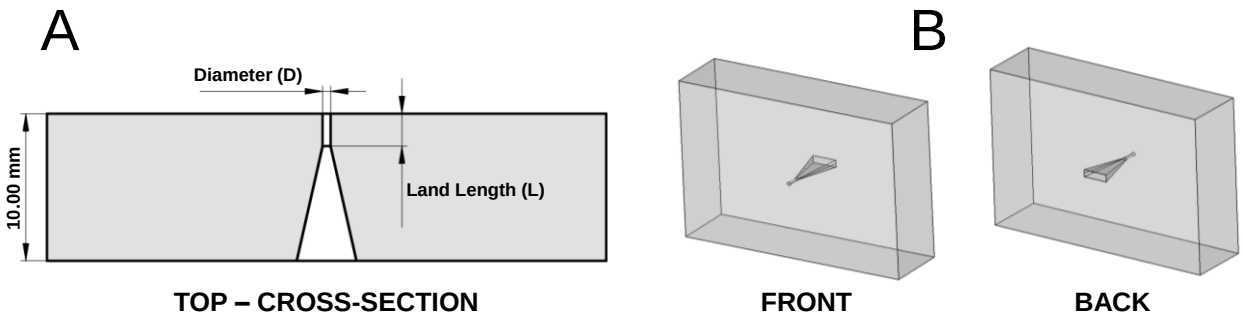

Figure 5.7. Simplified renderings of the reducing die affixed to the extruder showing just the reducing channel used to shape the dexamethasone intravitreal implants. The 2D cross-section (A) and 3D isometric views (B) illustrate how the rectangular profile of the melt leaving the extruder is converted to a circular profile.

	Die Diameter (D) (mm)	L:D Ratio	Land Length (L) (mm)	Reducing Channel Length (mm)	Total Length (mm)
1	0.48	2:1	0.96	9.04	10.00
2		4:1	1.92	8.08	
3	0.55	2:1	1.10	8.90	
4		4:1	2.20	7.80	
5		6:1	3.30	6.70	

Table 5.5. Dimensional specifications of the five die designs evaluated in this study.

All five runs successfully produced implants with diameters near the target value of 0.457 mm, demonstrating that smaller draw down ratios could be used to prepare the implants to the specification for diameter. Despite using identical extruder process parameters across the five runs, each die design produced implants with a unique internal void distribution and surface roughness. Figure 5.8 shows SEM images of the five implants produced with the five die designs evaluated. Qualitatively, total implant

porosity appeared to trend negatively with more restrictive dies. That is, dies with smaller diameter and longer land length produced less porous implants due to both a reduction in internal voids and surface roughness.

Since total porosity is a function of both internal voids and external surface roughness, the impact of both properties must be considered when targeting a specific total porosity during implant manufacture. The importance of this consideration can be emphasized by comparing the two implants produced with the 0.55 mm, 4:1 die (13.1% total porosity) and the 0.48 mm, 2:1 die (10.9% total porosity). Despite the number of internal voids being significantly higher in the 0.48 mm, 2:1 sample, the total porosity of the 0.55, 4:1 sample is higher due to a considerably rougher surface. These structural differences may impact the mechanisms of drug release from the long-acting implant (evaluated in Section 5.3.6). Although implant surface roughness was not extensively studied in this work, it is an important parameter to consider during manufacture of dexamethasone intravitreal implants due to its link with total porosity. In addition to SEM imaging, optical profilometry may also be a good technique for evaluating and quantifying surface roughness.[118]

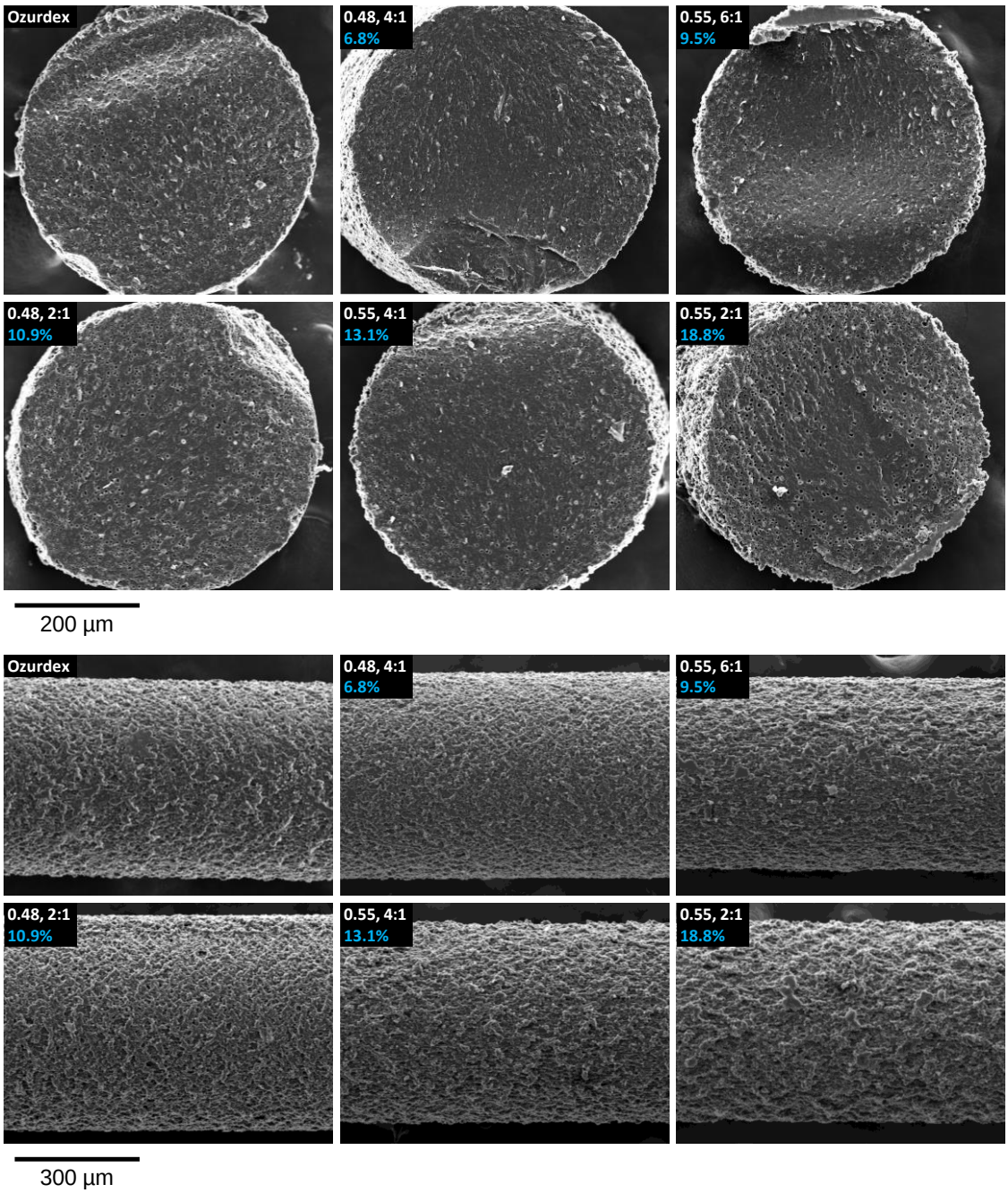

Figure 5.8. Scanning electron microscope images of Ozurdex and the five implants of different total porosity produced with the five dies evaluated in this study. Cross-section at 300× (top panel) and side view at 200× (bottom panel). The total porosity and die design for each sample is shown on the corresponding image.

The total porosity of the implants ranged from 6.8–18.8% across the five runs (see Figure 5.9B). Additionally, extruder torque during steady-state processing ranged from 83–148 N-cm across the runs (see Figure 5.9A). Steady-state extruder torque followed the opposite trend of total porosity, where more restrictive dies resulted in higher torque values. Figure 5.9C shows the relationship between extruder steady-state torque and total implant porosity. Higher torque values, indicative of higher barrel fill and increased melt pressure, resulted in reduced total implant porosity. The higher melt pressure required to force the melt through the more restrictive dies likely forced the trapped air bubbles that contribute to internal porosity out of gaps in the extruder barrel or backward through the feeding zone. Although not a perfect correlation, extruder process torque can be used as a proxy for total implant porosity in real-time during manufacture when evaluating different die designs at fixed extruder processing conditions.

In addition to unit dose potency, total implant porosity may also impact the mechanical strength of the implants. Implant strength may be an important consideration during intravitreal injection to reduce the risk of fracture during administration. The five implants of different total porosity were subjected to a three-point bend test based on the method described in ASTM D7264.[114] The loading force was increased until implant fracture occurred and the maximum force before fracture was recorded (see Figure S5.3). Intuitively, implants with higher total porosity required less force to induce fracture. The least porous implant (6.8%; 0.48 mm, 4:1) had a breaking force 66% higher than the most porous implant (18.8%; 0.55 mm, 2:1). It is likely that the implant fracture force would correlate more closely with the internal porosity of the implants (rather than the total implant porosity) as the external void volume was not expected to affect mechanical strength; however, a separate assessment of internal porosity was not performed in this work.

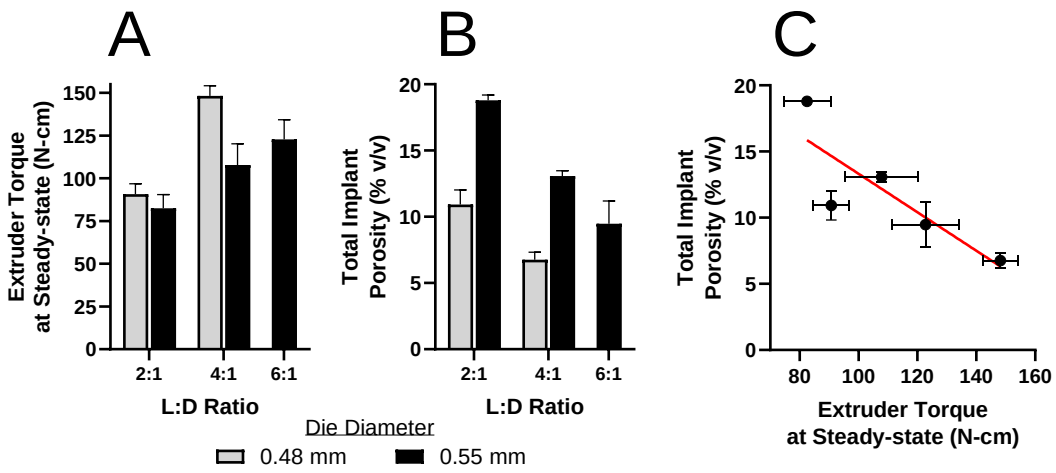

Figure 5.9. Extruder torque at steady-state (mean ± S.D., *n*=1500) (A) and total implant porosity (mean ± S.D., *n*=5) (B) for each die design evaluated. The relationship between the two parameters is presented in (C), with a least-squares regression line shown in red to emphasize the directionality of the relationship.

To better quantify the relationship between die design and total implant porosity, a multiple linear regression model for total implant porosity was fit to the two die parameters varied in this experiment (see Figure 5.10). A strong correlation was found with $R^2 = 0.991$. Both die diameter and die land length had a statistically significant impact ($p < 0.01$) on total implant porosity. The model emphasizes the importance of die design in melt extrusion of dexamethasone intravitreal implants and can be used to fine-tune die design parameters to reach a target total implant porosity.

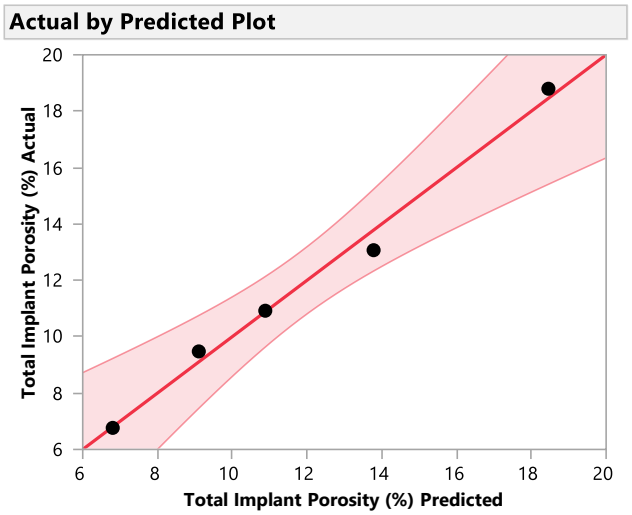

Summary of Fit

RSquare	0.9907
RSquare Adj	0.9814
Root Mean Square Error	0.6179
Mean of Response	11.805
Observations (or Sum Wgts)	5

Analysis of Variance

Source	DF	Sum of Squares	Mean Square	F Ratio
Model	2	81.299240	40.6496	106.4528
Error	2	0.763711	0.3819	Prob > F
C. Total	4	82.062951		0.0093 *

Parameter Estimates

Term	Estimate	Std Error	t Ratio	Prob>|t|
Intercept	-41.04	4.4337	-9.26	0.0115 *
Die Diameter (mm)	116.68	8.9759	13.00	0.0059 *
Die Land Length (mm)	-4.25	0.3641	-11.67	0.0073 *

Figure 5.10. Regression model for die design parameters and total implant porosity.

In addition to die design, extruder process parameters also play an important role in controlling total implant porosity. Although a comprehensive design of experiments (DOE) for extruder process parameters was not included in the scope of this study, experimentation revealed a similar trend between steady-state extruder torque and total implant porosity. Factors that reduced steady-state extruder torque, such as increasing die temperature or reducing screw speed, tended to increase total implant porosity (data not shown). Taken together, these findings associated with both extruder process parameters and die design suggest total implant porosity appears to be dictated by the melt pressure inside the extruder. Essentially, total implant porosity is directly related to the amount of trapped air from the feeding zone that is allowed to remain in the extrudate, which is controlled by the manufacturing parameters.

5.3.6. In vitro release testing

As discussed above, total implant porosity can be directly correlated to the unit dose assay of dexamethasone intravitreal implants; however, the impact of these porosity

differences on drug release was unclear. To address this gap, in vitro release testing was performed on the five implants of different total porosity in normal saline (0.9% (w/v) NaCl in water). In vitro release testing was performed in normal saline to match the method published by the manufacturer of Ozurdex.[38] Using normal saline accelerates the drug release profile approximately three-fold compared to phosphate-buffered media. Additionally, drug release in saline was observed to closely match the in vivo release profile of the dexamethasone intravitreal implants in rabbit eyes, as discussed in the Ozurdex patent documentation.[47]

Several studies throughout the literature have previously demonstrated that the porosity of PLGA–based dosage forms can have a significant impact to drug release.[60] In one example, risperidone microspheres with higher porosities showed faster PLGA degradation and a reduced duration of the lag phase of release due to improved access of water throughout the particles.[119] Pore closure in PLGA dosage forms has been well characterized in the literature and attributed to viscous flow of the polymer chains induced by the surface tension and curvature of the pores.[120] In another example, pore closure and opening was shown to be dynamic during release testing of protein-containing microspheres.[77] The temperature of the test conditions were shown to be a critical factor for the pore structure inside the microparticles throughout in vitro release testing, where higher temperatures promoted viscous flow of the polymer and subsequent pore closure.

The in vitro drug release profiles in normal saline of the five dexamethasone intravitreal implants of different total porosity were all substantially similar and very close to the release profile of the Ozurdex commercial product (see Figure 5.11A). In all samples, a limited burst release was seen on Day 1 (1–2%), followed by a one-week lag phase where limited drug release occurred (≤ 10%). Most of the drug release occurred in

the final phase, starting after Day 7. Although the curves show some separation at the Day 14 timepoint, they converge at Day 21 and all subsequent timepoints, resulting in release curves that are all very similar.

The finding that total implant porosity had limited impact to drug release was not unexpected based on our previous characterization of the drug release mechanisms of dexamethasone intravitreal implants.[51] Our previous studies showed that water ingress into the implant at early timepoints (Day 0 to Day 4) resulted in sufficient plasticization of the PLGA matrix at 37 °C to close the internal pores present at Day 0 and smooth the outer surface of the implants. Since the dexamethasone particles had limited intermolecular interaction with the PLGA, the polymer acted as a barrier to the water required for dissolution until sufficient polymer hydrolysis enabled its diffusion away from the implant. As a result, most of the drug release does not occur until after Day 7, the point at which the PLGA has degraded sufficiently to expose the dexamethasone crystals to substantial amounts of water for dissolution. The differences in total porosity between the implants were eliminated prior to the substantial drug release seen at Day 14 and beyond.

In vitro release testing was also performed in phosphate-buffered saline (pH 7.4) on three implants corresponding to the high, mid, and low values of the range of porosities prepared. Like the findings in normal saline, the three implants tested showed no major differences in drug release profile (see Figure 5.11B). As expected, the release profile in PBS was significantly longer than normal saline due to neutralization of the free acids liberated by hydrolysis, which limited the autocatalytic degradation of the PLGA. Like the normal saline samples, any initial differences in total porosity were likely eliminated during the lag phase of release due to moisture ingress and PLGA

plasticization, rendering the implants practically identical in structure prior reaching the final phase of the release profile where the majority of drug release occurs.

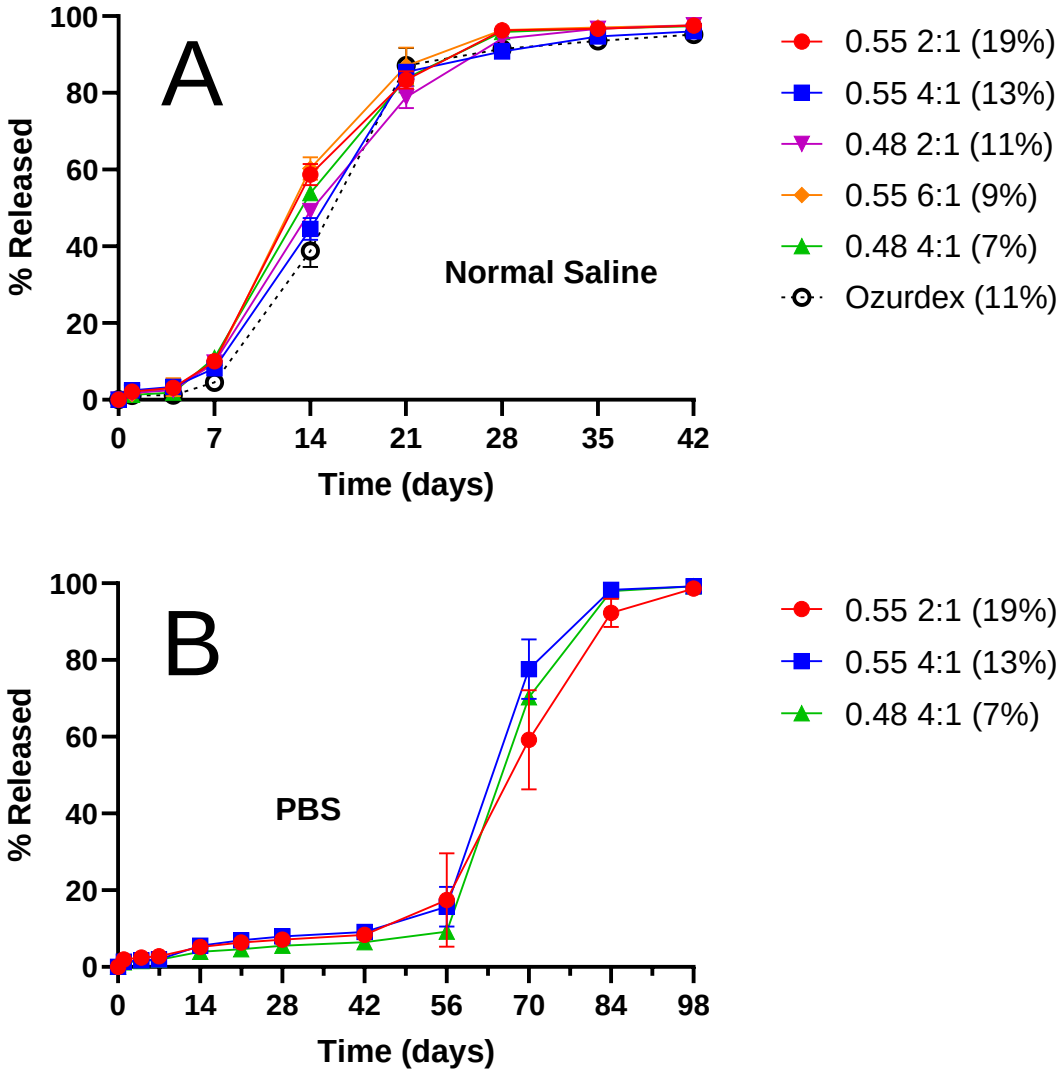

Figure 5.11. In vitro release testing of implants with different total porosity in normal saline (A) and phosphate-buffered saline (pH 7.4) (B). The release profile of the Ozurdex commercial product was also evaluated in normal saline. Mean ± S.D. reported; *n*=2 for Ozurdex in normal saline and *n*=3 for all other samples.

5.4. CONCLUSION

A continuous hot-melt extrusion process was developed to produce dexamethasone intravitreal implants similar to Ozurdex. Accurate control of implant structural characteristics during manufacture was required to maintain consistent unit dose potency. Implant diameter, internal porosity, and external surface morphology must all be controlled during manufacture to produce implants of appropriate label claim. Steady feeding of the melt-extrusion process was critical to reduce variability in implant diameter during the steady-state collection period of each run. The high solids load (60% w/w dexamethasone) of the extrudate melt gave it unique rheological properties that significantly limited the achievable draw down ratio, effectively requiring a die with a diameter less than 0.65 mm to produce implants of the target diameter (0.457 mm).

Changes to the extruder die design (land length and diameter) resulted in changes to total implant porosity. Despite the structural differences between the implants produced with different die designs, no differences in the in vitro release profiles were observed, and all profiles were similar to the Ozurdex commercial product. Mechanistically, the internal and external structural differences seen prior to in vitro release testing were eliminated during the first few days of testing due to polymer plasticization with water before any substantial drug release occurred.

The findings presented in this work suggest that changes to dexamethasone intravitreal implant morphology had a greater impact to unit dose potency and mechanical strength than the rate and duration of controlled drug release. Such a finding suggests some structural flexibility in the preparation of similar implants without compromising the drug release profile. The development of the hot-melt extrusion

process used to prepare the implants in this study may facilitate the development of generic implants referencing Ozurdex. Additionally, the process characterization methods applied here may be used during development of other melt extruded solid implant formulations.

ACKNOWLEDGEMENTS

This work was supported by the Broad Agency Announcement (BAA) Contract # 75F40120C00198 from the U.S. Food and Drug Administration (FDA). The content reflects the views of the authors and should not be construed to represent the views or policies of the U.S. FDA.

Chapter 6. Role of PLGA variability in controlled drug release from dexamethasone intravitreal implants*

ABSTRACT

Long-acting injectable formulations based on poly(lactide-co¬-glycolide) (PLGA) have been commercialized for over 30 years in at least 20 FDA–approved products. These formulations offer several advantages, including reduced dosing frequency, improved patient compliance, and maintenance of therapeutic levels of drug. Despite extensive study, the inherent complexity of the PLGA copolymer still poses significant challenges associated with the development of generic formulations having drug release profiles equivalent to the reference listed drug. In addition, small changes to PLGA physicochemical properties and/or the drug product manufacturing process can have a major impact on the drug release profile of these long-acting formulations.

This work seeks to better understand how variability in the physicochemical properties of similar PLGAs affects drug release from PLGA solid implants using Ozurdex (dexamethasone intravitreal implant) as the model system. Four 50:50, acid-terminated PLGAs of similar molecular weight were used to prepare four dexamethasone intravitreal implants structurally equivalent to Ozurdex. The PLGAs were extensively characterized using a variety of analytical techniques prior to implant manufacture using a continuous, hot-melt extrusion process. In vitro release testing of the four structurally-equivalent implants was performed in both normal saline and phosphate-buffered saline (PBS), yielding drastically different results between the two methods. In normal saline, no differences in the release profiles were observed. In PBS, drug release profiles were sensitive to small changes in residual monomer content, carboxylic acid end group

* This manuscript will be submitted for publication. Mark A. Costello wrote the manuscript and designed, executed, and interpreted the experiments.

content, and blockiness of the polymers. This finding further underscores the need for a physiologically relevant in vitro release testing method as part of a robust quality control strategy for PLGA–based solid implant formulations.

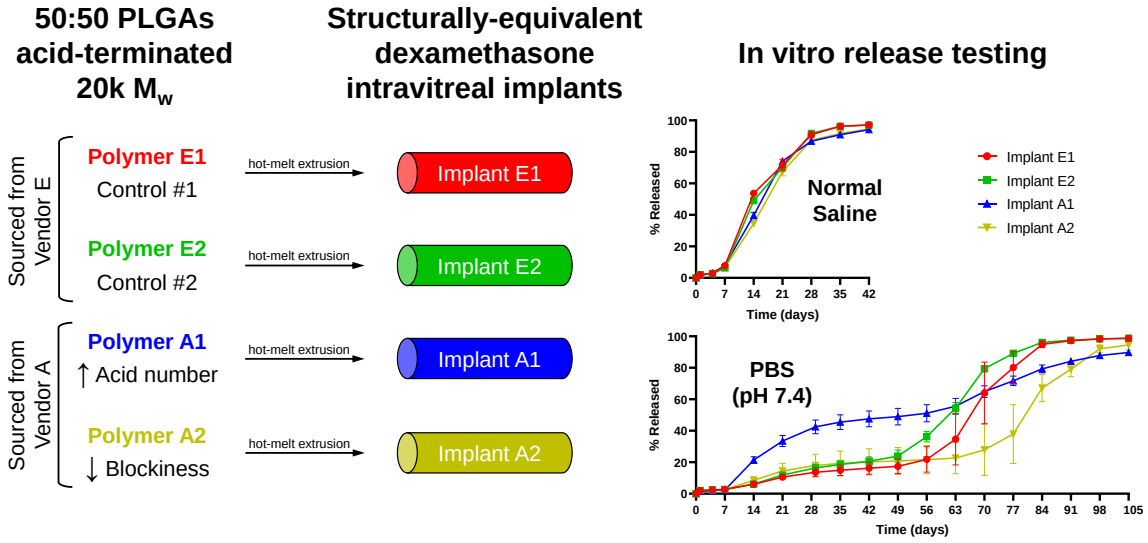

Illustration 6.1. Graphical abstract for Chapter 6.

6.1. INTRODUCTION

Biodegradable, long-acting injectable formulations based on poly(lactide-*co*-glycolide) (PLGA) have been applied for a variety of indications since the first PLGA–based product, Lupron Depot, gained FDA–approval in January 1989.[4] Since then, more than 20 other PLGA–based formulations have been approved by the FDA.[1] The copolymer, typically synthesized from lactide and glycolide by ring-opening polymerization, can be prepared under a variety of conditions to produce PLGAs with very different rate-controlling properties.

The inherent complexity of the PLGAs used to prepare these dosage forms is a double-edged sword. On one side, alteration of the polymer properties such as the

molecular weight, lactide/glycolide ratio, and chain capping enables extended delivery of small molecules and peptides for durations ranging from one week to six months. On the other side, the inherent heterogeneity of the polymer makes manufacture, scale-up, and development of generic equivalent formulations very challenging. This is especially evident by the limited number of approved generic PLGA–based formulations in the USA, despite many of the innovator drug products extending well beyond their marketing exclusivity period.[27]

Most of these dosage forms exist as microparticles prepared by an emulsion/solvent extraction process. It has been well documented that PLGA properties, the manufacturing conditions used, and the interplay between them directly impacts the microparticle properties and, most importantly, the drug release kinetics of these formulations.[60, 108, 121] Previous work by Wan et al. with leuprolide acetate microspheres showed that sourcing similar PLGAs from different suppliers produced microspheres with different physical properties (e.g., particle size, porosity) when using the same manufacturing process.[13] Consequently, the drug release profiles differed between the formulations. Similarly, when using risperidone as a model drug, small differences in PLGA properties resulted in microspheres with different particle size distributions and internal microstructures, again leading to significant variations in drug release kinetics.[122] In particular, this earlier study identified PLGA blockiness as a critical parameter affecting PLGA degradation rate and the drug release kinetics of the microparticles.

PLGA blockiness refers to the ordering of lactic acid and glycolic acid monomer units on the polymer chain.[123] Chemically, the methyl group present in the α position of polymerized lactic acid makes it more hydrophilic and less reactive due to steric hinderance when compared to glycolic acid. This renders the G-G linkage more prone to hydrolysis than the G-L or L-L linkages in the polymer.[22] Accordingly, PLGAs with

greater blockiness (more G-G linkages) are expected to degrade faster and release drug more quickly than less blocky PLGAs. Further assessment of the impact of blockiness on drug release from PLGA–based dosage forms is warranted.

In this work, the impact of small changes in PLGA properties (including blockiness) was investigated, using Ozurdex (dexamethasone intravitreal implant) as the model system. In contrast to the abovementioned microparticles, Ozurdex is a monolithic solid implant approximately 0.46 mm in diameter and 6 mm long produced by a continuous hot-melt extrusion process. Despite major differences in the size/shape of the dosage form compared to microparticles, the same PLGA degradation phenomena dictate drug release from the implant.[8]

The Ozurdex implant is comprised of a mixture of acid-terminated and ester-terminated 50:50 PLGAs. During melt extrusion, the dexamethasone and PLGAs are intimately mixed into a two-phase system of drug crystals uniformly dispersed in the PLGA matrix. The present study sourced four unique acid-terminated 50:50 PLGAs with similar molecular weights from two vendors to assess how subtle differences in physicochemical properties can impact implant manufacture and drug release in vitro. The four polymers were subjected to identical processing conditions to produce implants that were structurally equivalent to one another. This structural equivalence enabled an isolated study of how polymer properties can impact drug release in vitro. For developers considering sourcing PLGAs from various vendors, this work highlights the importance of thoroughly characterizing the polymers before, during, and after manufacture to develop products with release profiles equivalent to the reference listed drug (RLD).

6.2. MATERIALS AND METHODS

6.2.1. Materials

Ozurdex (dexamethasone intravitreal implant) (Allergan USA, Inc; Madison, NJ, USA) was purchased from a pharmacy supplier. Four lots of acid-terminated 50:50 poly(D,L-lactide-*co*-glycolide) (PLGA) were purchased from two vendors, two from Evonik Industries AG (Essen, Germany) and two from Akina Inc. (West Lafayette, IN). Ester-terminated 50:50 PLGA, Resomer RG 502, was also purchased from Evonik. Dexamethasone was purchased from Shenzhen Nexconn Pharmatechs Ltd. (Shenzhen, China). HPLC–grade acetone, HPLC–grade acetonitrile, ACS–grade sodium chloride, and 10x phosphate buffered saline (PBS) solution were purchased from Thermo Fisher Scientific (Waltham, MA, USA). Distilled, deionized water was obtained in the laboratory. All other reagents used in this work were of analytical grade.

6.2.2. Methods

6.2.2.1 Molecular weight distribution of PLGAs

Gel permeation chromatography (GPC) was used to determine the molecular weight of PLGA in a variety of samples throughout the study using a Waters GPC system equipped with a 2414 refractive index (RI) detector and an integrated 2707 autosampler (Waters Corporation; Milford, MA, USA). The 100% acetone mobile phase was pumped at a flow rate of 0.6 mL/min through two Tosoh TSKgel GMH_{HR}-L columns connected in series (Tosoh Corporation; Tokyo, Japan). A calibration curve was generated using nine poly(methyl methacrylate) (PMMA) standards (500–200,000 Da) (Agilent Technologies; Santa Clara, CA, USA). All PLGA samples and PMMA standards were dissolved in acetone and injected with a volume of 50 μL. All samples were evaluated in triplicate apart from the Day 28 sample taken during in vitro release testing in normal saline, in

which the three replicates were combined into a single sample to provide sufficient mass for GPC analysis. When evaluating the molecular weight of the PLGAs in the implant throughout the dissolution process using GPC, all samples were first lyophilized to remove residual water using the conditions listed in Section 6.2.2.12.

6.2.2.2 Thermal analysis of PLGAs

A Q20 DSC (TA Instruments; New Castle, DE, USA) was used to evaluate the glass transition temperature (T_g) of the neat PLGAs and the PLGAs in the implants throughout the manufacturing process. All samples were subjected to a heat–cool–heat cycle with the following parameters: 1) heat to 110 °C with a ramp rate of 20 °C/min, 2) hold isothermally at 110 °C for 5 minutes to remove residual moisture, 3) cool to -10 °C with a ramp rate of 20 °C/min, and 4) ramp to 75 °C at 4 °C/min under modulated heating conditions (± 1 °C every 45 s). The reversible heat flow signal from the second heating cycle was used to determine T_g for all samples tested.

6.2.2.3 Moisture content of PLGAs

Moisture content of the PLGAs was determined using a C20 Karl Fischer titrator (Mettler Toledo; Columbus, OH, USA). For each sample, 500 mg of PLGA was loaded into a glass vial that was then sealed with a rubber septum and charged with 7 mL of anhydrous methanol. Moisture extraction occurred for 1 h under continuous shaking on a tabletop shaker. 500 µL of the methanol extract was withdrawn from the vial using a 1 mL syringe and injected into the titrator. The water content of the anhydrous methanol was subtracted before reporting the moisture content of the sample.

6.2.2.4 Lactide/glycolide ratio, residual monomer, and blockiness of PLGAs[†]

^{1}H NMR was used to determine the lactide/glycolide ratio and the residual lactide and glycolide monomer content of the PLGAs. ^{1}H NMR samples were prepared by dissolving the PLGA in 0.7 mL of $CDCl_3$ (Cambridge Isotope Laboratories; Tewksbury, MA, USA) at *ca*. 50 mg/mL. Spectra were collected on an Avance III 500 NMR spectrometer (Bruker; Billerica, MA, USA) at 500 MHz using 32 scans with a 5 s relaxation delay. ^{1}H NMR spectra were phase- and baseline-corrected using MestreNova software (Mestrelab Research; Santiago de Compostela, Spain) before analysis. Integration areas from the resonances for the glycolyl repeat unit CH_2 (*ca.* 4.60-4.89 ppm), glycolide monomer CH_2 (*ca.* 4.89-4.96 ppm), lactide monomer CH (*ca.* 5.00-5.08 ppm), and lactyl repeat unit CH (*ca.* 5.08-5.28 ppm) were used for determining residual monomer and lactide/glycolide composition. See Figure S6.3 for an example ^{1}H NMR spectrum.

^{13}C NMR was used to quantify PLGA blockiness in the form of glycolate block length using a method similar to the one described by Engwicht et al.[124] Polymers were dissolved in $CDCl_3$ at a concentration of at least 50 mg/mL. Measurements were carried out at 125 MHz on the same Avance III 500 NMR spectrometer using Bruker's standard C13CPD pulse sequence. 1024 scans and a 1 s relaxation delay were used. Acquisition time was increased to 4.404 s to improve the resolution of the spectra. The chemical shifts relative to the residual chloroform resonance corresponding to the carbonyl in a G-G sequence and G-L sequence were *ca.* 166.5 ppm and 166.6 ppm, respectively. Since the G carbonyl resonance cannot be cleanly resolved into two peaks, all the resonances were split at the downfield side of the trough between the two large peaks, even in the

[†] Louise Kuehster collected and processed all NMR data shown in this chapter.

case where the upfield side of the trough was lower. See Figure S6.4 for an example ^{13}C NMR spectrum.

6.2.2.5 Acid number of PLGAs

The carboxylic acid end group content (i.e., the acid number) of the PLGAs was determined using an automated potentiometric titration method.[125] The PLGAs were dissolved in 80:20 acetonitrile:water (v/v) to a concentration of 5 mg/mL using a vortexer and brief sonication. The samples were titrated with an aqueous solution of 0.05 M NaOH under constant stirring while monitoring the pH. A 515 HPLC Pump (Waters Corporation; Milford, MA, USA) was used to deliver the titrant at 0.100 mL/min. Custom MATLAB software (MathWorks; Natick, MA, USA) was developed to record the pH from an Orion Versa Star Pro benchtop pH meter (Thermo Fisher Scientific; Waltham, MA, USA) every second during the titration. The acid number, corresponding to the inflection point of the titration curve, was determined programmatically using the first derivative test. The acid number is expressed in mg NaOH/g PLGA corresponding to the amount of strong base needed to deprotonate all exposed carboxylic acids on the polymer chains. See Figure S6.1 for example titration curves.

6.2.2.6 Melt rheology of implant formulations[‡]

Rheological properties of the implant formulations were evaluated using a 25 mm parallel plate setup on a Physica MCR 301 rotational rheometer (Anton Paar; Graz, Austria). The rheometer was fitted with a Peltier temperature control hood (H-PTD200) to maintain constant temperature during testing. Granules of each formulation taken after the first extrusion process (see Section 6.2.2.7) were used for testing. These granules

[‡] Joseph Liu collected all rheological data shown in this chapter.

were weighed to a target mass of approximately 670 mg and gently compressed in a hydraulic press (MTCM-I, GlobePharma; New Brunswick, NJ, USA) fitted with a 10 mm round die to produce consistent slugs for testing. All tests were performed at 99 °C with a 1 mm gap height. Immediately prior to testing, the slugs were softened at the testing temperature and pressed to the 1 mm gap height to fill the volume under the 25 mm plate. A rotational test was used to generate viscosity curves with shear rates logarithmically ramped from 0.01 – 10 s^{-1}. Viscoelastic behavior was evaluated using an oscillatory amplitude sweep of shear strain ranging from 0.01-100% at a frequency of 10 rad/s.

6.2.2.7 Manufacture of dexamethasone intravitreal implants

Dexamethasone intravitreal implants were manufactured using a double extrusion and shaping process, as described in our previous work.[8] The dual extrusion technique was necessary to accurately control the implant diameter and maintain consistent structural characteristics during implant manufacture. Briefly, both steps of the hot-melt extrusion process were performed using a Haake MiniLab twin-screw extruder (Thermo Electron (Karlsruhe) GmbH; Karlsruhe, Germany). In the first extrusion, a blend of micronized dexamethasone and jet-milled PLGA was extruded at 105 °C and shaped into rods using a 1 mm diameter die. After the first extrusion, the rods were milled to produce free-flowing granules that enabled steady feeding during the second extrusion. For the second extrusion, a dual-feeder setup was used to precisely control the feed rate of the milled extrudate (8.5 g/h) into the extruder (set to 105 °C and 75 rpm) fitted with a heated 0.55 mm diameter die at the discharge port set to 99 °C. A downstream puller (IMSTec USA, Inc.; Temecula, CA, USA) was used to draw down the melt to the target diameter of 457 μm (0.0180 in). Online process monitoring of extruder torque and implant diameter was performed using custom MATLAB software (MathWorks; Natick, MA,

USA). Implant rods of variable length were collected, allowed to cool down to room temperature, and manually cut to approximately 6 mm in length to produce individual implants.

6.2.2.8 Implant structural analysis

Scanning electron microscopy (SEM) was used to evaluate the internal and external structure of the melt extruded implants. The implants were carefully fractured to reveal a cross-section to visualize the size and distribution of internal voids. Prior to imaging, all SEM samples were attached to aluminum stubs using double-sided carbon tape, then sputter-coated with gold for 60 s at 40 mA (Electron Microscopy Sciences; Hatfield, PA, USA). Imaging was performed using a Quanta 650 FEG SEM (FEI Company; Hillsboro, OR, USA) using an accelerating voltage of 15 kV.

6.2.2.9 Total implant porosity

Total implant porosity was derived from the implant's dimensions, mass, and the true density of its components. This geometric approach to quantifying implant porosity assumed that the implant was a perfect cylinder. In actuality, imperfections on the surface of the implant formed voids between an imagined surrounding cylinder and the actual surface of the implant. Consequently, the *total porosity*, as applied in this work, included both the external void volume caused by surface imperfections and the internal void volume generated from closed pores.[63]

Digital calipers (CD-6" ASX, Mitutoyo Corp., Kanagawa, Japan) were used to measure the length of a 2–3 cm segment of melt extrudate. The diameter of the implant segment was measured at five equidistant points along the length using a laser micrometer (BETA LaserMike AccuScan 5012, NDC Technologies Inc.; Dayton, OH,

USA). The mass was measured using a microbalance (MSA3.6P0TRDM, Sartorius; Göttingen, Germany) with a precision of 0.001 mg. The true density of the dexamethasone–PLGA powder blend was previously determined to be 1.365 g/cm^3 using a helium pycnometer.[8] Equation 6.1 was used to calculate the implant porosity:

Equation 6.1.

$$Implant\ Porosity = \left(1 - \frac{\left(\frac{Implant\ Mass}{\pi \times \left(\frac{Avg.\ Diameter}{2} \right)^2 \times Length} \right)}{True\ Density} \right) \times 100\%$$

6.2.2.10 Dexamethasone assay

A Waters HPLC equipped with a 2996 photodiode array (PDA) detector and integrated 717plus autosampler (Waters Corporation; Milford, MA, USA) was used to quantify the dexamethasone content of whole implants and the release media during in vitro release testing. A flow rate of 1 mL/min of 60:40 acetonitrile:water (v/v) mobile phase was used along with a Luna 5 μm C18(2) 100 Å column (150 mm × 4.6 mm) (Phenomenex; Torrance, CA, USA) and a detection wavelength of 241 nm. Triplicate injections were used for all samples. The peak corresponding to dexamethasone had a retention time of 2.4 min. Whole implant samples were dissolved in mobile phase, subjected to a brief sonication to aid dissolution, and filtered using a 0.45 μm PTFE syringe filter. Duplicate 3-point calibration curves were generated from 0.1 to 10 μg/mL ($R^2 \geq 0.9999$) to quantify the dexamethasone content of the release media and whole implant fragments remaining at the final dissolution timepoint.

6.2.2.11 In vitro release testing

In vitro release testing was performed in 30 mL normal saline (0.9% NaCl (w/v)) or phosphate-buffered saline (PBS, pH 7.4) at 37 °C and 100 rpm using a New Brunswick Innova 40 incubator/shaker (Eppendorf; Hamburg, Germany). This volume was sufficient to maintain sink conditions (> 3×) throughout in vitro release testing as dexamethasone is a nonionizable molecule with a reported aqueous solubility of ~90 μg/mL at 37 °C.[35, 58] For the normal saline samples, sampling occurred on Days 1, 4, 7, and each week thereafter until Day 42. For the PBS samples, sampling occurred on Days 1, 4, 7, and each week thereafter until Day 105. At each timepoint, 25 mL of the release medium was removed for HPLC analysis and immediately replaced with 25 mL of fresh medium. Release data were normalized to the assay of the remaining implant fragment at the final timepoint: Day 42 for the normal saline samples and Day 105 for the PBS samples.

6.2.2.12 Mass loss, water content and lyophilization

Implant mass loss and water content were evaluated throughout in vitro release testing by recording the implant mass before and after lyophilization using a microbalance with a precision of 0.001 mg (MSA3.6P0TRDM, Sartorius; Göttingen, Germany). All samples for this analysis were staged in the incubator/shaker together on Day 0, as each sample was completely consumed at each timepoint for this analysis. The wet mass of the implant was determined by carefully recovering the sample from the dissolution medium and gently patting it dry with a Kimwipe (Kimberly-Clark Professional; Roswell, GA, USA) prior to measuring the mass with the microbalance. After recording the wet mass, all samples were transferred to a –20 °C freezer for holding until the final dissolution timepoint, at which all implants were lyophilized together using

a VirTis AdVantage EL-85 Freeze Dryer (SP; Warminster, PA, USA) with the following three-step method: (1) 1200 minute hold at −40 °C under 100 mTorr vacuum, (2) 1200 minute ramp from −40 °C to 25 °C under 100 mTorr vacuum, and (3) 1200 minute hold at 25 °C under 100 mTorr vacuum.

After lyophilization, the dry mass of each implant was measured using the microbalance. The total mass loss and moisture pick up were calculated using Equation 6.2 and Equation 6.3, respectively.

Equation 6.2.

$$\%\ Total\ Mass\ Loss\ (t) = \frac{Initial\ Mass\ -\ Dry\ Mass\ (t)}{Initial\ Mass} \times 100\%$$

Equation 6.3.

$$\%\ Moisture\ Pick\ Up\ (t) = \frac{Wet\ Mass\ (t)\ -\ Dry\ Mass(t)}{Dry\ Mass(t)} \times 100\%$$

6.3. RESULTS AND DISCUSSION

6.3.1. Sourcing the PLGAs

The four acid-terminated PLGAs studied in this work were purchased from two manufacturers: Evonik Industries AG (Essen, Germany) and Akina Inc. (West Lafayette, IN, USA). Evonik has been a long-time supplier of commercial PLGAs since their acquisition of the Resomer line of products from Boehringer Ingelheim in 2011.[65, 126] In this work, two lots of Resomer RG 502 H PLGA (Polymer E1, Polymer E2) and a single lot of ester terminated PLGA (Resomer RG 502) were sourced from Evonik. Notably, the

prescribing information for Ozurdex directly lists Resomer RG 502 H and Resomer RG 502 as the rate-controlling polymers in the Ozurdex implant.[56]

The other two acid-terminated polymers studied in this work were purchased from Akina Inc. Akina is a research company that offers a variety of biodegradable and biocompatible polymers for research purposes, including custom synthesis of PLGAs. The two polymers purchased from Akina were custom syntheses of 50:50 acid-terminated PLGA with molecular weights close to that of Evonik's Resomer RG 502 H. The reaction conditions of the two custom PLGAs were deliberately altered to produce polymers of different blockiness (Polymer A1 and Polymer A2). Higher temperatures during polymerization of lactide and glycolide promote transesterification in the PLGA, resulting in scrambling of the G–G and L–L repeat units and reducing blockiness.[21, 127] Polymer A2 was expected to be less blocky since the polymerization was performed at a higher temperature than Polymer A1.

The composition of the dexamethasone intravitreal implants prepared in this study resembling Ozurdex is presented in Table 6.1. The composition of the implant was deduced from both the literature and experimentation, as discussed in our reverse engineering study of the Ozurdex implant.[8] A single lot of dexamethasone and a single lot of ester-terminated PLGA were used to prepare the four implant formulations. The source of acid-terminated PLGA was varied between the four lots used in this study: Polymers E1, E2, A1, and A2.

Material	Mass per implant (mg)	% w/w
Dexamethasone (Form B, micronized)	0.700	60%
50:50 PLGA, acid terminated	0.350	30%
50:50 PLGA, ester terminated (Resomer RG 502)	0.117	10%
Total	1.167	100%

Table 6.1. Composition of the dexamethasone intravitreal implants resembling Ozurdex prepared in this study.

Studying Polymers E1 and E2 in Ozurdex-like implants enabled a proper evaluation of the impact of lot-to-lot variability of the polymer on manufacture and drug release of the dexamethasone intravitreal implants. Being commercially available materials, and the polymers used in Ozurdex, limited variation in drug release performance during in vitro release testing was expected between the two implants prepared with the two Evonik polymers (E1 and E2). On the other hand, developers of generic formulations referencing Ozurdex may consider sourcing their PLGAs from different suppliers. Evaluating PLGAs with similar properties made by a different supplier using a different manufacturing process was intended to reveal the sensitivity of small changes to PLGA properties on manufacture and controlled drug release during in vitro release testing from dexamethasone intravitreal implants.

6.3.2. Characterization of the acid-terminated PLGAs

Polymer	M_n (g/mol) (N=3)	M_w (g/mol) (N=3)	PDI (N=3)	T_g (°C) (N=3)	Moisture Content (%) (N=3)	L/G Ratio (N=1)	Total Residual Monomer (% w/w) (N=1)	G Block Length (N=1)	Acid Number (mg NaOH/g) (N=5)
E1 (●)	7264 (141)	19283 (324)	2.66 (0.05)	44.7 (0.6)	0.32 (0.01)	50/50	0.13	2.53	8.3 (0.2)
E2 (■)	7594 (100)	19875 (312)	2.62 (0.01)	44.7 (0.8)	0.36 (0.02)	51/49	0.10	2.45	8.0 (0.1)
A1 (▲)	7006 (111)	19387 (206)	2.77 (0.06)	42.6 (0.2)	0.29 (0.01)	52/48	0.26	2.54	9.7 (0.2)
A2 (▼)	7649 (129)	22487 (215)	2.94 (0.03)	43.6 (0.4)	0.32 (0.01)	52/48	0.31	2.25	8.6 (0.1)
Ester	10707 (281)	24076 (170)	2.25 (0.04)	43.3 (0.3)	0.25 (0.01)	51/49	0.08	2.56	N/A

Table 6.2. Properties of the four acid-terminated PLGAs evaluated in this study and the single lot of ester-terminated PLGA used in all implant formulations. Mean and standard deviation (in parentheses) reported, where applicable. The symbol and color convention presented in the first column is used throughout this work.

The four acid-terminated PLGAs used in this work were thoroughly characterized using a variety of analytical techniques to evaluate any differences in their physiochemical properties prior to manufacture of the dexamethasone intravitreal implants (see Table 6.2). First, GPC was used to evaluate the molecular weight distribution of the polymers. The chromatograms from GPC analysis showed practically identical curves for Polymers E1, E2, and A1 (see Figure 6.1). The chromatogram for Polymer A2 showed a slight shift to the left (shorter retention time) compared to the other three, leading to a slightly higher reported molecular weight. In general, the number-average molecular weights (M_n) of the four polymers were close to one another, with less than 10% difference between the highest and the lowest values. In this study, using polymers with comparable molecular weight distributions was deemed critical to properly evaluate the impact of polymer source variation on the manufacture and drug release of the dexamethasone intravitreal implants, as small differences in molecular weight are known to impact drug release from PLGA–based formulations.[128]

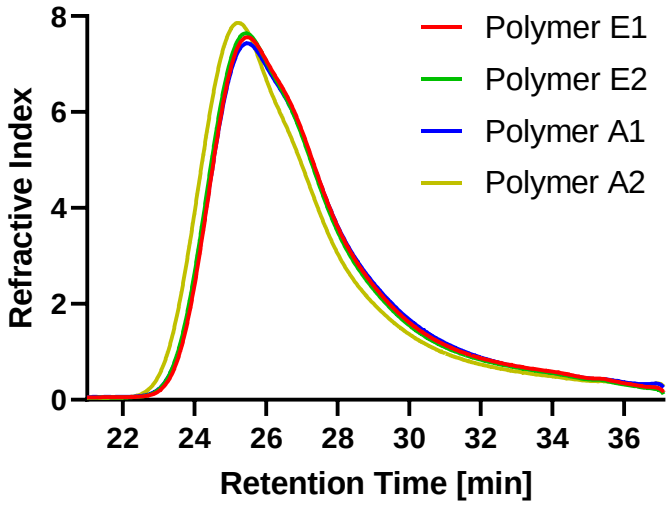

Figure 6.1. Area-normalized mean chromatograms (n = 3) from GPC analysis of the four acid-terminated PLGAs evaluated in this study illustrating their similar molecular weight distributions.

Differential scanning calorimetry (DSC) showed that the four polymers exhibited similar glass transition temperatures (T_g) on the second heating cycle in the range of 42–45 °C. The two Evonik polymers exhibited equal T_g; however, the two Akina polymers had T_g slightly lower than the Evonik polymers. In particular, the T_g of Polymer A1 was statistically lower than the two Evonik polymers ($p < 0.01$) with a difference of 2.1 °C. The measured T_g of PLGA can be impacted by several factors, including molecular weight distribution, the presence of residual monomers, residual solvents, and adsorbed moisture. Although the four polymers showed similar moisture content by Karl Fischer coulometric titration (see Table 6.2), the impact of moisture on T_g in this analysis was eliminated by removing bound water at 110 °C in the first heating cycle. Residual solvents from synthesis (e.g., toluene and acetone, per the manufacturer's certificate of analysis) were also likely removed at the elevated temperature. On the other hand, residual monomers left over from polymer synthesis may have remained and plasticized

the PLGA chains resulting in a lower reported T_g in samples with higher residual monomer.

NMR spectroscopy was also used to determine properties of the PLGAs used in this study, including the lactide/glycolide (L/G) ratio, the total residual monomer, and the blockiness (glycolate block length). ^{1}H NMR showed the L/G ratio of all polymers fell near the theoretical ratio of 50:50. ^{1}H NMR was also used to determine the residual lactide monomer and residual glycolide monomer remaining from the polymerization reaction. These two values were added together to determine the total residual monomer, as reported in Table 6.2. The total residual monomer was notably higher in the Akina polymers compared to the Evonik polymers. However, all samples had a total residual monomer content of $\leq$ 0.5%, in line with the total residual monomer content of other commercially available 50:50 PLGAs.[3]

^{13}C–NMR was used to determine the blockiness of the four acid-terminated PLGAs used in this study using a method similar to the one described by Engwicht et al.[124] The average glycolate block length of Polymers E1, E2, and A1 were all similar, with a value of about 2.5. The average glycolate block length of Polymer A2 was lower than the others, with a value of 2.25. Recall, the polymerization of Polymer A2 was deliberately performed at higher temperature than the polymerization of Polymer A1 to promote transesterification and scrambling of the glycolide and lactide dyads, resulting in a lower average glycolate block length. It should be noted that other reaction conditions, besides temperature, needed to be altered to synthesize Polymer A1 and A2 to a similar molecular weight; however, a detailed discussion of reaction conditions is not in the scope of this study.

Finally, the carboxylic acid end group content, or acid number, of the four acid-terminated PLGAs used in this study was evaluated using a potentiometric titration

method. A commonly applied method to determine the acid number of PLGAs is to perform organic phase titration of a PLGA solution with an organic solution of a strong base (typically KOH in methanol) using phenolphthalein as a visual indicator.[6, 129] Initial attempts to perform this titration with phenolphthalein resulted in significant sample-to-sample variability. Two factors were suspected to contribute to the observed variability using this method. Firstly, the subjective nature of using color change to indicate the 'light-pink' end point of the phenolphthalein titration can make it difficult to determine the true endpoint, as an overly-titrated sample may appear a similar shade of pink. Secondly, and perhaps more critically, the base-catalyzed hydrolysis of the PLGA with the titrant itself and adsorbed water from the air can cause the visually pink endpoint to revert to clear as the hydrolyzed PLGA chain ends expose additional carboxylic acid end groups. This in-process hydrolysis renders the time to complete the titration a critical parameter to avoid excessive contributions of the hydrolysis to the reported acid number.

To overcome both of these limitations, an automated, semi-aqueous titration of the PLGA was performed in an 80/20 acetonitrile/water mixture, building on the method described by Hong and Schwendeman.[125] Briefly, an HPLC pump was used to deliver an aqueous solution of NaOH to the acetonitrile/water PLGA solution under constant stirring while measuring the pH each second. The total time to complete this titration was approximately 5 minutes, minimizing the effects of base-catalyzed hydrolysis during testing. This method produced consistent titration curves between replicates (see Figure S6.1) and showed that Polymer A1 had a higher acid number than the other three polymers ($p < 0.0001$). The higher acid number indicated a larger number of carboxylic acid chain ends, potentially corresponding to a greater number of acid-terminated short-chain oligomers that are not easily detected by GPC. If true, these oligomers may contribute to the reduced T_g observed for Polymer A1.

6.3.3. Rheological properties of the dexamethasone/PLGA blends

Prior to preparation of the dexamethasone intravitreal implants, the melt rheology of each implant formulation (per the composition in Table 6.1) was evaluated using a rotational rheometer. Formulations were named per the unique acid-terminated PLGA used in each blend, e.g., Formulation A1 contained 30% (w/w) Polymer A1. A parallel plate setup was used with a heated chamber set to 99 °C, corresponding to the die temperature setpoint during melt extrusion. First, a rotational test was performed to generate viscosity curves in the low-shear range for the four formulations to evaluate any differences in the resistance to deformation (see Figure 6.2A). The four formulations proved to be very viscous and yielded similar viscosity curves. Although operating at least 50 °C above the glass transition temperature of the PLGA, the high loading of dexamethasone crystals in the formulation (60%, w/w) dramatically increased the formulation's resistance to deformation. The four curves terminated before the targeted shear rate of 10 s^{-1} due to reaching the 200 m-Nm torque limitation of the rheometer. Despite the high viscosity values, all samples exhibited shear-thinning behavior, as expected for polymeric melts. The small differences in viscosity seen at shear rates near 1 s^{-1} trended positively with the number average molecular weights determined via GPC, where the sample with the highest molecular weight exhibited the highest viscosity values.

To better understand the viscoelastic properties of the four formulations, an oscillatory amplitude sweep was performed (see Figure 6.2B). Oscillatory rheological tests can elucidate the elastic portion (i.e., the solid-state behavior) and the viscous portion (i.e., liquid-state behavior) of the overall viscoelastic behavior. The *storage modulus* (G′) represents the solid-like behavior, or the stored deformation energy when shear is applied. The *loss modulus* (G″) represents the liquid-like behavior, or the

deformation energy lost when flowing via internal friction when shear is applied. The four formulations exhibited similar curves for G′ and G″. At low strain, the storage modulus exceeded the loss modulus for all formulations, implying a solid, gel-like consistency of the sample. A transition from solid-dominant to liquid-dominant behavior occurred at shear strains less than 0.1% where the G′ and G″ curves crossed over. At higher strains, all samples became increasingly fluid. Taking this similar viscoelastic behavior together with the viscosity curves, the four formulations were expected to perform similarly during hot-melt extrusion and shaping of the dexamethasone intravitreal implants.

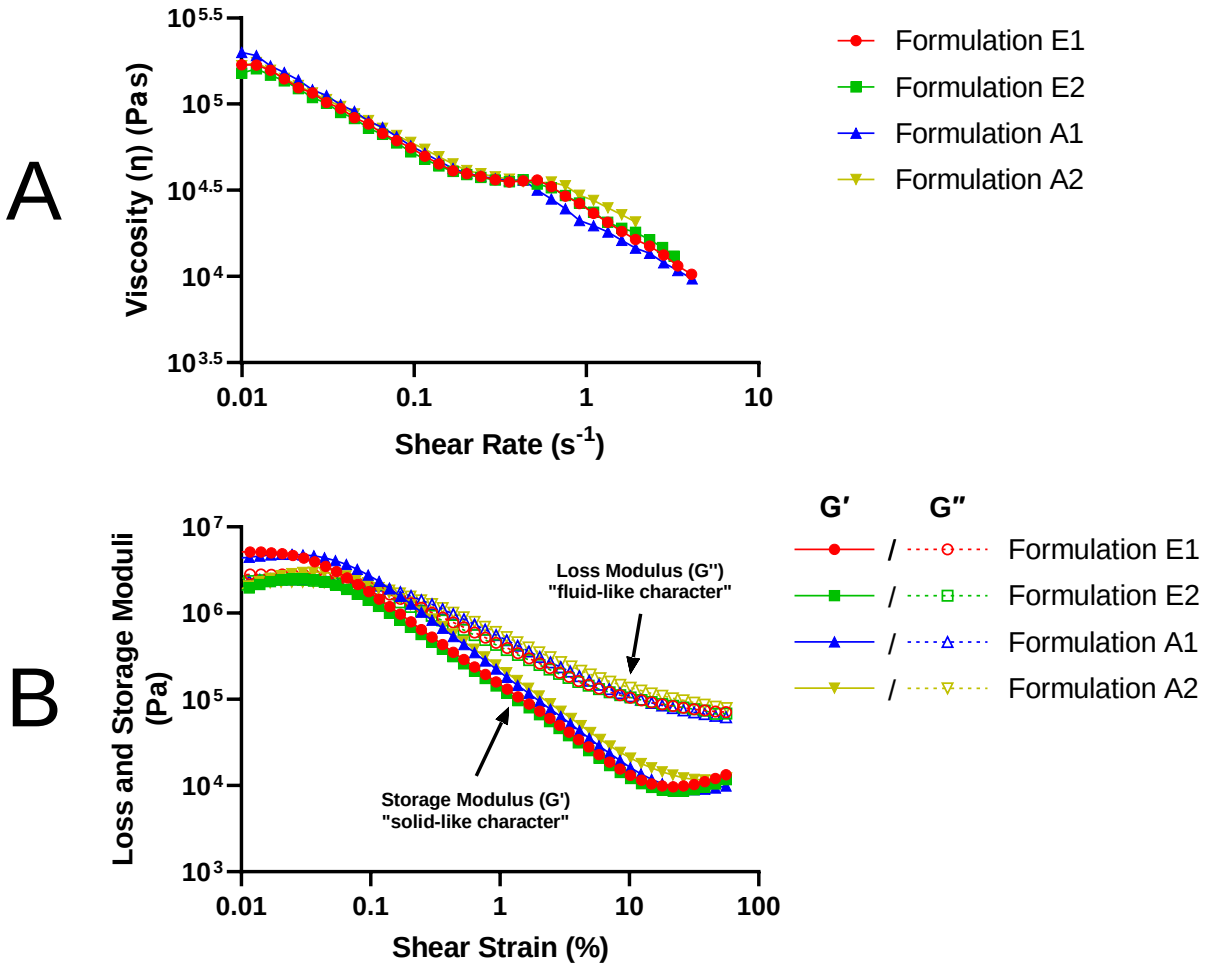

Figure 6.2. Melt rheology of the four implant formulations prepared with four different acid-terminated PLGAs at 99 °C. Viscosity curves from a rotational test (A) and viscoelastic behavior from an oscillatory test (B) are shown. Mean values (n = 2) reported.

6.3.4. Manufacture and characterization of the dexamethasone intravitreal implants

The first step in the preparation of the dexamethasone intravitreal implants was to jet-mill both the dexamethasone and the PLGAs. Dexamethasone was jet-milled to a $D_v(50)$ of 2.1 μm (mean, n = 3), to match the estimated particle size in Ozurdex. Jet-milling of the PLGAs served primarily to break up agglomerates and granules to promote

uniform powder mixing with the micronized dexamethasone during preparation of the pre-extrusion blend. Prior to jet-milling, the Evonik polymers (polymers E1 and E2) were fluffy in nature and exhibited a low bulk density. This remained the case after jet-milling, where the bulk density was likely reduced further based on visual observation. In contrast to this result, the Akina polymers (polymers A1 and A2) were received as dense agglomerates that required manual grinding with a mortar and pestle to enable feeding into the jet-mill. After jet-milling, these polymers remained dense, free-flowing granules, despite some apparent particle size reduction. A large difference in particle size and bulk density between the drug and the polymer could contribute to segregation during pre-extrusion blend preparation and handling[130], so assay of the implants after manufacture was planned.

Dexamethasone intravitreal implants were prepared using the two step, hot-melt extrusion process described in Methods. Identical process parameters were used for the four runs to evaluate the impact of PLGA variability on the manufacture of dexamethasone intravitreal implants. The first extrusion step was used primarily to densify the pre-extrusion blend into free-flowing granules that enabled steady feeding during the second extrusion. The first extrusion also eliminated the differences in bulk density of the pre-extrusion blends caused by the bulk density differences seen between the Evonik and Akina materials, as previously described.

Dexamethasone intravitreal implants resembling Ozurdex were collected for each formulation from the second extrusion run during steady-state operation. All implants consisted of a uniform dispersion of dexamethasone drug crystals embedded in a PLGA matrix. The implants had internal and external structural characteristics remarkably similar to each other and to Ozurdex (see Figure 6.3). All implants exhibited a rough, irregular surface and internal porosity from numerous internal voids, as seen in the SEM

images. The size and radial distribution of the internal voids was also similar between the implants, with the concentration of voids higher near the implant surface and few voids near the core.

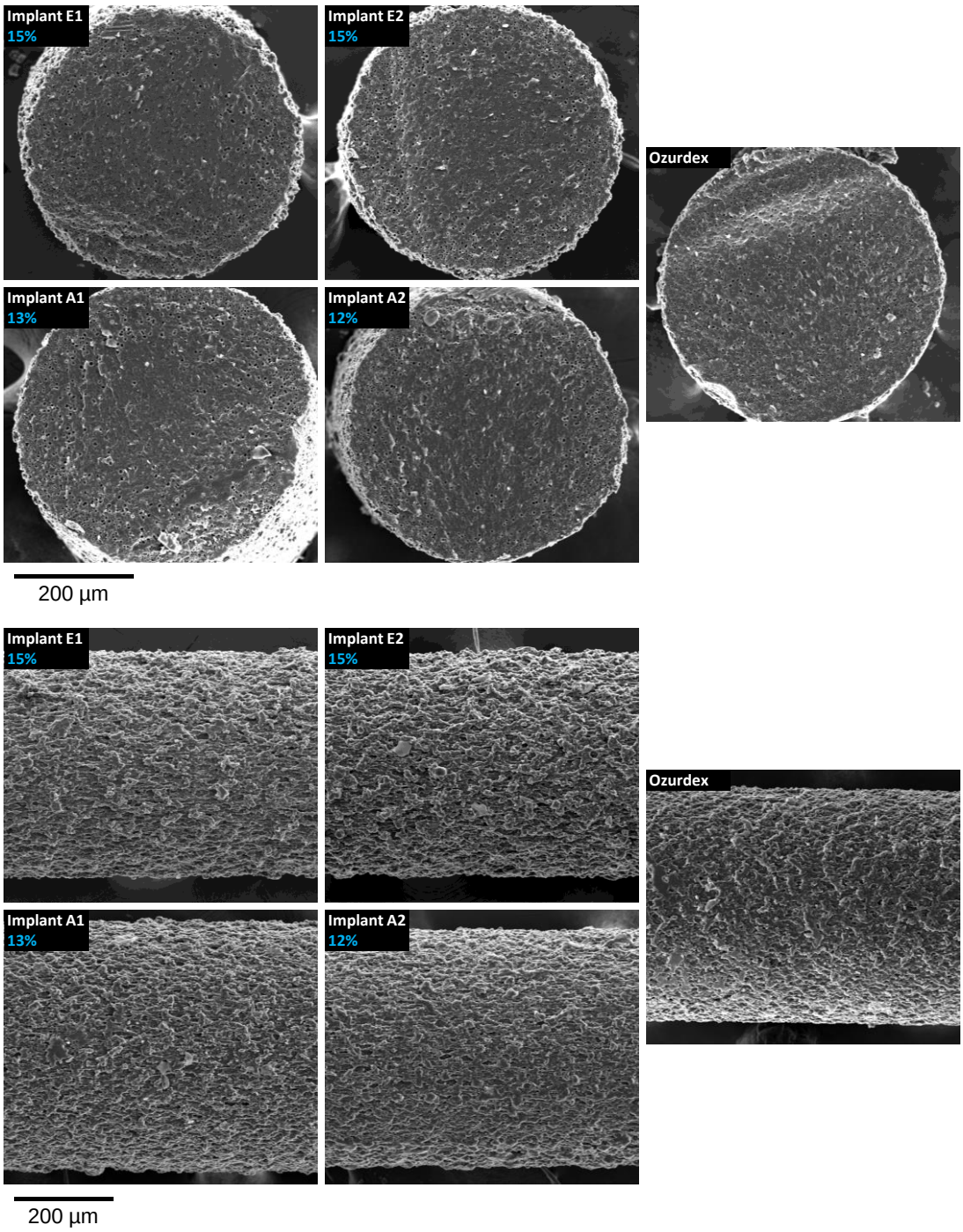

Figure 6.3. SEM images of Ozurdex and the four implants prepared with four different acid-terminated PLGAs. Cross-section at 300× (top panel) and side view at 250× (bottom panel). The total porosity for each sample is shown on the corresponding image.

Extruder torque was recorded throughout the 25-minute collection period for each formulation and averaged to evaluate any differences in processing behavior (see Figure 6.4). Polymers that are more resistant to deformation show higher torque values during processing as they require greater energy input by the rotating screws of the extruder to displace the material in the barrel. The average extruder torque of the two Evonik materials (Formulations E1 and E2) were practically-identical, suggesting limited lot-to-lot variability of Resomer RG 502 H when processing via hot-melt extrusion. Formulation A2 showed significantly higher process torque during manufacture than the other three formulations ($p < 0.0001$). Notably, Polymer A2 had the highest molecular weight by GPC analysis and showed the highest viscosity during evaluation of the melt rheology, although the magnitude of these differences was not large. Interestingly, the higher processing torque for Formulation A2 did not result in any significant structural changes to the implant when compared to the other three formulations.

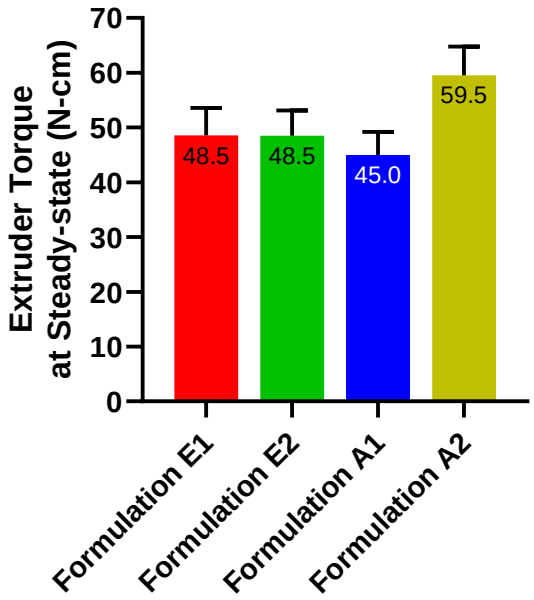

Figure 6.4. Extruder torque during manufacture of the dexamethasone intravitreal implants prepared with four different acid-terminated PLGAs. Mean and standard deviation, n = 1,500.

Table 6.3 presents the average diameter, total porosity, and unit dose potency of the four implants prepared. Accurate diameter control was achieved in all runs with all four implants having a mean diameter within one micron of the 457 μm target diameter (0.0180 in).[47] The implants also exhibited similar total porosity, ranging from 12 to 15%. The porosity of Implant A2 was the lowest of the four formulations, potentially due to a slightly smoother external surface of the implant. As discussed in Section 6.2.2.9, the geometric nature of porosity determination renders the reported total porosity a function of both internal voids and external surface roughness. The porosity of Implants E1 and E2 were practically identical, further demonstrating the consistent performance of Evonik's material during melt extrusion.

Implant	Diameter[a] (μm) (N=1,500)	Total Porosity (%) (N=5)	Unit Dose Potency (%) (N=6)
E1	458 (9)	15.2 (0.4)	100.9 (0.7)
E2	458 (9)	14.9 (0.6)	100.5 (0.4)
A1	458 (10)	13.5 (0.3)	97.2 (0.9)
A2	458 (8)	11.9 (0.2)	97.2 (0.7)

[a] Target implant diameter = 457 μm

Table 6.3. Properties of the dexamethasone intravitreal implants prepared with the four different acid-terminated polymers. Mean and standard deviation (in parentheses) reported.

The unit dose potency of Implants A1 and A2 was reduced compared to Implants E1 and E2 by about 3%. Although chemical degradation in these samples was not ruled out by evaluating the dexamethasone degradant profile before and after extrusion, this reduction in unit dose potency was attributed to material segregation in the pre-extrusion blend. As previously discussed, significant particle size differences between the jet-milled dexamethasone and the jet-milled but granular Akina polymers in the pre-extrusion blends may have contributed to material segregation. The micronized drug likely preferentially adhered to contact surfaces during handling (e.g., during screening of the blend) and extruder feeding, enriching the polymer portion of the blend and leading to a reduction of unit dose potency. Alternate milling techniques besides jet-milling should be evaluated when preparing dexamethasone intravitreal implants with dense granules of PLGA to further reduce particle size of the polymer and avoid the changes to unit dose potency seen here. Despite these differences in unit dose potency, all implants remained within the targeted range of 95–105%.

Samples were taken throughout the two step, hot-melt extrusion process to evaluate changes in PLGA molecular weight via GPC (see Figure 6.5). PLGAs are prone

to thermal degradation at the elevated temperatures experienced during melt extrusion.[67] The higher temperature, in combination with adsorbed moisture from the atmosphere, served to accelerate hydrolysis and reduce the average molecular weight of the PLGAs during processing. In all samples, a small reduction in molecular weight was seen after the first extrusion (1–3%). During the second extrusion, molecular weight degradation was greater and varied between the samples. Greater degradation during the second extrusion was expected as the residence time of the process, or the time the formulation spent inside the melt extruder, was much longer during the second extrusion compared to the first due to the slower feed rate used in the second extrusion. Since the primary goal of the first extrusion process was to densify the material, the material was passed through the extruder as fast as possible, resulting in minimal reduction in molecular weight due to shorter time spent at the elevated processing temperature.

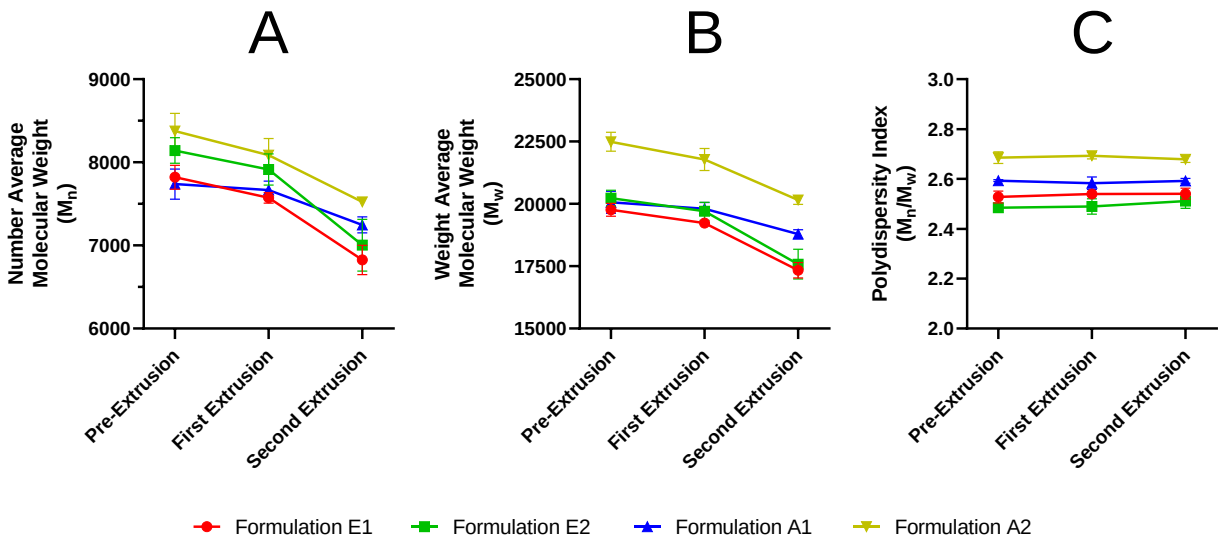

Figure 6.5. Number average molecular weight (A), weight average molecular weight (B), and polydispersity index (C) of the 3:1 acid-terminated:ester-terminated PLGA polymer mixture in the dexamethasone intravitreal implants throughout the two step extrusion process (Mean ± S.D., n = 3).

The two Evonik polymers showed a further reduction of about 10% in M_w after the second extrusion, totaling about 13% reduction when compared to the pre-extrusion blend. In contrast, Formulations A1 and A2 showed a reduction in M_w of 5% and 7% after the second extrusion, respectively, totaling 6% and 10% when compared to the pre-extrusion blend. Of note, the laboratory where these extrusions were performed was not under controlled humidity conditions. The relative humidity of the operating room can vary between 30–70% depending on local weather conditions. Concerningly, when plotting the relative humidity of the laboratory against polymer degradation during the second extrusion, a strong correlation (R^2 = 0.9996) developed for the four runs performed (see Figure S6.2). This finding emphasizes the importance of considering the environmental conditions during melt extrusion of polyesters susceptible to hydrolysis. Since changes in the room humidity were confounded with changes to the polymer during manufacture of the dexamethasone intravitreal implants, these two effects cannot be interpreted independently in this study. In other words, the PLGA degradation observed between the first and second extrusion process cannot be tied to the physicochemical properties of the polymers without further experimentation.

DSC was used to evaluate the impact of these molecular weight changes on the glass transition temperatures of the PLGAs. Figure 6.6 presents the T_g of the formulations throughout the two step, hot-melt extrusion process used to prepare the dexamethasone intravitreal implants. Despite the measured reduction in molecular weight via GPC, no change was seen in the glass transition temperatures of all samples after both extrusions. All samples had T_g between 43–45 °C, consistent with the T_g of the starting materials, as listed in Table 6.2. This result was consistent with the findings of Feuerbach et al., where a two-step extrusion process was shown to have little impact on the T_g of various PLGAs.[131]

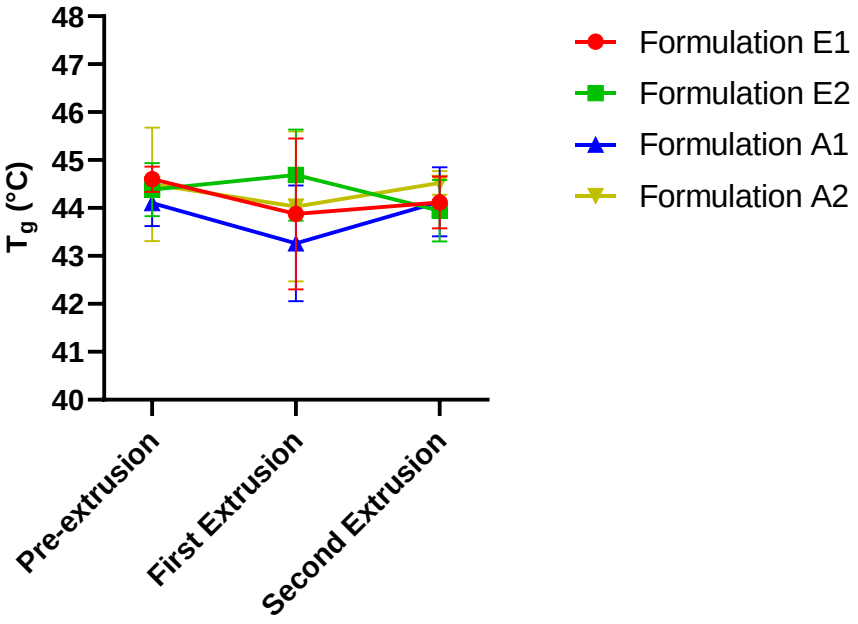

Figure 6.6. Glass transition temperatures of the 3:1 acid-terminated:ester-terminated PLGA polymer mixture in the dexamethasone intravitreal implants throughout the two step extrusion process (Mean ± S.D., *n* = 3).

In summary, characterization of the four dexamethasone intravitreal implants produced with the four different acid-terminated PLGAs showed strong similarities in implant structure and physiochemical properties. Similar behavior of the four formulations during the melt extrusion process resulted in production of implants with comparable diameter, total porosity, and potency. Hydrolytic degradation of the PLGAs during the two step, hot-melt extrusion was variable (6–13%), but no differences in the glass transition temperatures resulted. Altogether, the similarity of these implants enables a detailed assessment of the impact of PLGA physiochemical properties on controlled drug release from dexamethasone intravitreal implants like Ozurdex.

6.3.5. In vitro release testing

In vitro release testing of the four implants was performed in both normal saline (0.9% w/v NaCl) and phosphate-buffered saline (PBS, pH 7.4). In vitro release testing was performed in normal saline to match the method applied by the original manufacturer of Ozurdex to evaluate the impact of implant fragmentation on drug release.[38] In their study, fragmented and whole implants showed no difference in release profile in saline, which translated well to rabbit eye in vivo. Additionally, drug release from the dexamethasone intravitreal implants in saline was observed to closely match the in vivo drug release profile in rabbit eyes, as stated in the Ozurdex patent documentation.[47] The unbuffered nature of normal saline accelerates the drug release profile approximately three-fold compared to phosphate-buffered media, as the autocatalytic hydrolysis of the PLGA can proceed uninhibited.

The in vitro drug release profiles in normal saline of the four implants prepared with the four different acid-terminated PLGAs were very similar to one another (see Figure 6.7A). In all samples, a limited burst release was seen on Day 1 (1–2%), followed by a one-week lag phase where limited drug release occurred (< 10%). Most of the drug release occurred in the final phase, beginning after Day 7. On Day 14, the two Evonik implants (E1 and E2) showed greater release than the two Akina implants (A1 and A2). Despite this difference on Day 14, the release profile of all implants converged at Day 21 and all subsequent timepoints, resulting in release curves that were very similar.

The faster release observed on Day 14 from the two Evonik implants may be attributed to the lower PLGA molecular weight observed via GPC after the second extrusion process (see Figure 6.5). In our previous work, we demonstrated that the onset of significant drug release from the dexamethasone intravitreal implants after Day 7 is linked to the approach to the critical molecular weight of the PLGA.[51] The *critical*

molecular weight represents the point at which the hydrolytic PLGA degradation products become soluble in the release medium and can dissolve and/or diffuse away, exposing the dexamethasone crystals to sufficient water for drug release. Because the PLGA molecular weights of Implants E1 and E2 were lower at the start of in vitro release testing, the critical molecular weight would be reached sooner than Implants A1 and A2, resulting in more drug release at the Day 14 timepoint. Molecular weight changes of the implants throughout the first 28 days of in vitro release testing are discussed in more detail below.

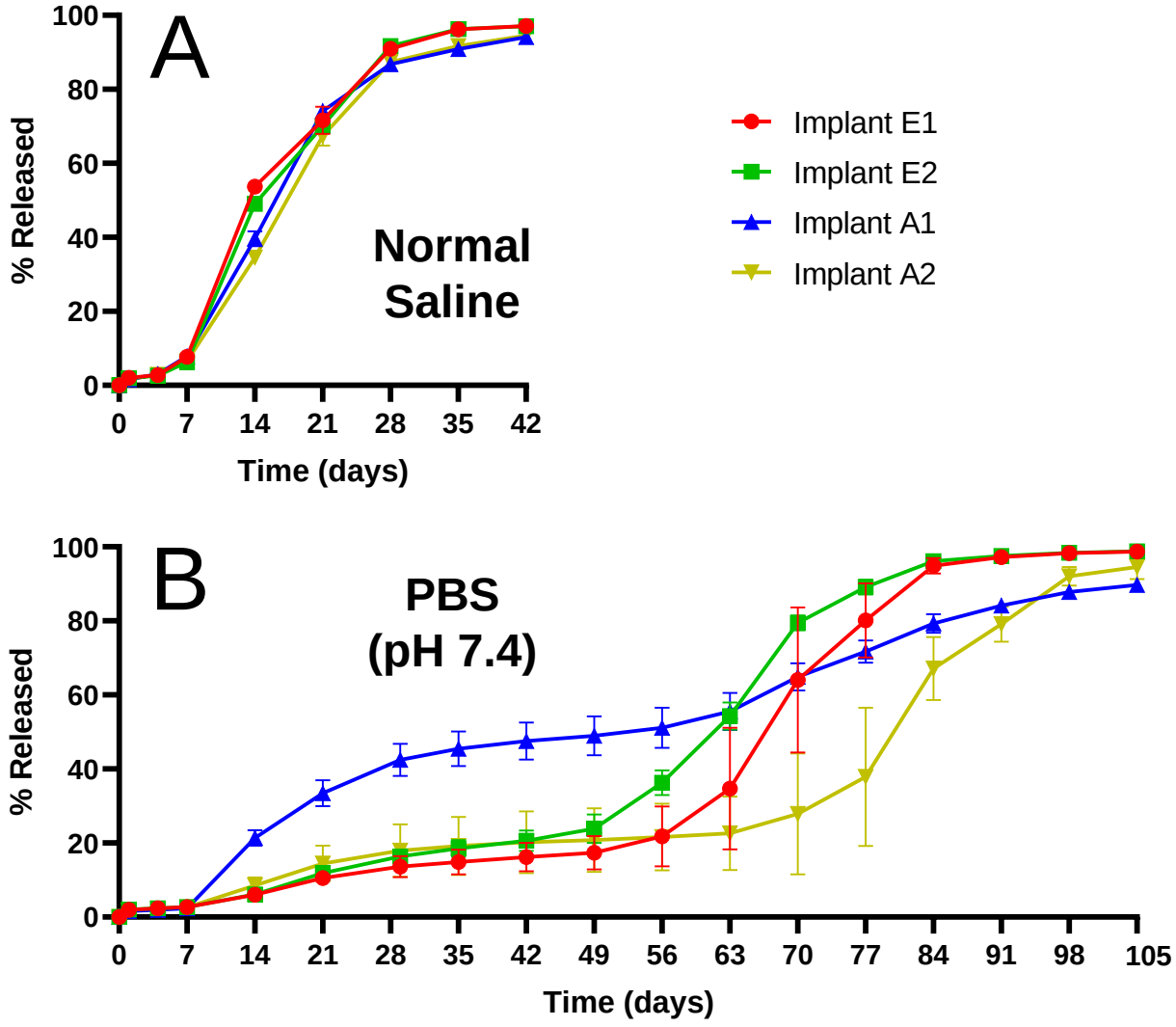

Figure 6.7. In vitro release testing of the four implants prepared with four different acid-terminated PLGAs in normal saline (A) and phosphate-buffered saline (pH 7.4) (B). Mean ± S.D., *n* = 6.

In contrast to the release profiles in normal saline, the in vitro drug release profiles in PBS of the four implants prepared with the four different acid-terminated PLGAs were all distinct from one another (see Figure 6.7B). As expected, the duration of drug release in PBS was extended approximately three-fold compared to normal saline

due to the buffering capacity of the PBS neutralizing the acidic PLGA hydrolysis products, dampening the impact of autocatalytic degradation. In all samples, a burst release of 1–2% was seen on Day 1, followed by a one-week period where limited drug release occurred, similar to what was observed in normal saline. Interestingly, after Day 7, the release profile of Implant A1 deviated considerably from the other three implants, releasing approximately two to three times more drug over the next month than the other three formulations where drug release remained slow in the lag phase. After Day 28, the expected slow-release behavior associated with the lag phase reemerged from Implant A1 and drug release remained slow until the end of this phase on Day 56.

The release profiles of Implants E1 and E2 were similar to one another, though the duration of the lag phase differed by about one week, with the lag phase extending to Day 49 for Implant E2 and to Day 56 for Implant E1. Implant A2 showed a long lag phase extending out to Day 70. The extended lag phase of Implant A2 was attributed to a difference in PLGA blockiness. From Table 6.2, this sample had the lowest average glycolate block length of the four acid-terminated PLGAs evaluated. In this less blocky sample, a higher proportion of G-L linkages were present on the polymer backbone and the G-G linkage became less common. The G-G linkage is known to be more reactive and more hydrophilic than the G-L linkage.[20] In this case, the overall rate of hydrolysis was slowed, resulting in a slower approach to the critical molecular weight, and an extended lag phase.

After the end of the lag phase in Implants E1, E2, and A2, drug release to completion occurred at a similar rate with the vast majority of drug being released over the subsequent five weeks. The rate of release after the end of the lag phase in Implant A1 was slowed compared to the other implants, and approximately 10% of the drug remained in the implant at the final timepoint (Day 105).

During in vitro release testing in PBS, it was visually observed that Implant A1 had a different appearance than the other three implants at all timepoints after Day 7. While all implants remained monolithic throughout in vitro release testing, all six replicates of Implant A1 appeared to split open after Day 7, coinciding with the substantial drug release seen on Days 14–28. To better visualize this event, SEM images of the four implants were acquired on Day 7 and Day 14 to evaluate any structural differences (see Figure 6.8). On Day 7, the implants had a generally similar appearance, although the surface of Implants E1 and E2 appeared to be rougher than the surface of Implants A1 and A2. The Day 14 images of Implant A1 confirmed the visual observations: the implant appeared to split open from the core outward, resulting in a greatly increased surface area and providing the dissolution medium direct access to the core of the implant. Minor cracking on the surface was also observed in Implant A2. Only a minor increase in swelling was seen between Day 7 and Day 14 in Implants E1 and E2, no cracking or structural breakdown was observed in these two samples.

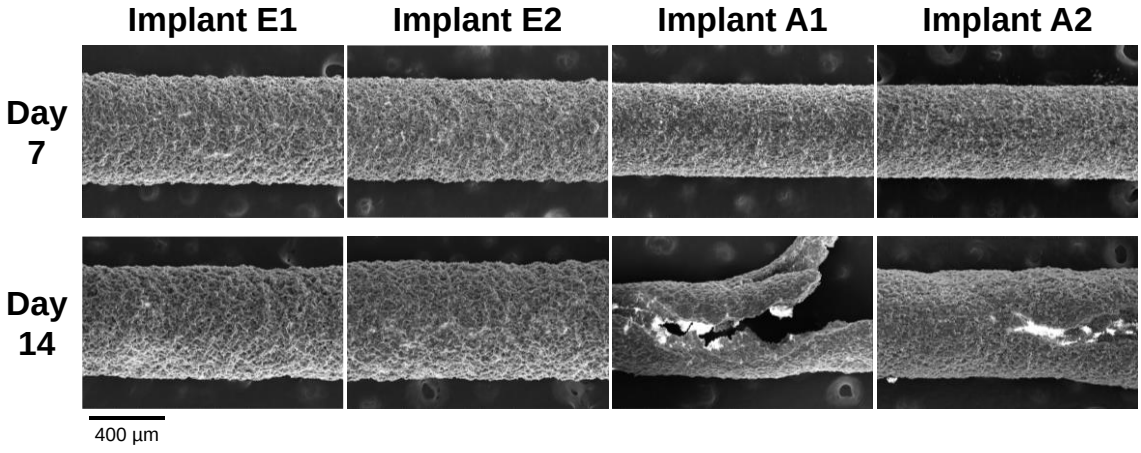

Figure 6.8. SEM images of the four implants prepared with four different acid-terminated PLGAs during dissolution in PBS (pH 7.4) after lyophilization on Day 7 and Day 14. Side view at 150×.

6.3.6. Implant characterization during in vitro release testing

To better understand the mechanisms behind the different drug release profiles of the four implants in PBS, additional characterization was performed throughout the first 28 days of in vitro release testing in both normal saline and PBS. GPC was used to trend the changes in PLGA molecular weight for the four implants. Total implant mass loss and moisture pickup were also trended throughout the 28-day period. Figure 6.9A shows the PLGA number average molecular weight change in normal saline. A rapid reduction in molecular weight was seen in all samples in the first seven days during the lag phase, prior to the onset of substantial drug release. The small differences in molecular weight measured on Day 0 remained until Day 21, after which all samples had the same average molecular weight. As previously mentioned, this difference in molecular weight may explain the slower release from Implants A1 and A2 on Day 14. Generally, the rates of PLGA degradation from the four implants in normal saline were very similar, leading to similar drug release profiles. In line with this result, the top panel of Figure 6.10 shows how the four implants lost mass (drug and polymer) and picked up moisture from the medium at equal rates.

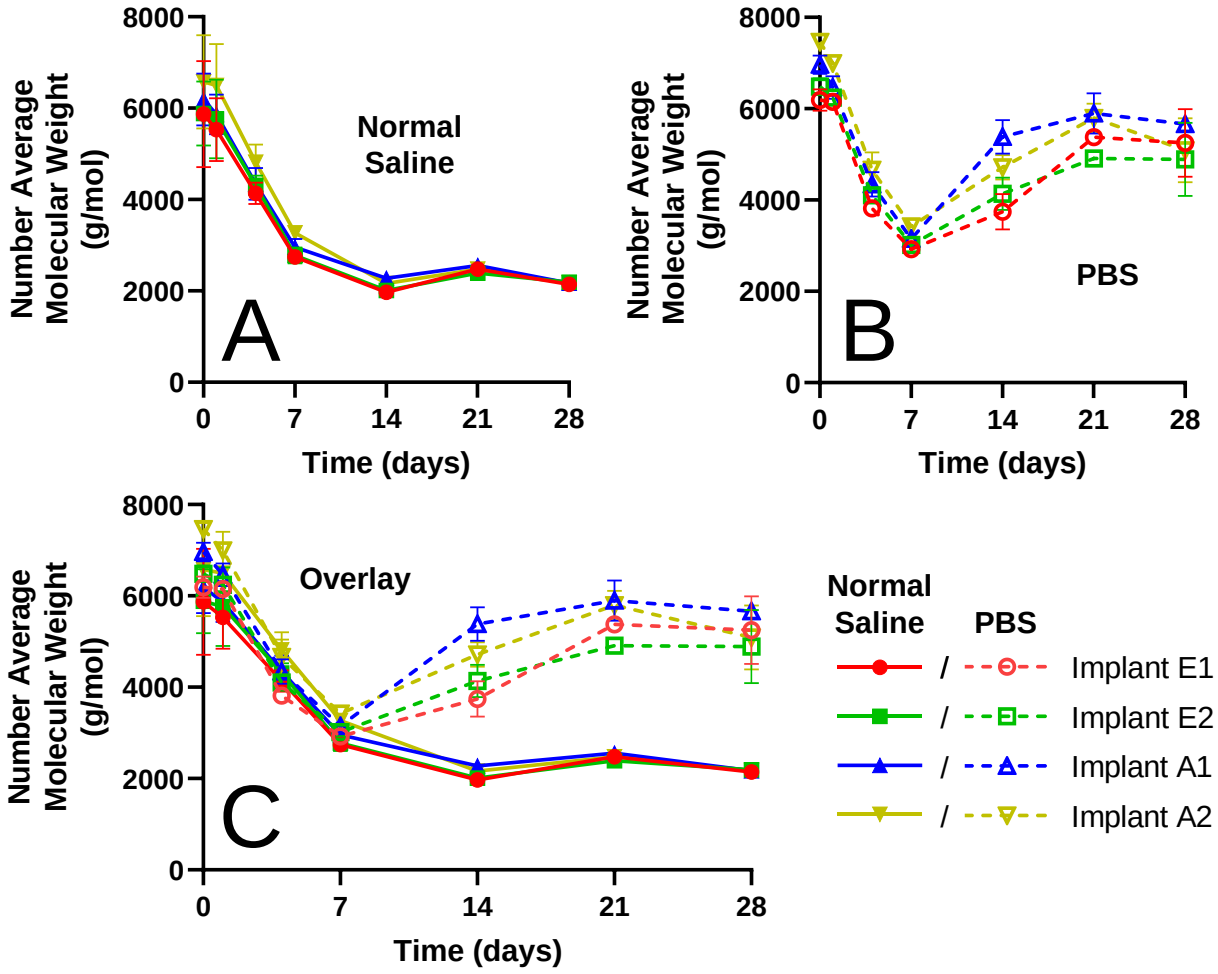

Figure 6.9. Change in PLGA molecular weight during the first 28 days of in vitro release testing of the dexamethasone intravitreal implants in normal saline (A), PBS (B), and their overlay (C). (mean ± S.D., *n* = 3).

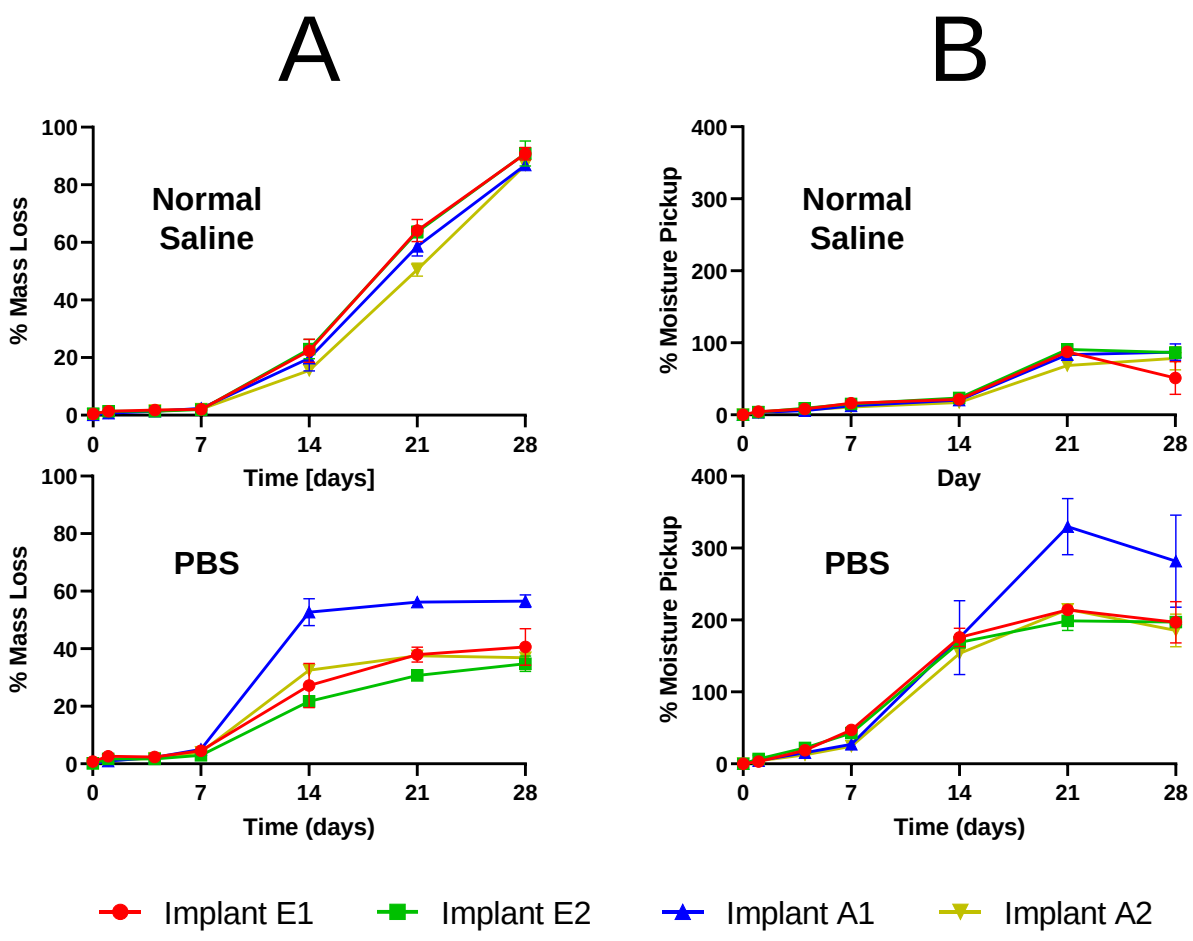

Figure 6.10. Total implant mass loss (A) and moisture pickup (B) during the first 28 days of in vitro release testing of the dexamethasone intravitreal implants in both normal saline (top) and PBS (bottom) (mean ± S.D., *n* = 3).

Figure 6.9B shows the PLGA number average molecular weight change in PBS. Like normal saline, all implants experienced a rapid decline in PLGA molecular weight in the first seven days of in vitro release testing. Unexpectedly, after Day 7, the average molecular weight of the PLGAs in all four implants increased on Day 14 and further on Day 21. This apparent increase in molecular weight was not due to polymerization of the PLGA, but due to dissolution of short chain oligomers into the medium, resulting in

enrichment of longer polymer chains in the implant fragment that were not soluble in the medium. The extent of this enrichment was variable between the four implants. Implant A1 showed the greatest increase in average molecular weight after Day 7 followed by Implant A2, then Implants E1 and E2 which showed a similar extent of increase. The splitting of Implant A1 and the cracking of Implant A2 may have contributed to the faster purge of short chain, soluble oligomers that would have otherwise remained trapped in the core.

The drug release process from dexamethasone intravitreal implants is dictated by the characteristic 'bulk erosion' of PLGA or the inside-out degradation of the dosage form, as discussed in detail in our previous study.[51] Figure 6.9C shows that the rate of PLGA degradation in the first seven days was practically identical between normal saline and PBS. During this phase, water from the release medium diffused through the PLGA matrix and polymer hydrolysis began. Autocatalytic hydrolysis occurred at an accelerated rate near the core of the implant due to diffusional limitations and osmotic effects from the degradation products pulling more water into the implant. After Day 7, sufficient water uptake and PLGA degradation had occurred in all samples to break down the internal structure of the implant core due to swelling and enabled the release of the trapped hydrolytic byproducts from the implant. In the case of unbuffered normal saline, autocatalytic hydrolysis of the PLGA continued inside the implant as drug and soluble oligomers diffused out of the core. In the case of PBS, the buffering capacity of the medium dramatically slowed the rate of PLGA hydrolysis as the trapped, water-soluble oligomers diffused away from the core, leaving behind longer PLGA chains undergoing hydrolysis at a much slower rate compared to normal saline.

The increased drug release from Implant A1 after Day 7 was attributed to amplified osmotic effects causing the implant to burst open and release drug and water-

soluble PLGA oligomers that would otherwise remain trapped in the core. The bottom-left plot of Figure 6.10 confirms that substantially greater mass loss occurred from Implant A1 after Day 7. As shown in Table 6.2, Polymer A1 had an elevated residual monomer content as well has the highest content of carboxylic acid chain ends (acid number). The increased hydrophilicity of this sample may have drawn more water into the core than all other implants, resulting in rapid and irregular swelling behavior that culminated in the implant bursting open between Days 7 and 14, releasing a greater quantity of dexamethasone. Polymer A2 also had elevated levels of residual monomer and an acid number slightly larger than the two Evonik polymers. This more subtle increase in hydrophilicity may have been enough to cause the minor cracking of the surface seen under SEM on Day 14 (see Figure 6.8). The outer surfaces of these implants had direct contact with the buffered medium and lacked the ability to trap hydrolytic degradation products, so this outer surface likely represented the least degraded, and correspondingly the most rigid, material in the implant. Under these conditions, it is conceivable that rapid swelling of the highly plasticized PLGA in the core could cause fracture of the surrounding skin layer, as observed in the SEM images.

The structural breakdown observed for Implants A1 and A2 in PBS was not observed in any of the normal saline samples during in vitro release testing. The more rapid and uniform degradation of the PLGAs in normal saline may have resulted in reduced sensitivity to small differences in PLGA physicochemical properties.

The goal of this work was to evaluate the role of PLGA variability in controlled drug release from dexamethasone intravitreal implants. Clearly, the in vitro release testing method selected to perform this evaluation had a major impact on the conclusions drawn. Release testing in normal saline showed no impact to drug release when preparing implants with acid-terminated PLGAs from different sources with similar molecular

weights. On the other hand, release testing in PBS showed clearly different performance between the four implants prepared, and suggested drug release was highly sensitive to small changes in residual monomer content, carboxylic acid end group content, and blockiness. These findings raised a question: which in vitro release testing method is more physiologically relevant?

6.3.7. Implications for IVIVC development

While PBS is often used to simulate the in vivo conditions of the posterior segment of the eye, it remains challenging to develop a predictive in vitro-in vivo correlation (IVIVC) in human eyes.[25] The inherent complexity of ocular physiology, including variations in vitreous viscosity and the possibility of multiple routes of elimination, complicates IVIVC development. Since collecting human ocular pharmacokinetic data from the posterior segment of the eye is impractical (if not impossible), developers of intraocular implants often rely solely on animal models and in vitro testing to develop their formulations before clinical validation of safety and efficacy.

Both monkey eye and rabbit eye were used as model systems during the development of Ozurdex.[44, 49] As previously mentioned, patent literature shows that the in vitro release data for Ozurdex in normal saline closely matched the in vivo release profile in rabbit eye, though the developers did not claim an IVIVC. Both the CHMP assessment report and TGA assessment report state that the 21-day in vitro testing method used for Ozurdex is mainly for quality control purposes to demonstrate reproducibility of the implant manufacturing process, and was not intended to represent the human in vivo performance of the dosage form.[46, 103]

For generic developers of dexamethasone intravitreal implants referencing Ozurdex, it would be beneficial to know which of the two in vitro release testing methods presented above is appropriate to discern meaningful differences in the formulations. Our future work includes plans to test some of the dexamethasone intravitreal implants prepared in this study in rabbit eye to better assess which in vitro release testing method is more appropriate for generic product development of implants referencing Ozurdex.

6.4. CONCLUSION

Extensive characterization of four 50:50, acid-terminated PLGAs from two vendors (Evonik and Akina) was performed to uncover any differences in physicochemical properties prior to dexamethasone intravitreal implant manufacture. The polymers were shown to be very similar in many regards, including molecular weight distribution, T_g, moisture content, and lactide/glycolide ratio. Differences in residual monomer content, blockiness, and carboxylic acid end group content were seen among the four polymers. Despite these differences, the four formulations prepared with the four polymers behaved similarly during hot-melt extrusion of the dexamethasone intravitreal implants. The implants were all structurally equivalent to one another and the Ozurdex reference product, isolating any effects from structural differences and enabling direct study of compositional differences in this system.

In vitro release testing in PBS was found to be dramatically more sensitive to subtle differences in PLGA properties than normal saline. The similar performance of the two Evonik polymers throughout the study demonstrated the consistent performance of the commercially-available Resomer products when formulated into dexamethasone intravitreal implants. The Akina polymers, deliberately synthesized with different blockiness, showed major differences in their release profile during in vitro release

testing in PBS but not in normal saline. Further studies are needed to clarify which in vitro release method is more physiologically relevant to better inform development of generic formulations referencing Ozurdex.

ACKNOWLEDGEMENTS

This work was supported by the Broad Agency Announcement (BAA) Contract # 75F40120C00198 from the U.S. Food and Drug Administration (FDA). The content reflects the views of the authors and should not be construed to represent the views or policies of the U.S. FDA. ^{1}H and ^{13}C NMR spectra were collected using the Bruker AVANCE III 500 associated with NIH Grant Number 1 S10 OD021508-01 in the University of Texas at Austin NMR facility.

Chapter 7. Concluding Remarks

7.1. DISSERTATION CONCLUSION AND OUTLOOK

To help address the absence of generic PLGA–based formulations in the market, the FDA–approved Ozurdex (dexamethasone intravitreal implant) was thoroughly researched in this dissertation. The implant was reverse-engineered to produce compositionally and structurally equivalent implants using a continuous hot-melt extrusion process. The physicochemical mechanisms of controlled drug release were evaluated in vitro using both unbuffered and buffered conditions. In vitro release testing showed that small changes to implant structure (e.g., porosity and surface morphology) did not impact drug release kinetics. On the other hand, research showed that buffered in vitro release testing was sensitive to subtle differences in PLGA purity (i.e., residual monomer content) and/or PLGA blockiness. Future work should consider the use of animal models to better understand the in vivo impact of these subtle differences in PLGA properties on drug release kinetics. Identifying an appropriate in vitro release testing method to detect meaningful differences between a generic formulation and the reference listed drug could help bring these cost-saving medicines to patients in need.

Appendix

SUPPLEMENTARY INFORMATION FOR CHAPTER 3

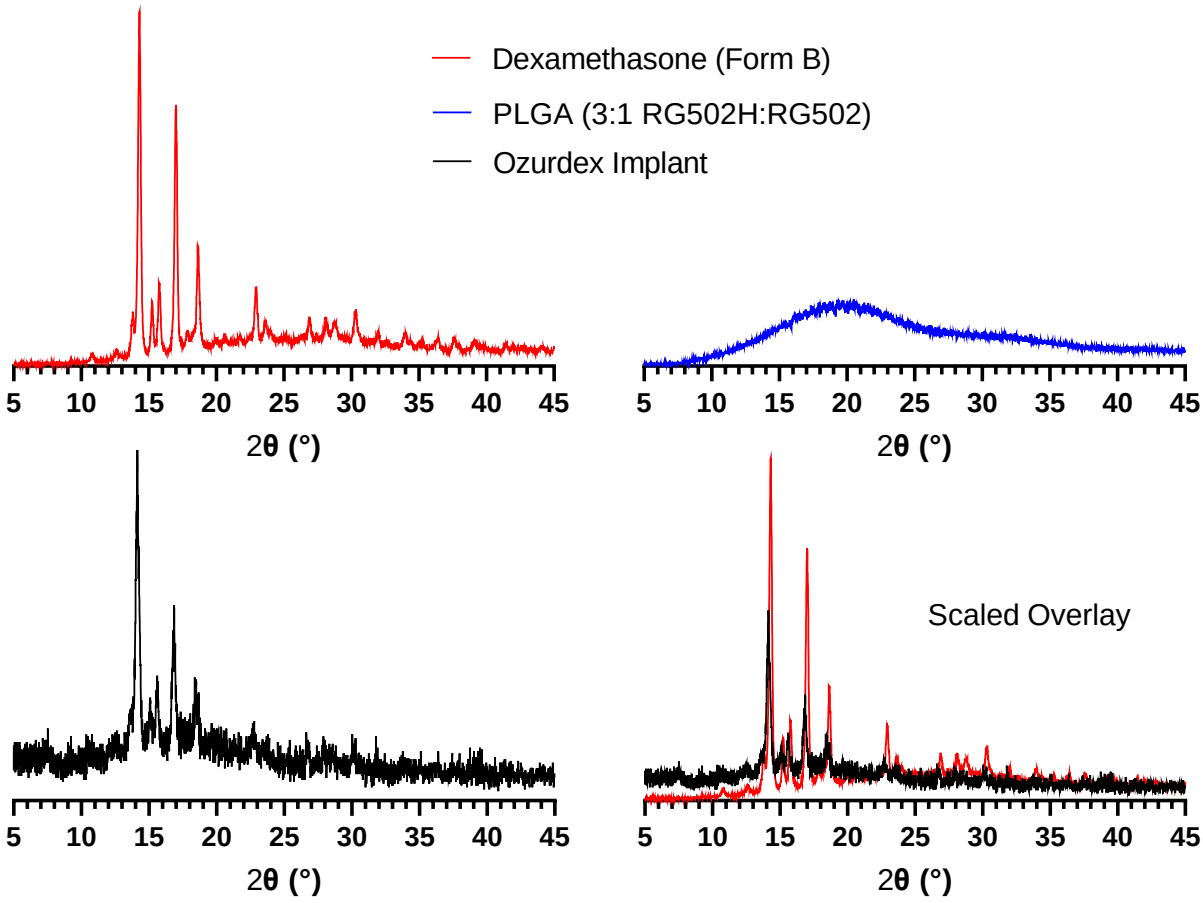

Figure S3.1. XRPD of dexamethasone Form B, PLGAs, and Ozurdex. A weak signal was obtained for the Ozurdex sample due to limited sample size.

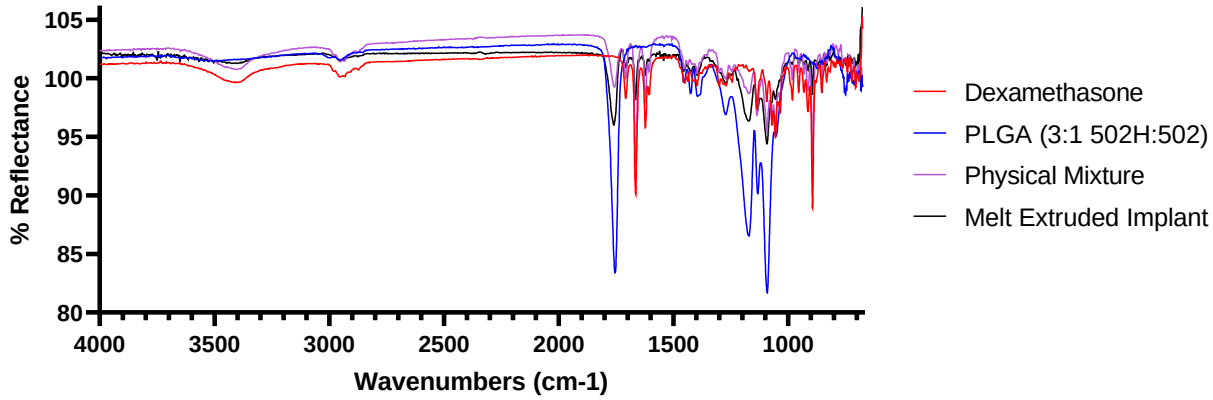

Figure S3.2. ATR-FTIR spectra of dexamethasone, PLGA (3:1 acid:ester blend), a physical mixture, and a melt-extruded implant.

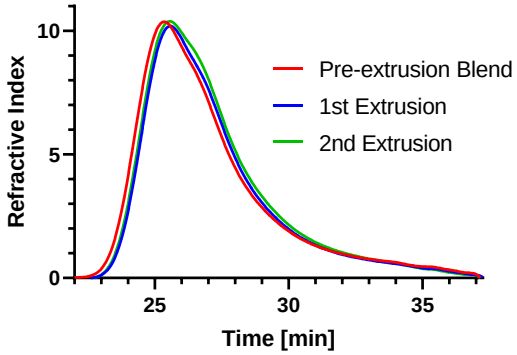

Sample	M_n	M_w	PDI	Change in M_n (%)
Pre-extrusion Blend	8650	21790	2.52	-
1st Extrusion	8137	19826	2.44	-6%
2nd Extrusion	8087	19684	2.43	-7%

Figure S3.3. GPC chromatogram of dexamethasone–PLGA blends before and after each extrusion.

SUPPLEMENTARY INFORMATION FOR CHAPTER 5

Assume implant is a perfect cylinder of known diameter and length:

$$Volume\ of\ Cylinder\ (mm^3) = \pi \left(\frac{Diameter(mm)}{2}\right)^2 \times\ Length\ (mm) \quad \text{(A)}$$

The total volume of the cylinder is comprised of two regions, solids and pores. As discussed in Methods, the total implant porosity includes both internal pores trapped inside the drug/polymer matrix and external pores between the true surface of the implant and the imagined perfect cylinder surrounding the implant:

$$Solid\ Fraction\ (\%) + Porosity\ (\%) = 100\% \quad \text{(B)}$$

Substitute (A) and (B) into (C) to find the total volume of solids (drug/polymer mixture):

$$Volume\ of\ Solids\ (mm^3) = Solid\ Fraction\ (\%) * Volume\ of\ Cylinder\ (mm^3) \quad \text{(C)}$$

Substitute (C) into (D) to find the total mass of the implant (the negligible mass of air in the pores can be neglected):

$$Total\ Implant\ Mass\ (mg) = Volume\ of\ Solids\ (mm^3) \times True\ Density\ \left(\frac{mg}{mm^3}\right) \quad \text{(D)}$$

Drug loading, determined during powder blending of the pre-extrusion blend, can be defined as:

$$Drug\ Loading\ (\%) = \frac{Drug\ Mass\ (mg)}{Total\ Implant\ Mass\ (mg)} \quad \text{(E)}$$

Substitute (D) into (F) to determine the unit dose assay of the implant:

$$Unit\ dose\ assay\ (mg) = Total\ Implant\ Mass\ (mg) \times Drug\ Loading\ (\%) \quad \text{(F)}$$

Per USP ⟨905⟩, the % label claim is defined as:

$$\%\ Label\ Claim = \frac{Unit\ Dose\ Assay\ (mg)}{Label\ Claim\ (mg)} \times 100\% \quad \text{(G)}$$

Finally, substitute (F) into (G), along with all preceding substitutions, to arrive at Equation 5.2:

$$\%\ Label\ Claim = \frac{\pi \times \left(\frac{Diameter\ (mm)}{2}\right)^2 \times Length\ (mm) \times True\ Density\ \left(\frac{mg}{mm^3}\right) \times Drug\ Loading\ (\%) \times \left(1 - Porosity(\%)\right)}{Label\ Claim\ (mg)} \times 100\%$$

Where:

$$True\ Density = 1.365\ \frac{mg}{mm^3}\left(or\ \frac{g}{cm^3}\right)$$

$$Drug\ Loading = 60\%$$

$$Label\ Claim = 0.700\ mg$$

Figure S5.1. Derivation of Equation 5.2. for calculation of implant % label claim based on dimensional and structural characteristics of the implant.

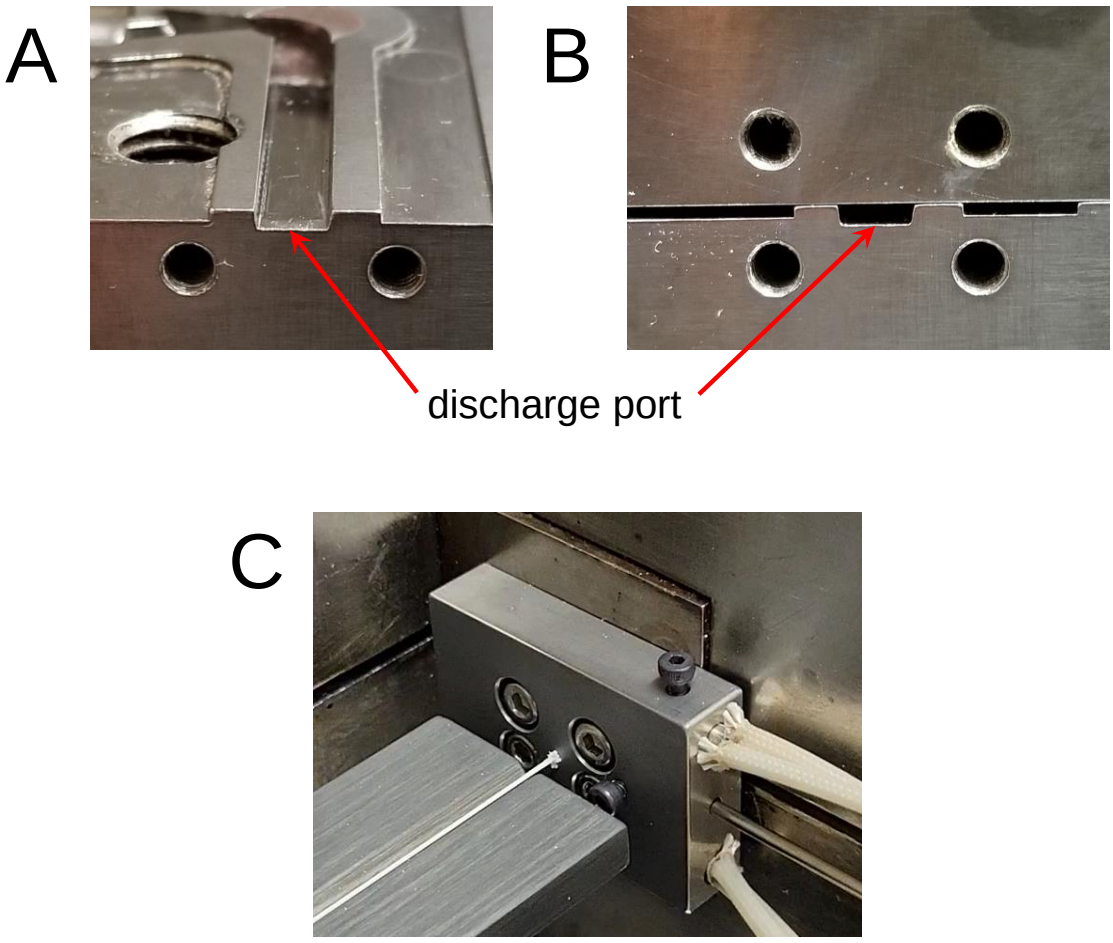

Figure S5.2. Discharge port of the Haake MiniLab extruder used to prepare the dexamethasone intravitreal implants with the clamshell lid open (A), with the clamshell lid closed (B), and fitted with a heated reducing die during melt extrusion (C).

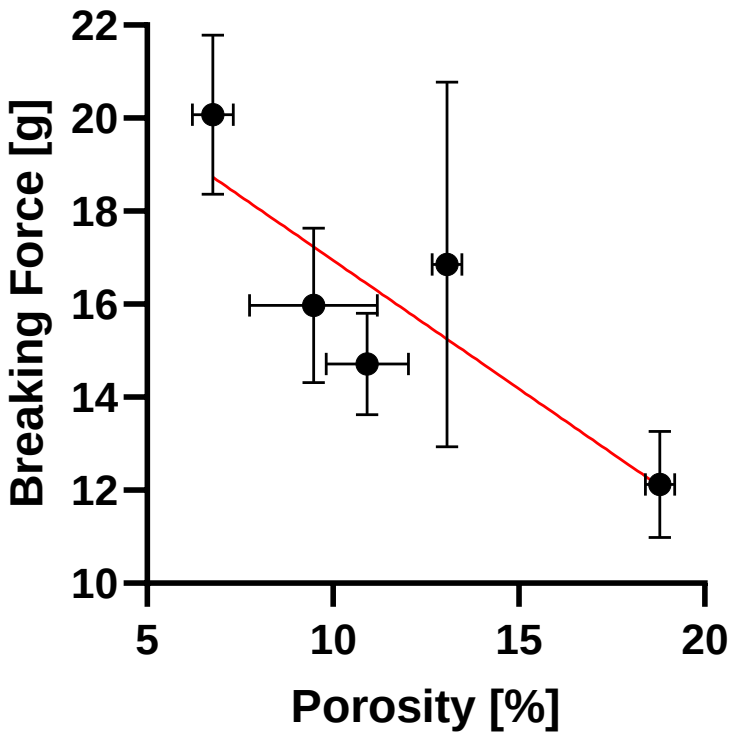

Figure S5.3. Impact of total implant porosity on breaking force using a 3-point bend test based on ASTM D7264. Mean ± S.D. are shown; n = 5 for porosity and n = 6 for breaking force. A least-squares regression line is shown in red to emphasize the directionality of the relationship.

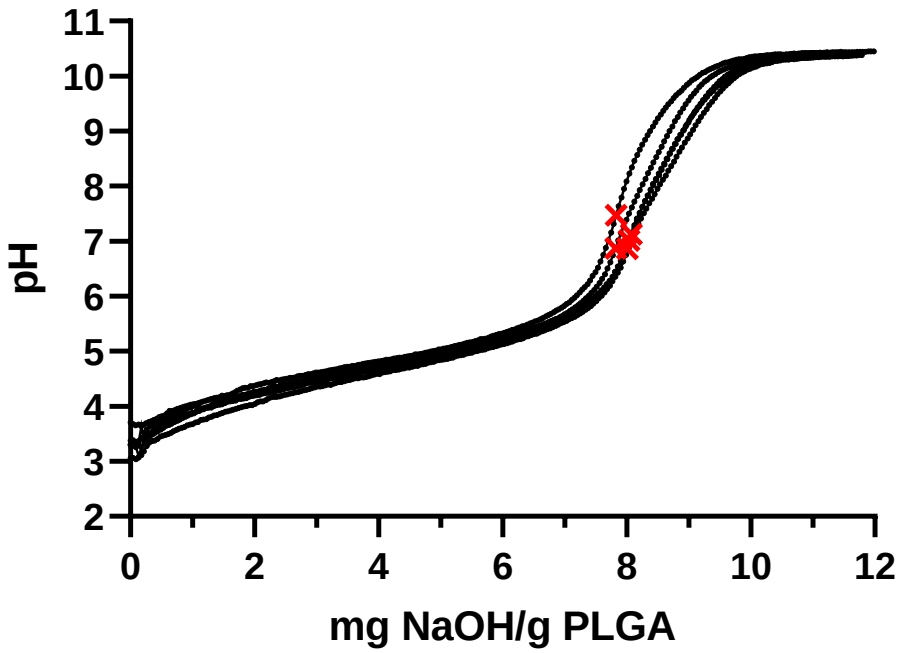

Figure S6.1. Acid number titration curves for the five replicates of Polymer E2. The red X's indicate the equivalence point of the titration determined by the first derivative test (the point on the titration curve where the slope is highest).

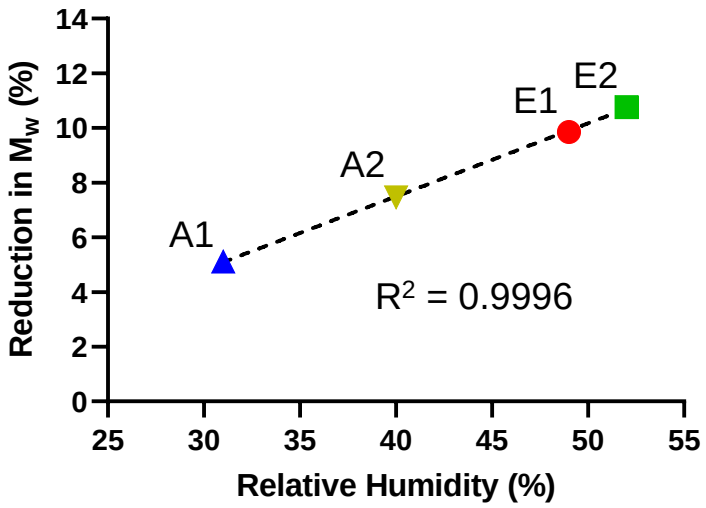

Figure S6.2. Relationship between laboratory humidity and the reduction in PLGA molecular weight in the dexamethasone intravitreal implants between the first and second extrusion runs.

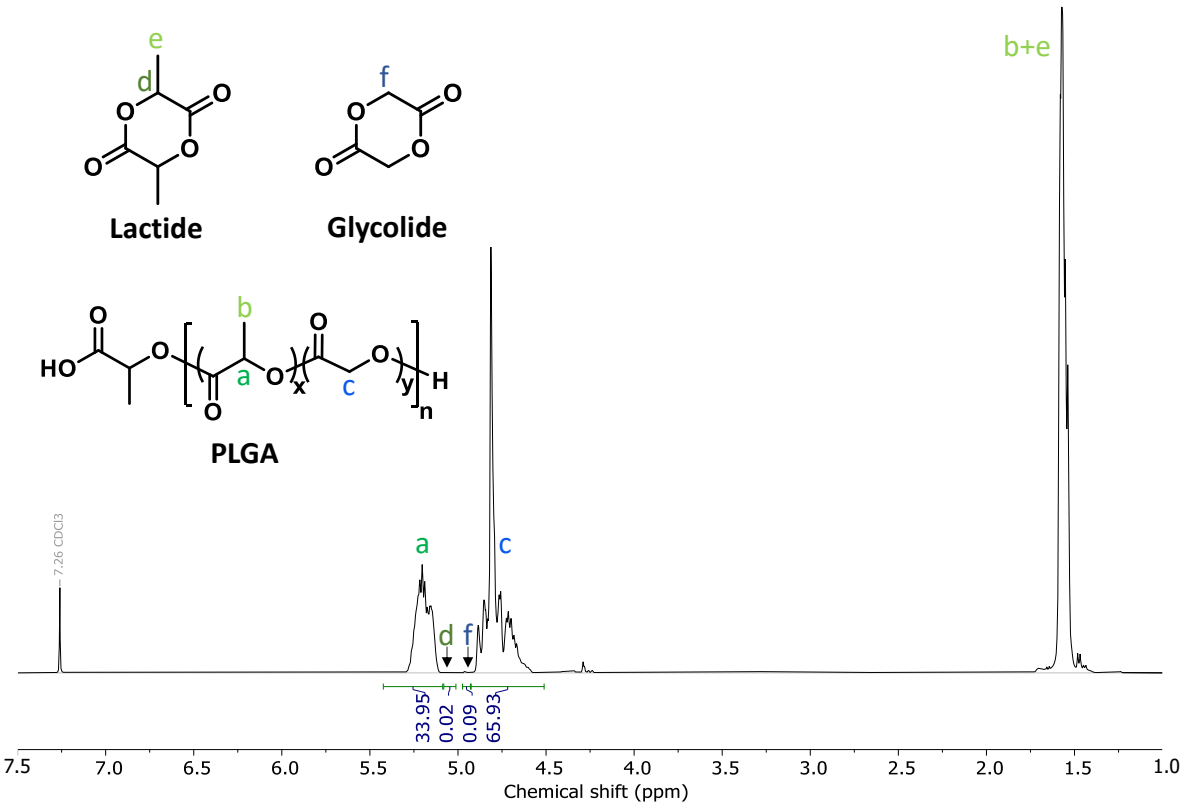

Figure S6.3. ^{1}H NMR spectrum of Polymer E2 used to determine the lactide/glycolide ratio and the total residual monomer.

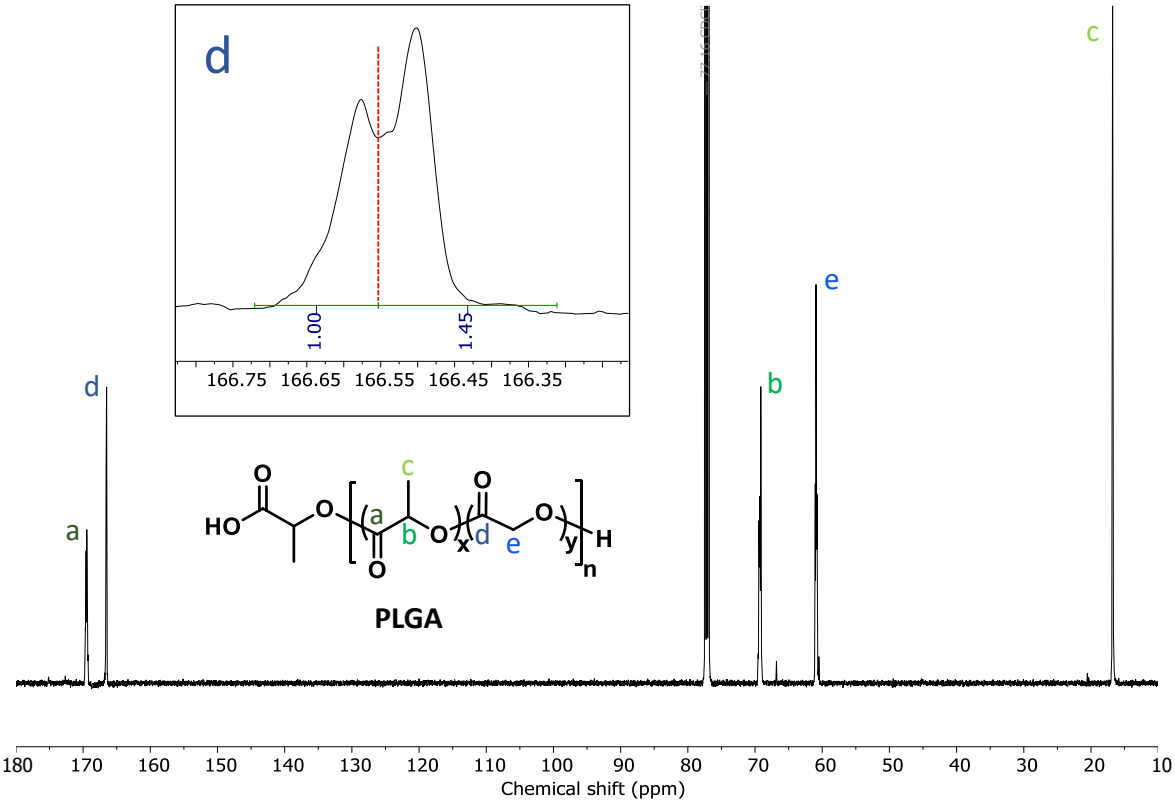

Figure S6.4. ^{13}C NMR spectrum of Polymer E2 used to calculate glycolate block length (blockiness).

References

1. Wang Y, Qin B, Xia G, Choi SH. FDA's Poly (Lactic-Co-Glycolic Acid) Research Program and Regulatory Outcomes. AAPS J. 2021;23(4):92.
2. Wan B, Bao Q, Burgess D. Long-acting PLGA microspheres: Advances in excipient and product analysis toward improved product understanding. Adv Drug Deliv Rev. 2023;198:114857.
3. Walker J, Albert J, Liang D, Sun J, Schutzman R, Kumar R, et al. In vitro degradation and erosion behavior of commercial PLGAs used for controlled drug delivery. Drug Deliv Transl Res. 2023;13(1):237-51.
4. Park K, Skidmore S, Hadar J, Garner J, Park H, Otte A, et al. Injectable, long-acting PLGA formulations: Analyzing PLGA and understanding microparticle formation. J Control Release. 2019;304:125-34.
5. Lim YW, Tan WS, Ho KL, Mariatulqabtiah AR, Abu Kasim NH, Abd Rahman N, et al. Challenges and Complications of Poly(lactic-co-glycolic acid)-Based Long-Acting Drug Product Development. Pharmaceutics. 2022;14(3).
6. Zhou J, Hirota K, Ackermann R, Walker J, Wang Y, Choi S, et al. Reverse Engineering the 1-Month Lupron Depot(R). AAPS J. 2018;20(6):105.
7. Beig A, Feng L, Walker J, Ackermann R, Hong JKY, Li T, et al. Physical-Chemical Characterization of Octreotide Encapsulated in Commercial Glucose-Star PLGA Microspheres. Mol Pharm. 2020;17(11):4141-51.
8. Costello MA, Liu J, Wang Y, Qin B, Xu X, Li Q, et al. Reverse engineering the Ozurdex dexamethasone intravitreal implant. Int J Pharm. 2023;634:122625.
9. Wang X, Bao Q, Wang R, Wan B, Wang Y, Qin B, et al. Reverse engineering of Perseris and development of compositionally equivalent formulations. Int J Pharm. 2023;639:122948.
10. Association for Accessible Medicines. The U.S. Generic & Biosimilar Medicines Savings Report2021. Available from: https://accessiblemeds.org/sites/default/files/2021-10/AAM-2021-US-Generic-Biosimilar-Medicines-Savings-Report-web.pdf.
11. Conrad R, Davis K, Glos L, Liu W. Estimating Cost Savings from New Generic Drug Approvals in 2018, 2019, and 20202022. Available from: https://www.fda.gov/media/161540/download.
12. Garner J, Skidmore S, Park H, Park K, Choi S, Wang Y. Beyond Q1/Q2: The Impact of Manufacturing Conditions and Test Methods on Drug Release From PLGA-Based Microparticle Depot Formulations. J Pharm Sci. 2018;107(1):353-61.
13. Wan B, Andhariya JV, Bao Q, Wang Y, Zou Y, Burgess DJ. Effect of polymer source on in vitro drug release from PLGA microspheres. Int J Pharm. 2021;607:120907.
14. Ding AG, Schwendeman SP. Determination of water-soluble acid distribution in poly(lactide-co-glycolide). J Pharm Sci. 2004;93(2):322-31.
15. Avgoustakis K. Polylactic-co-glycolic acid (PLGA). Encyclopedia of biomaterials and biomedical engineering. 2005;1(1):1-11.

16. Dechy-Cabaret O, Martin-Vaca B, Bourissou D. Controlled ring-opening polymerization of lactide and glycolide. Chem Rev. 2004;104(12):6147-76.
17. Garner J, Skidmore S, Hadar J, Park H, Park K, Kuk Jhon Y, et al. Analysis of semi-solvent effects for PLGA polymers. Int J Pharm. 2021;602:120627.
18. Miller RA, Brady JM, Cutright DE. Degradation rates of oral resorbable implants (polylactates and polyglycolates): rate modification with changes in PLA/PGA copolymer ratios. J Biomed Mater Res. 1977;11(5):711-9.
19. Tracy M, Ward K, Firouzabadian L, Wang Y, Dong N, Qian R, et al. Factors affecting the degradation rate of poly (lactide-co-glycolide) microspheres in vivo and in vitro. Biomaterials. 1999;20(11):1057-62.
20. Washington MA, Swiner DJ, Bell KR, Fedorchak MV, Little SR, Meyer TY. The impact of monomer sequence and stereochemistry on the swelling and erosion of biodegradable poly(lactic-co-glycolic acid) matrices. Biomaterials. 2017;117:66-76.
21. Kuehster L, Jhon YK, Wang Y, Smith WC, Xu X, Qin B, et al. Stochastic and Deterministic Analysis of Reactivity Ratios in the Partially Reversible Copolymerization of Lactide and Glycolide. Macromolecules. 2022;55(16):7171-80.
22. Washington MA, Balmert SC, Fedorchak MV, Little SR, Watkins SC, Meyer TY. Monomer sequence in PLGA microparticles: Effects on acidic microclimates and in vivo inflammatory response. Acta Biomater. 2018;65:259-71.
23. Dossarps D, Bron AM, Koehrer P, Aho-Glélé LS, Creuzot-Garcher C, Berthon L, et al. Endophthalmitis after intravitreal injections: incidence, presentation, management, and visual outcome. American journal of ophthalmology. 2015;160(1):17-25. e1.
24. Lee SS, Hughes P, Ross AD, Robinson MR. Biodegradable implants for sustained drug release in the eye. Pharm Res. 2010;27(10):2043-53.
25. Adrianto MF, Annuryanti F, Wilson CG, Sheshala R, Thakur RRS. In vitro dissolution testing models of ocular implants for posterior segment drug delivery. Drug Deliv Transl Res. 2021.
26. USP. ⟨1771⟩ Ophthalmic Products—Performance Tests. Rockville, MD2022.
27. U.S. Food & Drug Administration. Orange Book: Approved Drug Products with Therapeutic Equivalence Evaluations 2022 [Available from: https://www.accessdata.fda.gov/scripts/cder/ob/search_product.cfm.
28. EyePoint Pharmaceuticals I. Technology 2021 [Available from: https://eyepointpharma.com/technology/.
29. Alimera Sciences. What is ILUVIEN? 2021 [Available from: https://iluvien.com/iluvien-diabetic-macular-edema/.
30. Chen YC, Moseson DE, Richard CA, Swinney MR, Horava SD, Oucherif KA, et al. Development of hot-melt extruded drug/polymer matrices for sustained delivery of meloxicam. J Control Release. 2022;342:189-200.
31. Zhang S, Nagapudi K, Shen M, Lomeo J, Qin Y, Zhu A, et al. Release Mechanisms and Practical Percolation Threshold for Long-acting Biodegradable Implants: An Image to Simulation Study. J Pharm Sci. 2021.
32. Kelley RA, Ghaffari A, Wang Y, Choi S, Taylor JR, Hartman RR, et al. Manufacturing of Dexamethasone-Poly(d,l-Lactide-co-Glycolide) Implants Using Hot-

Melt Extrusion: Within- and Between-Batch Product Performance Comparisons. J Ocul Pharmacol Ther. 2020;36(5):290-7.
33. Schwendeman SP, Chang RS, inventorsCoated implants for long-term controlled release of antibody therapeutics2019.
34. Li D, Guo G, Fan R, Liang J, Deng X, Luo F, et al. PLA/F68/dexamethasone implants prepared by hot-melt extrusion for controlled release of anti-inflammatory drug to implantable medical devices: I. Preparation, characterization and hydrolytic degradation study. Int J Pharm. 2013;441(1-2):365-72.
35. Bode C, Kranz H, Fivez A, Siepmann F, Siepmann J. Often neglected: PLGA/PLA swelling orchestrates drug release: HME implants. J Control Release. 2019;306:97-107.
36. USP. ⟨1092⟩ The Dissolution Procedure: Development and Validation. Rockville, MD2022.
37. Jaffe GJ, Yang CH, Guo H, Denny JP, Lima C, Ashton P. Safety and pharmacokinetics of an intraocular fluocinolone acetonide sustained delivery device. Invest Ophthalmol Vis Sci. 2000;41(11):3569-75.
38. Bhagat R, Zhang J, Farooq S, Li XY. Comparison of the release profile and pharmacokinetics of intact and fragmented dexamethasone intravitreal implants in rabbit eyes. J Ocul Pharmacol Ther. 2014;30(10):854-8.
39. Stein S, Auel T, Kempin W, Bogdahn M, Weitschies W, Seidlitz A. Influence of the test method on in vitro drug release from intravitreal model implants containing dexamethasone or fluorescein sodium in poly (d,l-lactide-co-glycolide) or polycaprolactone. Eur J Pharm Biopharm. 2018;127:270-8.
40. Rawat A, Stippler E, Shah VP, Burgess DJ. Validation of USP apparatus 4 method for microsphere in vitro release testing using Risperdal Consta. Int J Pharm. 2011;420(2):198-205.
41. Zolnik BS, Leary PE, Burgess DJ. Elevated temperature accelerated release testing of PLGA microspheres. J Control Release. 2006;112(3):293-300.
42. Awwad S, Lockwood A, Brocchini S, Khaw PT. The PK-Eye: A Novel In Vitro Ocular Flow Model for Use in Preclinical Drug Development. J Pharm Sci. 2015;104(10):3330-42.
43. Kummer MP, Abbott JJ, Dinser S, Nelson BJ. Artificial vitreous humor for in vitro experiments. Annu Int Conf IEEE Eng Med Biol Soc. 2007;2007:6407-10.
44. Chang-Lin JE, Burke JA, Peng Q, Lin T, Orilla WC, Ghosn CR, et al. Pharmacokinetics of a sustained-release dexamethasone intravitreal implant in vitrectomized and nonvitrectomized eyes. Invest Ophthalmol Vis Sci. 2011;52(7):4605-9.
45. Stein S, Bogdahn M, Rosenbaum C, Weitschies W, Seidlitz A. Distribution of fluorescein sodium and triamcinolone acetonide in the simulated liquefied and vitrectomized Vitreous Model with simulated eye movements. Eur J Pharm Sci. 2017;109:233-43.
46. CHMP Assessment report - Ozurdex. London, UK; 2010.
47. Shiah J-G, Bhagat R, Blanda WM, Nivaggioli T, Peng L, Chou D, et al., inventors; Allergan, Inc., assignee. Ocular implant made by a double extrusion process. USA patent US8034366. 2011 10/11/2011.

48. Del Amo EM, Urtti A. Rabbit as an animal model for intravitreal pharmacokinetics: Clinical predictability and quality of the published data. Exp Eye Res. 2015;137:111-24.
49. Chang-Lin JE, Attar M, Acheampong AA, Robinson MR, Whitcup SM, Kuppermann BD, et al. Pharmacokinetics and pharmacodynamics of a sustained-release dexamethasone intravitreal implant. Invest Ophthalmol Vis Sci. 2011;52(1):80-6.
50. Siepmann J, Elkharraz K, Siepmann F, Klose D. How autocatalysis accelerates drug release from PLGA-based microparticles: a quantitative treatment. Biomacromolecules. 2005;6(4):2312-9.
51. Costello MA, Liu J, Chen B, Wang Y, Qin B, Xu X, et al. Drug release mechanisms of high-drug-load, melt-extruded dexamethasone intravitreal implants. Eur J Pharm Biopharm. 2023.
52. Yau JW, Rogers SL, Kawasaki R, Lamoureux EL, Kowalski JW, Bek T, et al. Global prevalence and major risk factors of diabetic retinopathy. Diabetes Care. 2012;35(3):556-64.
53. Tah V, Orlans HO, Hyer J, Casswell E, Din N, Sri Shanmuganathan V, et al. Anti-VEGF Therapy and the Retina: An Update. J Ophthalmol. 2015;2015:627674.
54. Gaballa SA, Kompella UB, Elgarhy O, Alqahtani AM, Pierscionek B, Alany RG, et al. Corticosteroids in ophthalmology: drug delivery innovations, pharmacology, clinical applications, and future perspectives. Drug Deliv Transl Res. 2021;11(3):866-93.
55. Robinson MR, Whitcup SM. Pharmacologic and clinical profile of dexamethasone intravitreal implant. Expert Rev Clin Pharmacol. 2012;5(6):629-47.
56. Highlights of Prescribing Information, OZURDEX (dexamethasone intravitreal implant) Madison, NJ: Allergan; 2020 [Available from: https://www.rxabbvie.com/pdf/ozurdex_pi.pdf.
57. Dugel PU, Bandello F, Loewenstein A. Dexamethasone intravitreal implant in the treatment of diabetic macular edema. Clin Ophthalmol. 2015;9:1321-35.
58. Cohen EM. Dexamethasone. In: Florey K, editor. Analytical profiles of drug substances. 2. New York and London: Academic Press; 1973. p. 163-97.
59. Bakri SJ, Boyer DS, Albini TA, Holekamp NM, Ferrone PJ, Bhagat R, et al. Comparison of the tissue penetration and glide force of 22-gauge thin-wall needles for intravitreal implant administration. Ophthalmic Surg Lasers Imaging Retina. 2014;45(5):430-5.
60. Fredenberg S, Wahlgren M, Reslow M, Axelsson A. The mechanisms of drug release in poly(lactic-co-glycolic acid)-based drug delivery systems--a review. Int J Pharm. 2011;415(1-2):34-52.
61. Zhou J, Walker J, Ackermann R, Olsen K, Hong JKY, Wang Y, et al. Effect of Manufacturing Variables and Raw Materials on the Composition-Equivalent PLGA Microspheres for 1-Month Controlled Release of Leuprolide. Mol Pharm. 2020;17(5):1502-15.
62. Garner J, Skidmore S, Park H, Park K, Choi S, Wang Y. A protocol for assay of poly(lactide-co-glycolide) in clinical products. Int J Pharm. 2015;495(1):87-92.
63. Webb PA. Volume and density determinations for particle technologists. Micromeritics Instrument Corp. 2001;2(16):01.

64. Oliveira PFM, Willart J-F, Siepmann J, Siepmann F, Descamps M. Using Milling To Explore Physical States: The Amorphous and Polymorphic Forms of Dexamethasone. Crystal Growth & Design. 2018;18(3):1748-57.
65. Evonik Industries AG. Biodegradable polymers for controlled release 2023 [Available from: https://healthcare.evonik.com/en/pharmaceuticals/parenteral-drug-delivery/parenteral-excipients/bioresorbable-polymers/standard-polymers.
66. Thompson SA, Davis DA, DiNunzio JC, Martin C, Williams RO, Zhang F. Melt Extrusion. In: Williams Iii RO, Davis Jr DA, Miller DA, editors. Formulating Poorly Water Soluble Drugs. Cham: Springer International Publishing; 2022. p. 327-76.
67. Bassand C, Benabed L, Verin J, Danede F, Lefol LA, Willart JF, et al. Hot melt extruded PLGA implants loaded with ibuprofen: How heat exposure alters the physical drug state. Journal of Drug Delivery Science and Technology. 2022;73.
68. Park K, Otte A, Sharifi F, Garner J, Skidmore S, Park H, et al. Potential Roles of the Glass Transition Temperature of PLGA Microparticles in Drug Release Kinetics. Mol Pharm. 2021;18(1):18-32.
69. Moseson DE, Taylor LS. The application of temperature-composition phase diagrams for hot melt extrusion processing of amorphous solid dispersions to prevent residual crystallinity. Int J Pharm. 2018;553(1-2):454-66.
70. Prudic A, Lesniak AK, Ji Y, Sadowski G. Thermodynamic phase behaviour of indomethacin/PLGA formulations. Eur J Pharm Biopharm. 2015;93:88-94.
71. Gasmi H, Siepmann F, Hamoudi MC, Danede F, Verin J, Willart JF, et al. Towards a better understanding of the different release phases from PLGA microparticles: Dexamethasone-loaded systems. Int J Pharm. 2016;514(1):189-99.
72. Kothari K, Ragoonanan V, Suryanarayanan R. The role of drug-polymer hydrogen bonding interactions on the molecular mobility and physical stability of nifedipine solid dispersions. Mol Pharm. 2015;12(1):162-70.
73. Andhariya JV, Jog R, Shen J, Choi S, Wang Y, Zou Y, et al. Development of Level A in vitro-in vivo correlations for peptide loaded PLGA microspheres. J Control Release. 2019;308:1-13.
74. Wang C, Hou H, Nan K, Sailor MJ, Freeman WR, Cheng L. Intravitreal controlled release of dexamethasone from engineered microparticles of porous silicon dioxide. Exp Eye Res. 2014;129:74-82.
75. Tamani F, Bassand C, Hamoudi MC, Danede F, Willart JF, Siepmann F, et al. Mechanistic explanation of the (up to) 3 release phases of PLGA microparticles: Diprophylline dispersions. Int J Pharm. 2019;572:118819.
76. Rothstein SN, Little SR. A "tool box" for rational design of degradable controlled release formulations. Journal of materials chemistry. 2010;21(1):29-39.
77. Kang J, Schwendeman SP. Pore closing and opening in biodegradable polymers and their effect on the controlled release of proteins. Mol Pharm. 2007;4(1):104-18.
78. Meyer CH, Liu Z, Brinkmann CK, Rodrigues EB, Bertelmann T, German Retinal Vein Occlusion G. Penetration force, geometry, and cutting profile of the novel and old Ozurdex needle: the MONO study. J Ocul Pharmacol Ther. 2014;30(5):387-91.

79. Baird DG, Collias DI. Polymer Processing : Principles and Design. 2nd ed. ed. Somerset: John Wiley & Sons, Incorporated; 2014.
80. Skomski D, Liu Z, Su Y, John CT, Doty A, Forster SP, et al. An Imaging Toolkit for Physical Characterization of Long-Acting Pharmaceutical Implants. J Pharm Sci. 2020;109(9):2798-811.
81. Makadia HK, Siegel SJ. Poly Lactic-co-Glycolic Acid (PLGA) as Biodegradable Controlled Drug Delivery Carrier. Polymers (Basel). 2011;3(3):1377-97.
82. Zolnik BS, Burgess DJ. Effect of acidic pH on PLGA microsphere degradation and release. J Control Release. 2007;122(3):338-44.
83. Hickey T, Kreutzer D, Burgess DJ, Moussy F. Dexamethasone/PLGA microspheres for continuous delivery of an anti-inflammatory drug for implantable medical devices. Biomaterials. 2002;23(7):1649-56.
84. Matter B, Ghaffari A, Bourne D, Wang Y, Choi S, Kompella UB. Dexamethasone Degradation in Aqueous Medium and Implications for Correction of In Vitro Release from Sustained Release Delivery Systems. AAPS PharmSciTech. 2019;20(8):320.
85. Whitcup SM, Robinson MR. Development of a dexamethasone intravitreal implant for the treatment of noninfectious posterior segment uveitis. Ann N Y Acad Sci. 2015;1358:1-12.
86. Gan IM, Ugahary LC, van Dissel JT, van Meurs JC. Effect of intravitreal dexamethasone on vitreous vancomycin concentrations in patients with suspected postoperative bacterial endophthalmitis. Graefes Arch Clin Exp Ophthalmol. 2005;243(11):1186-9.
87. Hausberger AG, DeLuca PP. Characterization of biodegradable poly(d,l-lactide-co-glycolide) polymers and microspheres. Journal of Pharmaceutical and Biomedical Analysis. 1995;13(6):747-60.
88. Blasi P, D'Souza SS, Selmin F, DeLuca PP. Plasticizing effect of water on poly(lactide-co-glycolide). J Control Release. 2005;108(1):1-9.
89. Brunner A, Mäder K, Göpferich A. pH and Osmotic Pressure Inside Biodegradable Microspheres During Erosion1. Pharmaceutical Research. 1999;16(6):847-53.
90. Ding AG, Schwendeman SP. Acidic microclimate pH distribution in PLGA microspheres monitored by confocal laser scanning microscopy. Pharm Res. 2008;25(9):2041-52.
91. Blasi P, Schoubben A, Giovagnoli S, Perioli L, Ricci M, Rossi C. Ketoprofen poly(lactide-co-glycolide) physical interaction. AAPS PharmSciTech. 2007;8(2):Article 37.
92. Acharya G, Shin CS, Vedantham K, McDermott M, Rish T, Hansen K, et al. A study of drug release from homogeneous PLGA microstructures. J Control Release. 2010;146(2):201-6.
93. Rapier CE, Shea KJ, Lee AP. Investigating PLGA microparticle swelling behavior reveals an interplay of expansive intermolecular forces. Sci Rep. 2021;11(1):14512.
94. Korber M. PLGA erosion: solubility- or diffusion-controlled? Pharm Res. 2010;27(11):2414-20.

95. Siepmann J, Elkharraz K, Siepmann F, Klose D. How autocatalysis accelerates drug release from PLGA-based microparticles: A quantitative treatment. Biomacromolecules. 2005;6(4):2312-9.
96. Burkersroda Fv, Schedl L, Göpferich A. Why degradable polymers undergo surface erosion or bulk erosion. Biomaterials. 2002;23(21):4221-31.
97. Gasmi H, Danede F, Siepmann J, Siepmann F. Does PLGA microparticle swelling control drug release? New insight based on single particle swelling studies. J Control Release. 2015;213:120-7.
98. Gasmi H, Willart JF, Danede F, Hamoudi MC, Siepmann J, Siepmann F. Importance of PLGA microparticle swelling for the control of prilocaine release. Journal of Drug Delivery Science and Technology. 2015;30:123-32.
99. He P, Xu S, Guo Z, Yuan P, Liu Y, Chen Y, et al. Pharmacodynamics and pharmacokinetics of PLGA-based doxorubicin-loaded implants for tumor therapy. Drug Deliv. 2022;29(1):478-88.
100. Kamel R, Abbas H. PLGA-based monolithic filaments prepared by hot-melt extrusion: In-vitro comparative study. Annales Pharmaceutiques Francaises. 2018;76(2):97-106.
101. Bassand C, Freitag J, Benabed L, Verin J, Siepmann F, Siepmann J. PLGA implants for controlled drug release: Impact of the diameter. Eur J Pharm Biopharm. 2022.
102. Saraf I, Kushwah V, Alva C, Koutsamanis I, Rattenberger J, Schroettner H, et al. Influence of PLGA End Groups on the Release Profile of Dexamethasone from Ocular Implants. Mol Pharm. 2023.
103. Australian Public Assessment Report for Dexamethasone - Ozurdex. Australian Capital Territory, Australia; 2011.
104. Hausberger AG, Kenley RA, DeLuca PP. Gamma irradiation effects on molecular weight and in vitro degradation of poly(D,L-lactide-CO-glycolide) microparticles. Pharm Res. 1995;12(6):851-6.
105. Faisant N, Siepmann J, Richard J, Benoit JP. Mathematical modeling of drug release from bioerodible microparticles: effect of gamma-irradiation. Eur J Pharm Biopharm. 2003;56(2):271-9.
106. Park TG. Degradation of poly(d,l-lactic acid) microspheres: effect of molecular weight. Journal of Controlled Release. 1994;30(2):161-73.
107. Park TG. Degradation of poly(lactic-co-glycolic acid) microspheres: effect of copolymer composition. Biomaterials. 1995;16(15):1123-30.
108. Park K, Otte A, Sharifi F, Garner J, Skidmore S, Park H, et al. Formulation composition, manufacturing process, and characterization of poly(lactide-co-glycolide) microparticles. J Control Release. 2020.
109. Lee SL, O'Connor TF, Yang X, Cruz CN, Chatterjee S, Madurawe RD, et al. Modernizing Pharmaceutical Manufacturing: from Batch to Continuous Production. Journal of Pharmaceutical Innovation. 2015;10(3):191-9.
110. Chahal HS, Patel R, Shimer M. Marketing of First Generic Drugs Approved by U.S. FDA from January 2010 to June 2017. 2021.

111. U.S. Food & Drug Administration. Generic Drugs: Questions & Answers2021. Available from: https://www.fda.gov/drugs/frequently-asked-questions-popular-topics/generic-drugs-questions-answers.
112. Wahl PR, Hörl G, Kaiser D, Sacher S, Rupp C, Shlieout G, et al. In-line measurement of residence time distribution in melt extrusion via video analysis. Polymer Engineering & Science. 2018;58(2):170-9.
113. Poulesquen A, Vergnes B. A study of residence time distribution in co-rotating twin-screw extruders. Part I: Theoretical modeling. Polymer Engineering & Science. 2003;43(12):1841-8.
114. ASTM D7264/D7264M−21. Standard Test Method for Flexural Properties of Polymer Matrix Composite Materials. West Conshohocken, PA: ASTM International; 2021.
115. Blackshields CA, Crean AM. Continuous powder feeding for pharmaceutical solid dosage form manufacture: a short review. Pharm Dev Technol. 2018;23(6):554-60.
116. Engisch WE, Muzzio FJ. Feedrate deviations caused by hopper refill of loss-in-weight feeders. Powder Technology. 2015;283:389-400.
117. Kostic MM, Reifschneider LG. Design of extrusion dies. Encyclopedia of chemical processing. 2006;10:633-49.
118. Seitavuopio P, Rantanen J, Yliruusi J. Use of roughness maps in visualisation of surfaces. Eur J Pharm Biopharm. 2005;59(2):351-8.
119. Kohno M, Andhariya JV, Wan B, Bao Q, Rothstein S, Hezel M, et al. The effect of PLGA molecular weight differences on risperidone release from microspheres. Int J Pharm. 2020;582:119339.
120. Huang J, Mazzara JM, Schwendeman SP, Thouless MD. Self-healing of pores in PLGAs. J Control Release. 2015;206:20-9.
121. Muddineti OS, Omri A. Current trends in PLGA based long-acting injectable products: The industry perspective. Expert Opin Drug Deliv. 2022;19(5):559-76.
122. Wan B, Bao Q, Zou Y, Wang Y, Burgess DJ. Effect of polymer source variation on the properties and performance of risperidone microspheres. Int J Pharm. 2021;610:121265.
123. Sun J, Walker J, Beck-Broichsitter M, Schwendeman S. Characterization of Commercial PLGAs by NMR Spectroscopy. 2021.
124. Engwicht A, Girreser U, Muller BW. Characterization of co-polymers of lactic and glycolic acid for supercritical fluid processing. Biomaterials. 2000;21(15):1587-93.
125. Hong JKY, Schwendeman SP. Characterization of Octreotide-PLGA Binding by Isothermal Titration Calorimetry. Biomacromolecules. 2020;21(10):4087-93.
126. Evonik Industries AG. Evonik finalizes acquisition of Boehringer Ingelheim's RESOMER® business 2011 [Available from: https://corporate.evonik.com/en/media/press-releases/corporate/evonik-finalizes-acquisition-of-boehringer-ingelheims-resomer-business-103186.html.
127. Garner J, Hadar J, Skidmore S, Jessmon F, Park H, Park K, et al., editors. Effect of Reaction Temperature on PLGA Properties and Semi-Solvent Interactions. Controlled Release Society Annual Meeting, Virtual Meeting; 2021.

128. Kumskova N, Ermolenko Y, Osipova N, Semyonkin A, Kildeeva N, Gorshkova M, et al. How subtle differences in polymer molecular weight affect doxorubicin-loaded PLGA nanoparticles degradation and drug release. J Microencapsul. 2020;37(3):283-95.
129. Dorati R, DeLuca PP. Effect of Hydration on Physicochemical Properties of End-Capped PLGA. Advances in Biomaterials. 2014;2014:1-9.
130. Higashitani K, Masuda H, Gotoh K. Powder Technology Handbook. New York: CRC Press LLC; 1997.
131. Feuerbach T, Callau-Mendoza S, Thommes M. Development of filaments for fused deposition modeling 3D printing with medical grade poly(lactic-co-glycolic acid) copolymers. Pharm Dev Technol. 2019;24(4):487-93.

Vita

Mark Allen Costello was born in Warren, MI and raised in Shelby Township, MI. After graduating valedictorian from Dwight D. Eisenhower High School in 2008, he entered the Chemical Engineering program at the University of Michigan – Ann Arbor, from which he graduated with a Bachelor of Science in Engineering in 2012. From 2012–2015, he was employed as a formulation scientist at AbbVie (formerly Abbott Laboratories) in North Chicago, IL, where he assisted in the commercialization of hepatitis C treatment Viekira XR. In 2015, he joined the Formulation Development group at Vertex Pharmaceuticals in Boston, MA, where he was involved in the development of several clinical-stage programs and commercialization of the Orkambi pediatric tablet for treatment of cystic fibrosis. In September 2020, he joined Dr. Feng Zhang's research group in the College of Pharmacy at the University of Texas at Austin in pursuit of his doctoral degree.

Email: Mark.Costello@utexas.edu